Effects of pyroptotic inhibitors on Infectious Laryngotracheitis Virus (ILTV) induced inflammation in chicken epithelial cells

Thesis

Submitted to the
DEEMED UNIVERSITY
ICAR-Indian Veterinary Research Institute
Izatnagar - 243 122 (U.P.), India

Dr. Parvatha Rama Sai Revathi
Roll No. M-6151

IN PARTIAL FULFILMENT OF THE REQUIREMENTS FOR THE DEGREE OF

Master of Veterinary Science
(Veterinary Microbiology)

2023

Dedicated To...

My Beloved Family,
Guide
and
Co-Guide

भा.कृ.अनु.प.–भारतीय पशु चिकित्सा अनुसंधान संस्थान
(सम विश्वविद्यालय)
इज्जतनगर –243122, (उ.प्र.), भारत

DIVISION OF VETERINARY MICROBIOLOGY
ICAR-INDIAN VETERINARY RESEARCH INSTITUTE
(Deemed University)
IZATNAGAR - 243 122, U.P., INDIA

Dr. Kuldeep Dhama
M.V.Sc., Ph.D.
Principal Scientist

Dated: 15/12/2022

Certificate

This is to be certified that the research work embodied in this thesis entitled **"Effects of pyroptotic inhibitors on Infectious Laryngotracheitis Virus (ILTV) induced inflammation in chicken epithelial cells"** *submitted by* **Dr. Parvatha Rama Sai Revathi, Roll No. M-6151,** *for the award of* **Master of Veterinary Science** *Degree in* **Veterinary Microbiology** *at Indian Veterinary Research Institute, Izatnagar, is the original work carried out by the candidate herself under my supervision and guidance.*

It is further certified that **Dr. Parvatha Rama Sai Revathi, Roll No. M-6151,** *has worked for more than 21 months in the Institute and has put in more than 150 days attendance under me from the date of registration for the* **Master of Veterinary Science** *Degree in this Deemed University, as required under the relevant ordinance.*

(KULDEEP DHAMA)
Chairman
Advisory Committee
DR. KULDEEP DHAMA
Principal Scientist
Avian Disease Section
Indian Veterinary Research Institute
Izatnagar (U.P.) 243 122

Certificate

We the undersigned members of Advisory Committee of **Dr. Parvatha Rama Sai Revathi, Roll No. M-6151,** *a candidate for the degree of* **Master of Veterinary Science** *with the major discipline in* **Veterinary Microbiology,** *agree that the thesis entitled* **"Effects of pyroptotic inhibitors on Infectious Laryngotracheitis Virus (ILTV) induced inflammation in chicken epithelial cells"** *may be submitted in partial fulfilment of the requirement for the degree.*

We have gone through the contents of the thesis and are fully satisfied with the work carried out by the candidate, which is being presented for the award of **Master of Veterinary Science** *Degree of this Institute.*

It is further certified that the candidate has completed all the prescribed requirements governing the award of **Master of Veterinary Science** *Degree of the Deemed University, Indian Veterinary Research Institute, Izatnagar.*

Signature
Name D. V. Rai
External Examiner
Date : 27-1-23

(Kuldeep Dhama)
Chairman
Advisory Committee
Date : 25/1/2023

MEMBERS OF STUDENT'S ADVISORY COMMITTEE

Dr. M.K. Singh, Senior Scientist
Immunology Section, ICAR-IVRI, Izatnagar .....

Dr. Gaurav Kumar Sharma, Senior Scientist
CADRAD, ICAR-IVRI, Izatnagar .....

Dr. Ajay Kumar, Senior Scientist
Division of Veterinary Biochemistry, ICAR-IVRI, Izatnagar .....

Dr. Asok Kumar M, Scientist (SS)
Division of Pathology, ICAR-IVRI, Izatnagar .....

ACKNOWLEDGEMENTS

First of all, it is always a pleasure to look back and cherish the joy of thanking the good hearts behind us. Though a few words of acknowledgements will not equilibrate the real feeling of gratitude towards them, but I believe to some extent it will fulfil a part of it definitely.

A formal statement of acknowledgement will hardly do justice to my deeply felt sincere and loyal gratitude to the chairman of my advisory committee, **Dr. Kuldeep Dhama,** Principal Scientist, Avian Disease Section, Division of Pathology, IVRI, Izatnagar for his scholastic guidance, diligent help, continuous inspiration and critical appreciation during the entire course of this study and in the preparation of manuscript.

I would like to extend my heartfelt gratitude and sincere thanks to my respected Advisor and Co-guide **Dr. Asok Kumar M.**, Scientist, Division of Pathology, ICAR-IVRI, for his insightful advice at every phase of the execution and planning of the research, unfailing guidance, continuous motivation and critical appreciation during the entire course of this study and in the preparation of manuscript which I am unable to express in words. It is an honour to thank my advisor, whom I consider to be my best teacher, for adopting me as a student and adding a new layer to my academic life.

I express my heartfelt appreciation and gratitude to the Late **Dr. M. Palanivelu,** Scientist, Division of Pathology for his brilliant design of the research project that shaped my research abilities. May his soul rest in peace, his legacy will live on forever.

I wish to record my gratitude and sincere thanks to the members of the advisory committee, **Dr. M. K. Singh** (Senior Scientist, Immunology Section), for his patient and scholastic guidance, inspirational words, constant supervision and diligent help throughout my research. I warmly thank **Dr. Gaurav. K. Sharma** (Senior Scientist, CADRAD, ICAR-IVRI, Izatnagar), **Dr. Ajay Kumar** (Senior Scientist, Division of Animal Biochemistry), for their assistance and guidance during my research work. I express my sincere gratitude to **Dr. M. Karikalan,** Scientist, Centre for wild life Studies, who provided me necessary facilities to carry out my work, cooperation during my research work in general. Without your help it wasn't easy to finish work in time.

I would also take this opportunity to thank all the scientists of Immunology section **Dr. S. Dandapat**, Incharge, Immunology Section, **Dr. R. Saravanan,** Principal Scientist, Immunology Section, **Dr. T. K. Goswami**, Emeritus Scientist, Immunology Section, **Dr. Alka Tomar**, Retired Incharge, Immunology Section, **Dr. Vishal Chander** (Senior Scientist, Immunology Section), **Dr. Shyma K. Latheef** (Scientist, CADRAD, ICAR-IVRI, Izatnagar), for their inspiration, encouragement, active persuasion and help rendered to make this task an accomplishment.

I am very grateful to the **Director, Joint Director (Research), Joint Director (Acad)**, and **Scientific Coordinator** for providing me the necessary facilities to carry out the research work, I owe a very special debt of gratitude to the ICAR for providing me financial support during this work.

I am especially grateful to my Ph.D senior **Dr. Megha Sharma** for her constant encouragement , affection and valuable advice during my research work and my laboratory mate **Dr. Sayali Kohale**, for her valuable advice helped and guided me through my work in the Avian Disease Section Laboratory.

I extend my sincere thanks to my seniors from the veterinary microbiology division **Dr. Bindu S** for her constant encouragement, **Dr. Abinaya K, Dr. Manikandan R,** for their constant support and valuable help during my research work.

I am also very thankful to my seniors and colleagues **Dr. Rohit, Dr. Hitheshwar, Dr. Vinay Kumar, Dr. Faslu Rahaman, Dr. Shubham, Dr. Basant, Dr. Mir Hussain, Dr Tanuj, Dr. Sourabh Babu** for their guidance, support, expertise, unreserved help and invaluable inspirations throughout my research work.

I genuinely appreciate the ever-willing help given by my batchmates of Veterinary microbiology division Dr(s). **Firdous, Alona, Goparam, , Indu, Amani, Mounica, Lakshmi Prakasan, Lulu, Dengam, Prabodh, Santanu, Sunil, Eben** I thank all of them for their constant help, and joyful company during my course work.

I am truly thankful to all my batchmates in IVRI Dr (s). **Laharika, Sai Vinay, Yaswanth, Sai simha reddy, Prudhvi, Naveen, Praveen, Indu, Chandini, Jitha, Hema, Parul, Naveena** and specially my Ph.D senior **Lakshmi Kanth sir,** I feel emotional to remember the company and support I have enjoyed with all my colleagues during the entire life of my IVRI

carrier and making my research life sweet and memorable. I would like to express special thanks to my seniors Dr(s). **Neha mam, Devansh sir, Venu, Arpita mam, Khushboo mam, Satyabrat Dutta sir, Vidya mam, Safoora mam, for** their valuable suggestions and support. I am also thankful to my juniors Dr.(s) **Sarath Chandra, Sri Harsha, Balaji, Akhil raj, Arun Chatla, Revathi, Varshini, Haritha, Sariga, Priyanshi, Purushottam, Bhanu Kumar, Rajendar** for their help during this study. I wish to acknowledge my seniors and friends and other members of IVRI for their help and support throughout my study.

Special thanks to **Dr.Drashini** for being my constant support system throughout my reasearch. Without your help it wasn't easy to finish work in time. You always stood by me, cared for me when I was in need, cheered me up in my bad times and always inspired me with words of wisdom.

I extend my special mention to **Dr.Kiranmayee** for being my lovely companion in IVRI, canteen, parties and outings. You people will always be cherished in my memories, and the time I spent with you at IVRI was bliss thanks for bearing my all nonsense.

I have the good opportunity to sincerely thank my best friend **Dr. V. Vijay Kumar** for his generosity towards me and his constant support and motivation was a driving force for the successful completion of my thesis. My heartfelt thanks to my best pals **Dr. Samanvitha, Dr.Venkatesh Abburi, Dr. Sravani, Dr.Khadeer Basha, Dr. Sumana, Surekha, Sharath** for their constant support and affection throughout my journey.

Words cannot describe the help and good association to my lovable seniors and juniors at **Karnataka mess**, IVRI, for their immense encouragement, helping and providing friendly environment during the present study. A special thanks to **Chandan** bhaiya, **Bharath** bhaiya and mess workers for providing us with good food all the times and taking care of us.

I am thankful to **Mr. Dharmendra** (Chachu) and **Mr. Kuldeep** for their great help rendered for bringing up this thesis to a proper shape.

I would like to mention special thanks to the staff members of Pathology lab, **Umesh Singh ji, Sartaj ji** for their patience, support, timely co-operation with my experiments and **Manoj ji, Ismail ji** including for their timely help during my research and I acknowledge the help from Immunology lab staff members **Raju ji, Amardeep ji, Kunwarsen ji,Rathuri ji, Rahul ji, Sudheer ji, Bikesh ji, Shamruddin ji, Bhuparam ji, Lalaram ji**including for their timely help during my research.

Finally, I'd like to take this opportunity to express my gratitude to my beloved nanna and amma **Mr. P.Ch. Rami Reddy,** and **Mrs. M.V. Vijaya** and my loving sisters **Sumithra**, and **Keerthi** and my family members especially **mummy,** and **mama**. Whatever I am today, it is because of their unconditional love and support. I will never be able to repay their sacrifices. I also want to thank them for their continuous blessings, prayers, and encouragement.

This list is obviously incomplete but allow me to submit that the omissions are inadvertent and I once again record my deep felt gratitude to all those associated with me in this endeavour.

Date: 15/12/22 ***(Parvatha Rama Sai Revathi)***

Place: *ICAR-IVRI, Izatnagar*

ABBREVIATIONS

%	:	Percent
<	:	Less than
>	:	Greater than
° C	:	Degree Celsius
β	:	beta
γ	:	gamma
µL	:	Microliter
µM	:	Micromolar
µm	:	Micrometer
BIT	:	Bovine serum albumin, insulin, transferrin
bp	:	Base pairs
BSA	:	Bovine serum albumin
CAM	:	Chorioallantoic membrane
CEO	:	Chicken embryo origin
DMEM	:	Dulbecco's Modified Eagle Medium
DNA	:	Deoxyribonucleic acid
dNTP	:	Deoxynucleotide triphosphates
DTT	:	DL-Dithiothreitol
DS	:	Dissociation solution
DW	:	Distilled water
EDTA	:	Ethylene diamine tetra acetic acid
ELISA	:	Enzyme-linked immunosorbent assay
Fig.	:	Figure
GAPDH	:	Glyceraldehyde 3-phosphate dehydrogenase
gC	:	Glycoprotein C
GSDMD	:	Gasdermin D
hpi	:	Hour(s) pre infection
hpoi	:	Hour(s) post infection
HVT	:	Herpesvirus of turkey
ILTV	:	Infectious Laryngotracheitis virus
IVRI	:	Indian Veterinary Research Institute
LPS	:	Lipopolysaccharide
LTR	:	Long terminal repeats
min	:	Minute(s)
mM	:	Millimolar

nm	:	nanometer
NTC	:	No template control
NFW	:	Nuclease free water
Pmol	:	Picomole
PBS	:	Phosphate-buffered saline
PCR	:	Polymerase chain reaction
RNA	:	Ribonucleic acid
TBE	:	Tris-Borate-EDTA
TCO	:	Tissue culture origin
VCN	:	Viral copy numbers

LIST OF TABLES

LIST OF FIGURES

CONTENTS

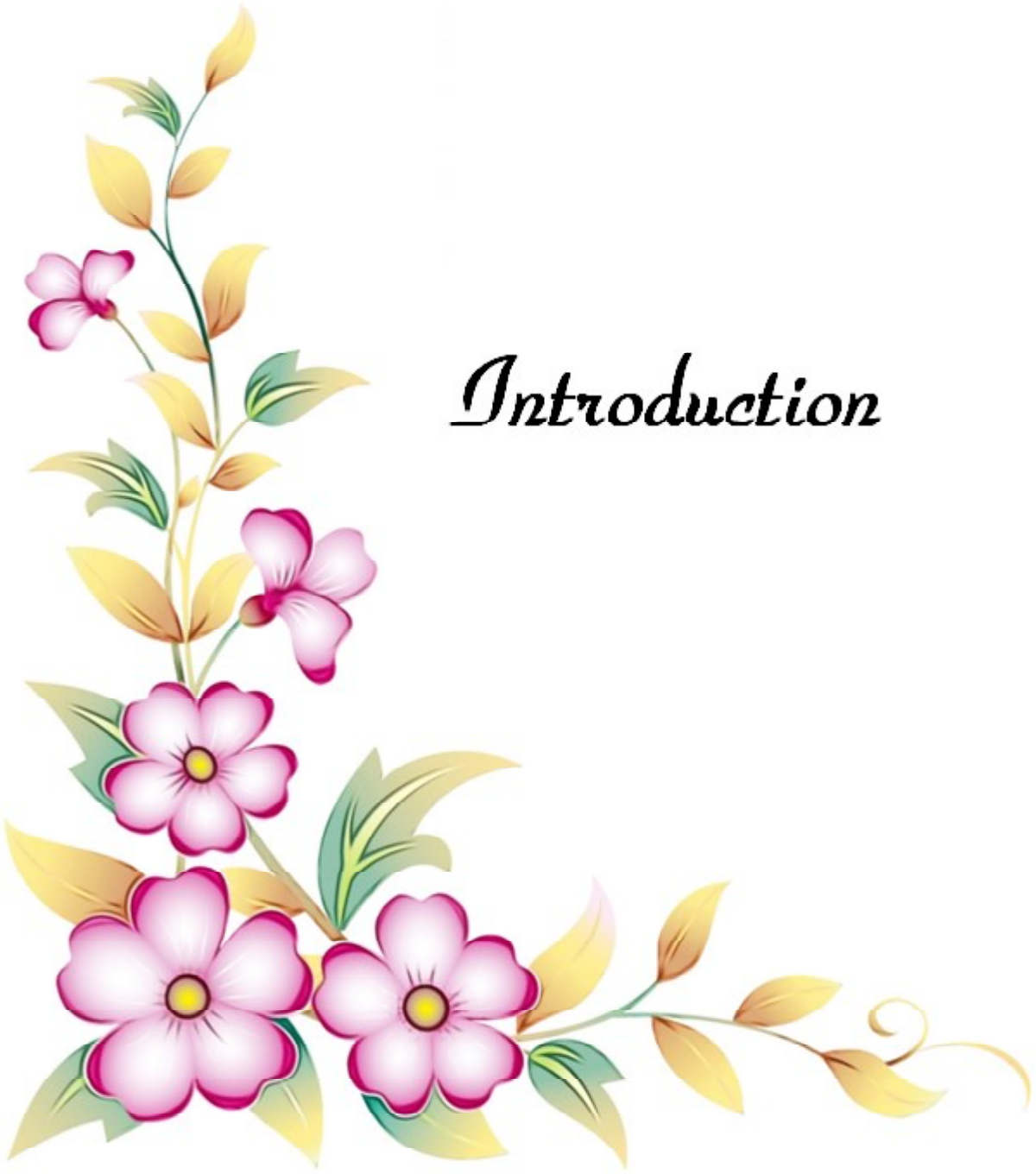

Introduction

1 INTRODUCTION

Poultry farming is one of the fastest-growing industries, and it plays a key role in global food security and the economy. Poultry producers frequently increase production in the most cost-effective way to get high economical benefits and to meet the demands of consumers. Close confinement and multi-age group poultry rearing are used in intensive rearing systems to maximise profits, but they also pose a significant risk of disease spread. In an outsized poultry flock with such proximity, mutation and recombination of live virus vaccines could result in the appearance of a replacement variant, resulting in significant losses. As a result of the evolution of industrialization, diseases that were once easily preventable have resurfaced or simply spread across geographic boundaries, causing great concern. Rapid and confirmatory diagnosis of different diseases of poultry helps in formulating timely and adequate prevention and control measures to lessen the economic losses in poultry farming promoting and commercializing the poultry industry (Hafez *et al*., 2020). Prophylactic vaccination in poultry is the major means to safeguard the health of birds from the threats of economically important pathogens via developing protective immunity, and for this purpose, various kinds of vaccines are available (Dhama *et al*., 2014). Adopting appropriate and timely treatment options and exploiting advances in developing newer therapeutic regimens by optimally exploring the fields of immunology, pharmacology, biotechnology and molecular biology are paving way for designing novel therapeutics against different pathogens of poultry.

Disease challenges have evolved alongside the poultry industry with its rapid expansion, resulting in holistic approaches to prevent clinical and sub-clinical diseases. Infectious laryngotracheitis (ILT), caused primarily in chickens by Gallid herpesvirus-1 infection, is one

of the emerging diseases that pose such a complex problem for the poultry industry, causing severe production losses due to high morbidity and mortality and also by mass vaccination (Garcia and Spatz, 2020; Gowthaman *et al.,* 2020). The species Gallid herpesvirus-1(GaHV-1) belongs to the genus *Iltovirus*, subfamily *Alphaherpesvirinae* and the family of *Herpesviridae* (Davison *et al.,* 2009). The ILTV genome spans 150-155kb and is a double-stranded DNA virus. The linear dsDNA of the virus is enclosed by a tegument layer and an outer glycoprotein envelope, giving it a diameter of 200-350nm (Granzow *et al.,* 2001). At least 80 open reading frames (ORFs) code for the entire length of the ILTV genome, in terms of position and structure of the deduced translation products, 63 ORFs show similarities to the Herpes Simplex Virus-1 (HSV-1) genome and the highly conserved glycoproteins are critical for replication and eliciting an immune response in the target host (Piccirillo *et al.,* 2016). In chickens, ILTV infection causes respiratory distress characterised by bloody mucus coughing, gasping, and open mouth breathing, as well as high morbidity and variable mortality (more than 50%) (OIE, 2014). Although ILTV is primarily associated with chickens, the natural infection has been documented in pheasants, peafowl, and turkeys (Winterfield and So, 1968; Crawshaw and Boycott, 1982). Infected birds spread the virus by contaminating surfaces, litter, and equipment with their respiratory discharges, or by direct contact with uninfected birds (Dufour-Zavala *et al.,* 2008). Gasping, bloody mucus expectoration, decreased egg production and decreased broiler weight gain are all symptoms to look out for (Aziz, 2010). In developing countries, the lack of safe vaccines contributes to the fact that ILTV is in its most severe form. The virus can also remain latent in the trigeminal ganglion and reactivate when infected birds are exposed to certain stressors, making the disease even more difficult to control (Bagust *et al.,* 1986). As a result of ILTV infection, the farm suffers a multimillion-dollar loss, which is caused by either mortality, reduced egg production, or both (Garcia and Spatz, 2020). ILTV was found to co-exist with other viral agents such as Avian influenza virus (AIV), Chicken anaemia virus (CAV), Avian pathogenic *Escherichia coli* (APEC), *Mycoplasma synoviae* (MS), and *Mycoplasma gallisepticum* (MG) in flocks from Uttar Pradesh and Tamil Nadu, according to a molecular analysis of the virus (Gowthaman *et al.,* 2017) thus the disease pathology is further complicated. Experiments on the immunological reactions of the host to

ILTV have been conducted, although they are not comprehensive. Bursectomized and vaccinated chickens resist the virus (Fahey *et al.,*1983), but thymectomized chickens do not (Fahey *et al.,*1984), demonstrating that the bird relies on cellular immunity rather than antibodies to fight the virus. In ILTV-infected chicken embryo lung cell culture, Lee *et al.* (2010) discovered that 789 genes were differentially expressed, many of which were involved in cellular growth, proliferation, and cell death. The CEO vaccine activates proteins in the MHC-I and MHC-II signalling pathways, such as B2M and TAP (Luo *et al.,* 2014).

ILT has become more common in India in recent years, four decades after its first report, which necessitates a deeper knowledge of its pathophysiology for developing control and treatment strategies. While more knowledge about the pathology of ILT has been gained, the molecular aspects of cell death and inflammation are still unknown. In general, microbes cause cell death by three major programmed cell death pathways which include apoptosis, necroptosis, and pyroptosis (Place and Kanneganti 2019; D'Arcy, 2019). Kumar *et al.* (2015) mentioned a group of non-inflammatory caspases (for example, caspase-8 in the mitochondrial pathway and caspase-9 in the death receptor pathway) that initiates apoptosis, which is primarily carried out by caspase-3. ILTV has so far been shown to evade apoptosis (Reddy *et al.,* 2014) and actively block chemokines via glycoprotein G (Coppo *et al*., 2018). Li *et al.* (2018) observed that p53 gene expression in "bystander" cells reduced not only the rate of apoptosis but also the rate of ILTV replication. In 2000, Brennan and Cookson reported that cell death distinct from apoptosis occurs in macrophages. They discovered that the entire process was reliant on caspase-1, which resulted in inflammation, and they named it pyroptosis. The term pyroptosis was coined from Greek origins "pyro" (fire or fever) and "ptosis" (falling). It's a great way to get rid of intracellular pathogens while also alerting the immune system to the intruder. When certain sensors detect danger signals, the creation of an inflammasome, which converts inactive procaspase-1 to caspase-1, is initiated by the cell pathways. This caspase-1 then activates the pro-forms of cytokines interleukin (IL-1β, IL-18) to make them active. Gasdermin-D is cleaved into N-GsdmD and C-GsdmD by caspase-1 at the same time. N-GsdmD then polymerizes in the cell membrane-forming pores through which inflammatory cytokines are released, resulting in cell death (Ding *et al.,* 2016). Since then, many scientists

have discovered that pyroptosis plays an essential role in innate immunity. It is implicated in several traumatic brain injuries (Sun *et al.,* 2020), chronic inflammation (Zhang *et al.,* 2019), cancers (Wu *et al.,* 2020), and metabolic disease pathogeneses (Chen *et al.,* 2020). Pathogens can avoid pyroptosis through the following mechanisms: i) Preventing ligands from binding to sensors by inhibiting their expression; ii) Modifying ligand binding to the inflammasome, and iii) Directly inhibiting inflammasomes. HSV-1 genome induced inflammasome activation in early infections in human foreskin fibroblast cells, and later suppressed the canonical pathway of pyroptosis failing IL-1 secretion with the help of actin clusters, trap caspase1, and NLRP3 inflammasome (Johnson *et al.,* 2013). The study demonstrates how HSV-1 evolved to avoid and block the proinflammatory cascade as well as cell death to preserve its niche. Anti-caspase-1 drugs inhibit the pyroptosis-dependent depletion of "bystander" CD4+ cells, which leads to acquired immunodeficiency disease (AIDS) in HIV-positive patients, according to similar evidence (Doitsh *et al.,* 2014). The infection of major respiratory viruses in birds, such as Newcastle disease and avian influenza has been studied using chicken tracheal cell culture (Zaffuto *et al.,* 2008). Even though the trachea is known to be the site of ILTV replication, studies on the isolation and behaviour of ILTV in chicken tracheal epithelial cell culture have yet to be published.

ILTV vaccination is efficient in preventing infection. Aside from their efficacy, CEO and TCO vaccines have the unfavourable property of reverting to the virulent form upon bird-to-bird transmissions, resulting in vaccinal laryngotracheitis in the field (Dufour-Zavala, 2008; Chacon *et al.,* 2015). Vaccination can sometimes result in the development of latent carrier birds, which serve as a source of infection for unvaccinated populations (Bagust, 1986). Apart from vaccination, therapeutic approaches for ILTV must be explored further. Seeing as ILTV infection causes intense inflammatory pathology in the conjunctiva and respiratory mucosa of chickens, pyroptosis could be important in the pathogenesis of ILTV, according to our hypothesis. Since elucidating the mode of cell death that aggravate inflammation in ILT will aid in identifying the root cause of inflammation, intervention strategies to block that specific cell death pathway can be devised using inhibitors, which will help to reduce the negative effects of ILT virus-induced inflammation. We assume that, by blocking this proinflammatory cell death

pathway (pyroptosis), the pathology associated with exacerbated inflammation during infectious laryngotracheitis might be reduced. Keeping this in view, the current study has been proposed with the following objective.

OBJECTIVE

i) To assess the effects of pyroptotic inhibitors on Infectious Laryngotracheitis virus (ILTV) induced inflammation in epithelial cells of chicken origin

Review of Literature

2 REVIEW OF LITERATURE

Infectious laryngotracheitis (ILT), caused predominantly in chickens by Gallid herpesvirus-1 infection, is one of the diseases that pose such integrated challenges and costs the poultry industry millions of dollars (Garcia and Spatz, 2020; Gowthaman *et al.,* 2020). After primary infection, an incubation period of 3–12 days is followed by an acute phase lasting 1–2 weeks. During this time, the virus replicates mainly in the trachea, larynx and conjunctiva, leading to respiratory disorders such as gasping, coughing, expectoration of bloody mucus and open mouth breathing, less frequently conjunctivitis, amidst, high morbidity, and variable mortality (more than 50%) in chickens (OIE, 2014).

When a virus enters the body, the innate immune system identifies it and reacts quickly. The adaptive immune system is subsequently activated, and the pathogen is neutralised. Apart from acting physical barrier in the mucosal innate immune system it also carries IgA, collectins, interferons, defensins, and lactoferrins, (Vareille *et al.,* 2011), which reduces herpes virus invasion by 100-fold compared to water (Cone, 2009). Chemokines and cytokines direct both innate and adaptive immunity once the mucosal epithelium has been penetrated (Vareille *et al.,* 2011). Infected lung cells from chicken embryos in vitro with ILTV demonstrated differential expression of 786 genes affecting cell development and death, 54 genes involved in inflammatory response pathways, and 60 genes involved in cell signalling pathways, according to Lee *et al.,* (2010). IL-8, IL-6, and CXC K60 expressions were also revealed to be more significant than chemokines and cytokines. Mild oedema and infiltration of inflammatory cells (CD4+ and CD8+) are seen between 3 to 5 days after infection after which the outcome of the disease is the result of the type of inflammatory cells present (Devlin *et al.,* 2010). Vagnozzi

et al. (2018) found that around 3–5 dpi, the tracheal mucosal epithelium upregulates chemokine binding ligand-2 and IL-1, as well as INF-genes. The inflammatory response was thought to be controlled by simultaneous overexpression of IL-10 genes. During ILTV infection, chickens rely significantly on cell-mediated immunity rather than antibody-dependent protection, according to multiple experimental investigations (Hayles *et al.,* 1976a; Fahey *et al.,* 1983a). Chen *et al.* (2011) found that a recombinant fowlpox virus encoding ILTV glycoprotein B (gB) and interleukin-18 (IL18) produced a stronger protective response than a recombinant vaccination alone. T-cell responsiveness and antibody-specific T-cell proliferation both were enhanced by this cytokine. The necessity of a Th-1 response against ILTV infection was discussed in this study. A transcriptome study of tracheal cells following ILTV infection indicated that 91 gene categories were differentially expressed out of 158 genes. Several collagen family genes were downregulated, whereas cytokine receptors, MHC I (2-microglobulin (B2M), transporter 2, ATP-binding cassette, sub-family B (TAP), CD8A, and CD8B, and MHC II (B locus M molecule1(BMA1/MHC-II), CD74 molecule (CD74), and CD4 were elevated, indicating a Th1 response (Luo *et al.,* 2014). Even though Glycoprotein G is not required for viral replication, it has been identified as a virulence factor in ILTV infection due to its chemokine binding and cytokine transcription regulation. An increase in the thickness of the tracheal mucosa of hens infected with gG-ILTV indicates that it regulates inflammatory cell chemotaxis and renders chemokines inaccessible (Devlin *et al.,* 2006).

Apoptosis in ILTV infections is also not well understood. It allows researchers to experiment with diverse cell death pathways such as necroptosis, ferroptosis, Entotic cell death, NETotic cell death, Parthanatos and pyroptosis (Galluzzi *et al.,* 2018). Reddy *et al.* (2014) attempted to characterise the function of apoptosis in ILTV infection, they observed only in bystander cells. A similar pattern of cell death was observed in human bystander CD4+ T cells which resulted in their depletion due to human immunodeficiency virus (HIV) infection (Doitsh *et al.,* 2014). They were able to activate caspase-1 in uninfected cells by using fluorochrome-labelled inhibitors of caspases FLICA. He repeated his experiments on the human lymphoid aggregated culture (HLAC) system, suppressing the maturation and release of pro-IL-1 in uninfected cells using Z-YVAD-FMK (caspase-1 inhibitor), finally preventing its depletion. As a result, apoptosis may not play a significant role in ILTV-infected epithelial

cells; however, the role of other major cell death pathways, such as pyroptosis and necroptosis, in the tracheal epithelial cell death pathogenesis of ILTV in chickens has yet to be investigated.

2.1. Pyroptosis

Programmed cell death is one of the natural ways by which cells die, often known as cell suicide (Raff, 1998). Since dying cells produce pro-inflammatory cytokines in a bursting manner, the name pyroptosis was created from the Greek origin "pyro" (fire or fever) and "ptosis" (falling) (Cookson and Brennan, 2001). Brennan and Cookson (2000) discovered proinflammatory programmed cell death in *Salmonella* Typhimurium infected mouse macrophages and created the name pyroptosis to distinguish it from apoptosis, which is caspase-3 dependent and non-inflammatory cell death. They said extensive DNA fragmentation, intact nucleus shape, fast membrane damage, inflammation, and caspase-1 activation distinguish this cell death process from apoptosis. Apoptotic cells had their poly-ADP ribose polymerase (PARP) cleaved and inactivated, however, *Salmonella* Typhimurium-infected macrophages' PARP remained uncleaved and active. PARP is a cofactor of NF-kB in caspase-11 transcription driven by lipopolysaccharide (LPS) (Yoo *et al.*, 2011). Inflammatory caspases regulate the pyroptosis pathway, followed by the creation of holes in the plasma membrane that release immunomodulatory cellular contents, resulting in positive propidium iodide (PI) and 7-aminoactinomycin (7-AAD) tests. The inner side of the plasma membrane is exposed during cell lysis, resulting in positive Annexin V staining. However, Annexin-V is unable to differentiate between apoptotic and pyroptotic cells, because the PS is exposed on the extracellular surface owing to the flippase enzyme, providing a positive Annexin-V. Unlike necrotic cell death, apoptotic cells break and inactivate the poly ADP ribose polymerase (PARP) enzyme to preserve ATP supply, however, the pyroptosis mechanism is unaffected in PARP knockdown macrophages, demonstrating that PARP activity is not necessary for pyroptosis (Jorgensen and Miao, 2015). In pyroptotic cells, the inhibitor of caspase activated DNase (ICAD) is attached to CAD, indicating that ICAD DNA proteolysis is not part of the pyroptosis process (Fink and Cookson, 2006).

2.1.1. Molecular mechanism of pyroptosis

Pyroptosis is a kind of programmed death that is mediated by proinflammatory caspases-1/4/5 (in humans) (Jorgensen and Miao, 2015), and Caspase-11 (in mice) (Stowe *et al.,* 2015). It not only aids in antimicrobial infection, however, it is also linked to non-pathogenic infection. The discovery of novel targets for disease therapy will be aided by understanding the molecular process of pyroptosis. Pyroptosis is carried out by members of the gasdermin family (Shi *et al*., 2017). This will be triggered by the activation of an inflammasome induced caspase-1 cleavage of gasdermin D (GSDMD); caspase-11/4/5 or caspase-8 cleavage of GSDMD; caspase-3 cleavage of GSDME; or granzyme -A mediated cleavage of GSDME (He *et al.,* 2015; Zhou *et al.,* 2020).The membrane pore-forming activity of the gasdermin-N domain of GSDMD is responsible for pyroptosis execution, which executes the necrotic function of pyroptosis, suggesting a new definition of pyroptosis as gasdermin-mediated programmed necrosis (Shi *et al.,* 2016). Dr Jurg Tschopp's group came up with the term "inflammasome" when they discovered the NALP1-Pycardcaspase-1 complex responsible for IL-1β production (Martinon *et al.,* 2002). Pattern recognition receptors (PRRs) such as toll like receptors (TLRs), C-type lectin receptors (CLRs), retinoic acid inducible gene (RIG) like receptors (RLRs), and nod like receptors (NLRs) recognise pathogen associated molecular patterns (PAMPS)/ damage associated molecular patterns (DAMPS) and trigger the formation of inflammasomes (Takeuchi and Akira, 2010). Similarly, molecules including Nigericin, Val-boroPro and L-allo-Ileisoindoline can cause pyroptosis by activating procaspase-1 through a mechanism that is currently unclear (Okondo *et al.,* 2017).

2.1.2. The canonical inflammasomes

Inflammasome activation is critical in the immunological response to viral infection and is a potential target for drug- or vaccine-based therapies to reduce excessive inflammasome activation and immunopathology or to regulate viral replication (Shrivastava *et al*., 2016). Inflammasomes are multi-protein signalling complexes that form when cellular disturbances or intracellular microbial ligands are detected (Jorgensen and Miao, 2015). Caspase-1 (canonical), caspase-1 inflammasome independent (non-canonical), and alternate pathways are all used to activate the inflammasome (Man *et al.,* 2015). A sensor protein, apoptosis-associated speck-

like protein (ASC), a pro-caspase-1 recruiter, and caspase-1 make up the canonical inflammasome. NLRP1 inflammasome, NLRC4 inflammasome, NLRP3 inflammasome, AIM2 inflammasome, IFI16 inflammasome, and Pyrin inflammasome are examples of these inflammasomes (Lamkanfi and Dixit, 2014). PYD domain, NACHT domain, and Leucine Rich Repeats (LRRs) are shared by all NLRs (excluding NLRC4, which has a CARD domain instead of a PYD domain) (Platnich and Muruve, 2019). Inflammasomes with the CARD domain (NLRC4, NLRP1, NLRP1a, NLRP1b) can signal with or without caspase-1 recruitment and processing (Broz *et al.*, 2010). The PYD domain binds to the PYD domain on ASC (the adaptor molecule) also known as the caspase-1 recruiter. To complete the inflammasome structure, this ASC molecule creates a CARD-CARD interaction with caspase-1 (Martinon and Tschopp, 2007). PYD domains are found in some non-NLR proteins (AIM2) that can form inflammasomes and signal via ASC and caspase-1 processing (Fernandes-Alnemri *et al.,* 2009).

NLRP3 is the most researched and well-characterized inflammasome. NLRP3 mainly contains the NACTH, pyrin, and leucine-rich repeat (LRR) domains. When activated, NLRP3 oligomerizes via homotypic interactions with NIMA-related kinase 7 (NEK7) and then recruits apoptosis-associated speck-like protein containing a CARD (ASC) and procaspase 1 to form an inflammasome, which results in procaspase 1 cleavage and subsequent maturation of pro-inflammatory cytokines IL-1 β and IL-18 (Chen *et al.,* 2018). Mature IL-1 and IL-18 are released from the cell through the transmembrane complex formed by gasdermin D (GSDMD). In sterile inflammation or microbial infection, the NLRP3 inflammasome signalling pathway is triggered by Signal 1 and Signal 2, or the so-called canonical and non-canonical pathways, except that when a microbial infection occurs, the reaction is considerably faster and stronger. Shrivastava *et al.* (2016) referenced that the activation of the NLRP3 inflammasome is related to three major processes. Firstly, NLRP3 activators such as alum, silica, nigericin, and asbestos stimulate the production of reactive oxygen species (ROS) by nicotinamide adenine dinucleotide phosphate (NADPH) oxidase, which stimulates the efflux of potassium ions (K+) leading to NLRP3 inflammasome activation. The second mechanism is the 'lysosomal rupture model,' in which NLRP3 activators (silica, asbestos, etc.) create aggregates that are phagocytosed and cause lysosome rupture, resulting in the release of

cathepsin B, which further activates NLRP3. Finally, the 'ion channel model' proposes that a high concentration of extracellular ATP can stimulate the development of cell membrane pannexin-1 holes and K+ efflux via the P2X7 ATP-gated ion channel, hence facilitating the entry of PAMPs and DAMPs, which are critical for NLRP3 activation. Rossol *et al.* (2012) mentioned the role of calcium in NLRP3 inflammasome activation in their two different studies. Microbial antigens, such as the bacterial wall component LPS, frequently trigger both signals at the same time. In addition, the canonical and non-canonical NLRP3 inflammasome activation serves as a feedback loop to further activate the NLRP3 inflammasome under chronic disease conditions (Chen *et al.,* 2020).

2.1.3. Caspase-1- dependent classical pyroptosis pathway

Monocytes, macrophages, dendritic cells, and epithelial cells have all been reported to be affected. Canonical pyroptosis is triggered by a variety of microbial structures, including bacterial flagellin, double-stranded DNA, anthrax deadly toxin, and bacterium modified host Rho GTPases (Lamkanfi and Dixit, 2014; Broz and Dixit, 2016). Intracellular PRR gets signal stimulation in the conventional pyroptosis pathway, which is followed by inflammatory body construction, development of intracellular macromolecular protein complex, and the production of inflammatory corpuscles, which activates caspase-1 precursor (Gong *et al*., 2020). Canonical pathway of inflammasome activation takes place only via the activation of caspase-1 by inflammasomes.CARD-CARD domain interaction converts procaspase-1 to caspase-1 in these inflammasomes with their caspase activation and recruitment domain (CARD) (Martinon and Tschopp, 2007). Finally, these activated caspases then i) convert proinflammatory cytokines (IL-1â and IL-18) to their active form (Man *et al.,* 2015) and ii) split Gasdermin D molecules into GSDMD-C (p20) and GSDMD-N (p30) polymers in the plasma membrane to create a 1.1-1.24 nm pore (Fink and Cookson, 2006). The full execution of pyroptosis occurs when a pore forms, causing the release of activated cytokines (Man and Kanneganti, 2015). Although this pathway normally activates caspase-1, In the absence of ASC, the NAIP-NLRC4 and Nlrp1b scaffolds may activate pro-caspase-1 without inflammasome complex formation or autoproteolysis (Guey *et al.,* 2014; Van Opdenbosch *et al.,* 2014)

2.1.4. Caspase-11/-4/-5-dependent non-classical pyroptosis pathway

Caspase-4/-5 in humans and Caspase-11 in mice are homologous proteins with similar characteristics (Shi *et al.*, 2014). The activation of human derived caspase 4/5 and murine derived caspase-11 is a non-canonical mechanism for inflammasome activation. It acts by attaching directly to Lipopolysaccharides of Gram-negative bacteria (Aachoui *et al.*, 2013) then operating on GSDMD to release the active N-terminal domain; it also, opens membrane channel P2 × 7 by activating the pannexin-1 channel, which releases ATP (Gong *et al*., 2020); also aids K+ efflux rather than directly triggering proinflammatory cytokines causing NLRP3 inflammasome activation of the canonical pathway (Ruhl and Broz, 2015).

2.1.5. Other pathways of pyroptosis:

Recent studies say that pyroptosis can be activated through apoptotic caspases. Sarhan *et al.* (2018) found that apoptotic caspase that can trigger pyroptosis is caspase-8, which can induce the cleavage of GSDMD to elicit pyroptosis during Yersinia infection. Recently, studies have demonstrated that caspase-3 cleaves GSDME after Asp270 to produce a necrotic GSDME-N fragment that targets the plasma membrane, thereby inducing pyroptosis (Kayagaki *et al.,* 2015; Schmid-Burgk *et al.,* 2015). Granzyme-A/B-dependent pyroptosis pathway, Granzyme-mediated cell death was previously generally presumed to be apoptosis. Feng Shao et al. (2020) first found that cytotoxic lymphocytes mediate the death of GSDMB-expressing cells by inducing pyroptosis. Further mechanistic studies showed that lymphocyte-derived granzyme-A cleaved GSDMB at Lys within the interdomain linker and released the N-terminal fragment to induce cell pyroptosis. Furthermore, interferon derived from activated cytotoxic lymphocytes increases the expression of the GSDMB transcript, which further contributes to GZMA- and GSDMB-mediated pyroptotic cell death (Zhou *et al.,* 2020). Judy Lieberman et al. (2020), in the same year showed that granzyme B derived from cytotoxic lymphocytes directly cleaved GSDME after D270 to trigger caspase-independent pyroptosis in GSMDE-positive cells (Zhang *et al.,* 2020). Thus, these two studies altered our view by showing that granzyme not only induces cell apoptosis but also induces caspase-independent pyroptosis in GSDME- or GSDMB-positive cells.

2.1.6. Pyroptosis in viral infections

The role of inflammasome activation and GSDMD in viral infection is not well studied. Viruses activate Toll-like receptors that sense viral nucleic acids on the cell surface or in endosomes to prime expression of innate immune genes. NLRP3 inflammasomes are activated by DNA and RNA viruses (Lupfer *et al.,* 2015), which disturb cellular homeostasis and contribute to the classic route of inflammasome activation.Influenza, measles, RSVD, Newcastle disease, vesicular stomatitis, rabies, polio, hepatitis C, dengue, West Nile fever, varicella zoster, and myxoma virus are known to activate NLRP3, thus contributing to viral pathogenesis (Kuriakose and Kanneganti, 2019). According to Sanders *et al.* (2011), influenza A virus (IAV) causes inflammatory responses by killing respiratory epithelial cells, and the proinflammatory response from respiratory epithelial cells triggers the migration of macrophages and neutrophils, resulting in excessive inflammation. However, the cell death pathway has not been outlined. Recently Lee *et al.* (2018) have demonstrated that influenza A virus (IAV) causes cell death in bronchial epithelial cells by both apoptosis and pyroptosis and that pyroptosis causes inflammasome formation and IL-1β release by infected epithelial cells. The AIM2 inflammasome is known to be activated by HSV-1, MCMV, and vaccinia virus (Rathinam *et al.,* 2010). Furthermore, HSV-1 promotes and then inhibits the generation of the IFI16 and NLRP3 inflammasomes. The replication features of ILTV in the respiratory and conjunctival mucosae were studied by Reddy *et al.* (2014), who detected apoptosis in bystander cells but not in ILTV-infected epithelial cells.Inhibition of caspase-1 or gasdermin-D in the Naip5/ NLRC4/ASC inflammasome allows caspase-8 activation, according to Danielle *et al.* (2017). As caspase-8 is key apoptosis initiating caspase, its activation triggers the intrinsic apoptosis pathway. In addition to the infections indicated above, caspase-1-mediated pyroptosis causes the death of uninfected quiescent CD4+ T cells, resulting in immunosuppression (Doitsh *et al.,* 2014). Brazilian researchers have discovered a surge in serum IL-1β in COVID-19 patients, indicating either canonical or non-canonical pyroptosis mechanisms. Furthermore, they contribute to the fact that 30% of COVID-19 patients died as a result of a cytokine storm and sepsis event, which they believe is caused by pyroptosis in lymphocytes (Duran and Favaro, 2020). Recently, de Vasconcelos *et al.* (2018) studied pyroptosis dynamics in single cells and discovered that gasdermin D (GSDMD)-mediated intracellular processes occur prior to plasma

membrane rupture in macrophages. Viruses have evolved mechanisms and channels to prevent pyroptosis, which the virus perceives as a danger. Many documented examples exist where the virus can i) evade sensory detection by the PRRS, ii) suppress the development of inflammasomes, or iii) inhibit the activation of proinflammatory cytokines. These operations are carried out by particular viral modulators (Stewart and Cookson, 2016).

Pyroptosis-mediated cell death aids in the destruction of intracellular pathogens such as viruses, it also triggers the release of proinflammatory cytokines, which activate antiviral defences. According to Kuriakose and Kanneganti (2019), the precise benefit contribution to antiviral systems is obscured since these two processes, cell death and cytokine-mediated response, coincide**.** Deciphering the function of pyroptosis in viral inflammation would assist in strategically constructing ways of reducing tissue damage owing to increased inflammation since new pyroptotic inhibitors are being found and tested for therapeutic application in a variety of disorders (Lei *et al.,* 2017; Rathkey *et al.,* 2018).

2.1.7. Pyroptosis inhibitors

Many studies have focused on inhibiting pyroptosis to treat inflammatory diseases by targeting NLRP3, caspase-1, or GSDMD. Necrosulfonamide was originally identified as a cysteine reactive drug that targeted MLKL to inhibit necroptosis (Sun *et al.* 2012) and might also inhibit multiple steps of the pyroptotic pathway (Rathkey *et al.,* 2018). LDC7559 inhibited NET formation, presumably by binding and suppressing GSDMD pore formation (Sollberger *et al.,* 2018). In human and mouse cells, Hu *et al.* (2018) found that the drugs disulfiram (1,1',1",1"'- [disulfanediylbis (carbonothioylnitrilo)] tetraethane, the substance that is used to treat alcoholism and Bay 11-7082 ((E)-3-(4-Methylphenylsulfonyl)-2-propenenitrile), an NF-êB inhibitor inhibited gasdermin D (GSDMD) pore formation and blocked proinflammatory IL-1â release. In addition, disulfiram has been shown to decrease IL-1â production in mice when given at a therapeutically acceptable dosage. Both of these chemicals covalently change a conserved Cys in gasdermin D, which is required for pore formation (Liu *et al.,* 2016; Ruan *et al.,* 2018). Disulfiram also inhibited TLR-induced priming at higher concentrations, and both disulfiram and Bay 11-7082 attenuated ASC speck formation and the protease activities of caspases 1 and 11 (Chauhan *et al.,* 2022). Bay 11-7082 selectively inhibits the NLRP3

inflammasome pathway according to the studies conducted by (Juliana *et al.*, 2010) in NG5 cell lines. Deng *et al.,* (2020) found that disulfiram (DSF) could inhibit NLRP3, therefore inhibiting the release of IL-1β and the occurrence of cell pyroptosis in mouse J774 A.1 and human THP-1 macrophage cell lines. As a result, these chemicals might be appealing therapeutics for preventing pyroptotic cell death and reducing inflammation.

Table 1. Different types of inhibitors and their mechanism of action

Type of Inhibitors	MOA	Reference	
NLRP3 inhibitors	Bay-11-7082, Parthenolide, BOT-4-one, MNS, OLT1177, JC-171 etc	Inhibits ATPase activity Binding site is unknown	Coll *et al.* (2022)
GSDMD inhibitors	Necrosulfonamide, Dimethyl fumarate, Disulfiram	Either binds, succinates C191, Modifies the blocking of GSDMD oligomerization	Coll *et al.* (2022)
Caspase-1 inhibitors	CrmA, p35 family,Z-YVAD-FMK,VX 765	Exact mechanism unknown	Dhani *et al.* (2021)

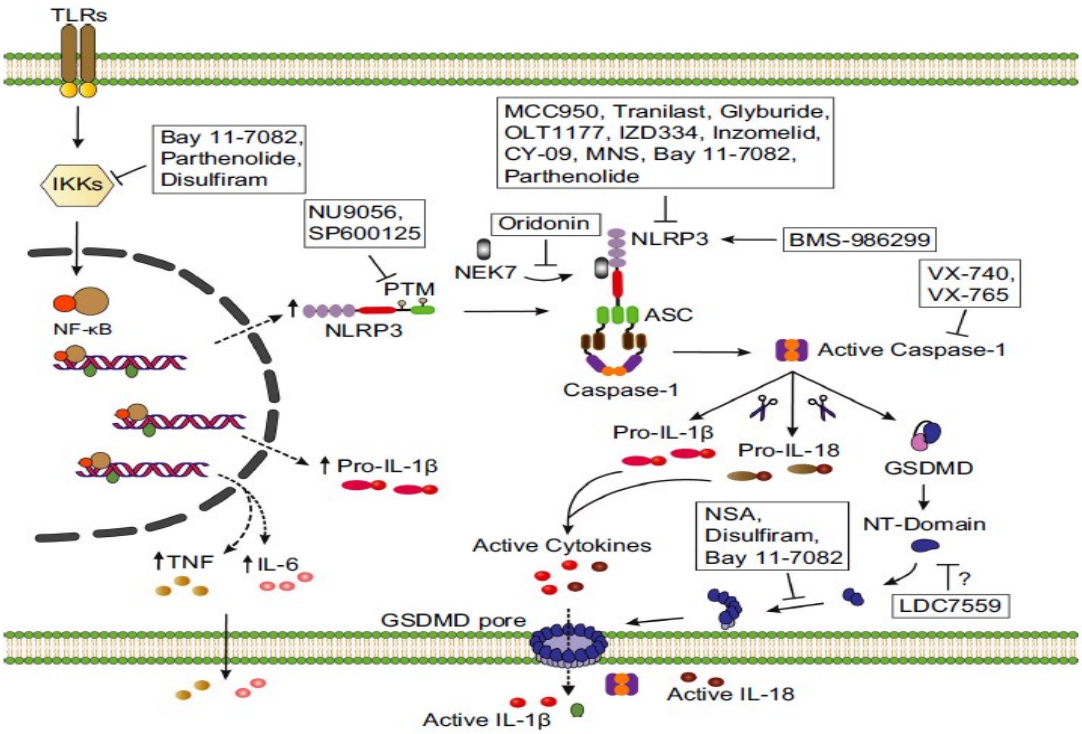

Fig. 1. Schematic image of pharmacological targeting of inflammasomes.

2.1.8. The importance of pyroptosis in chicken infections and its hypotheses

Pyroptosis is verified in humans, and it is also found to have a part in the aetiology of numerous avian illnesses, as previously indicated**.** A comprehensive analysis of the pathophysiology of avian Influenza revealed that highly produced caspase-1 colocalized with influenza A nucleoprotein, implying an association, which was further substantiated by the high production of IL-1β by lung alveolar cells (Solberg *et al.,* 2019). Interestingly, pyroptosis in ducks was linked to the pathophysiology of molybdenum-induced renal tubular injury, and additional treatment with a caspase-1 inhibitor decreased the pyroptosis cell death. Elevated mRNA expression levels and protein levels of pyroptosis-related factors were the bits of information.

The first study of caspase-1-mediated cell death was published in chickens infected with the novel Avian leukosis virus-subgroup J, where they were able to demonstrate changes in the expression of NLRP3, caspase-1, IL-1, and IL-18, and then used immunohistochemical methods to identify the caspase-1 enzyme in artificially infected chicken livers. On 5 dpi, the expression of NLRP3, caspase-1, IL-1β, and IL-18 increased, peaked at 7 dpi, and then declined after 9 dpi, according to their observations (Liu *et al.,* 2016). Liao *et al.,* (2019) infected primary chicken hepatocytes with varying concentrations of copper sulphate ($CuSO_4$) to see if pyroptotic markers (NLRP3, caspase-1, IL-1, IL-18) mRNA expression increased. Copper promotes pyroptosis *in vitro*, as evidenced by the presence of proinflammatory cytokines (IL-1β, IL-18) in the supernatant and subsequent downregulation of expression of the same markers with the addition of a caspase inhibitor (Z-YVAD-FMK). Many analysts claim that cytokines like 1L-β and IL-18 have a role in avian illnesses like Newcastle disease and avian influenza by causing severe inflammatory lesions. Birds infected with NDV produced IL-1β mRNA in their gut tissue. Following that, the source of IL-1β was discovered to be caspase-1-mediated pyroptosis and other discoveries, such as the detection of caspase-1 activity in DF1 chicken fibroblast cells infected with the virulent GM NDV strain, backed up the findings (Gao *et al.,* 2020).

In comparison to TOCs infected with deleted glycoprotein G virus (ΔgG-ILTV), Coppo *et al.* (2018) found a total loss of epithelial mucosa in tracheal organs cultures infected with

revived glycoprotein G virus (ΔgGREV-ILTV). The trachea was thickened by inflammatory cells in addition to the entire loss of mucosa, indicating that gG has chemokine binding properties. It may be determined that the proinflammatory activity of infiltrating inflammatory cells may be the cause of severe pathological abnormalities in the trachea. Gobel *et al*. (2003) identified the involvement of IL-18 cytokine in chickens. They believe that IL-18 is responsible for T-cell proliferation and upregulation of MHC-II antigens. When the micro RNAs (iltv-miR-I5 and I6) flanking the gene ICP4 in the IRs and TRs flanking the gene ICP4 were discovered in 2011, apoptosis evading by the ILTV virus was speculated. The particular route that causes a Th-1 type response, in response to ILTV infection is yet unknown, and there is a scarcity of research on the subject. The mechanism by which these cytokines are produced and how they contribute to the pathophysiology of ILT is uncertain.

2.2. Aetiology

The infectious laryngotracheitis virus belongs to the *Herpesviridae* family, *Alphaherpesvirinae* subfamily, and genus *Iltovirus*, with linear 150-155kb of double-stranded DNA and 48.16 per cent G+C content (Lee *et al.*, 2011). The ILTV genome comprises 148665 base pairs and two distinct sequences: one long (UL), one short (US), and two inverted repeats (internal and terminal) flanking the US portions (Thureen and Keeler, 2006). The nucleic acid is contained within a 100 μm diameter icosahedral capsid, which is encoded by a proteinaceous tegument layer and a 200-300 μm outer glycoprotein layer (Granzow *et al.,* 2001). At least 80 open reading frames (ORFs) code for the entire length of the ILTV genome, in terms of position and structure of the deduced translation products, 63 ORFs show similarities to the Herpes Simplex Virus-1 (HSV-1) genome and the highly conserved glycoproteins are critical for replication and eliciting an immune response in the target host (Piccirillo *et al.,* 2016). Glycoproteins gB, gC, gD, gE, gG, gH, gI, gJ, gK, gL, and gM are encoded by ORFs UL27, UL44, US6, US8, US4, UL22, US7, US5, UL53, UL1, and UL10, respectively, are present on the envelope and preserved, according to the author. ILTV propagation and elicitation of humoral and cell-mediated immune responses in the host are dependent on viral glycoproteins (Roizman and Pellett 2001). UL2 (uracil-DNA glycosylase), UL3 (non-essential phosphoprotein), UL3.5 (not in HSV-1 and -2), UL4 (replication essential protein), and UL5 (makes helicase with US52 and UL8 gene products) have great homologies to HSV-1 and -

2, EHV-1, BHV-1, PRV, and MDV (Fuchs and Mettenleiter, 1996).In 1999, by the same team, other sites such asUL6(DNA cleavage and packaging), UL8 (helicase complex component), UL9 (origin binding protein), UL11 (myristylated membrane protein), UL12 (alkaline nuclease), UL15, UL17 (DNA cleavage and packaging), UL18 (capsid protein), UL19 (major capsid protein) and UL20 (intrinsic membrane protein) were found to share homologies with HSV-1(á), VZV(á), EHV-1(á), EBV(ã) and HCMV(â) and also stated that in comparison to other herpesviruses, UL10(gM) lacks an N-glycosylation site.Despite the similarities, two clusters of genes, one found between UL45 and UL22 coding for ORF A-E and the other between UL-1 and ICP4, absence of UL16 homolog distinguish *Itlovirus*.While studying the gene organisation of the UL region, Zeimann *et al.* (1998) noticed an internal inversion and localisation of UL47 in the US area.UL0 and UL (-1), two ILTV unique genes, have been duplicated (Thureen and Keeler, 2006). Nadimpalli *et al.,* (2017) mentioned that the UL (-1) gene is crucial for ILTV replication.The ILTV genome, like that of other *Alphaherpesviruses*, has three replication origins: an OriL in the UL region, two copies of OriS in the I internal repeats and Terminal repeats areas, (Lee *et al.,* 2011).

2.3. History

The history of infectious tracheitis in chicken's dates back to the mid -1920s in the United States, as a coinfection with the poultry pox virus was first observed in 1926 (Beach, 1926). It was also known as tracheolaryngitis (May and Tittsler, 1925), infectious bronchitis (Beach, 1926), and infected tracheitis (Beach, 1926) before the American Veterinary Medical Association (AVMA) approved the term infectious laryngotracheitis (ILT) in 1931. Cover, (1996) analysed the first reports of ILT in Canada (1925), Australia (1935), the United Kingdom (1935), Sweden (1940), Poland (1948), Germany (1959), India (1964), and Finland (1965), as well as a demonstration by Beaudette in 1930. Cruickshank *et al.* (1963) established the virus's initial dimensions, Brandly (1935) successfully reproduced the virus artificially on chorioallantoic membrane (CAM), and Gibbs (1934) contributed significantly to the early development of ILT vaccination.

2.4. Epidemiology

May and Thittsler (1925) were the first to report the disease in the United States, followed by Australia, the United Kingdom, and Europe (Cover 1996) then throughout the world. A field epidemic occurred in layer farms in Namakkal District, Tamilnadu, in 2012, according to current reports on ILT outbreaks in India (Srinivasan *et al.,* 2012) after those cases of ILT have recently been documented in India's major poultry belts, with severe respiratory distress, different degrees of conjunctivitis, and death rates of up to 80% (Gowthaman *et al.,* 2020). Increased ILT outbreaks have been attributed to the tendency toward shorter production cycles, high flock density, rearing multi-age and multifunctional chicken within the same geographical region, and inappropriate vaccination and biosecurity breaches (Garcia *et al.*, 2013; Blakey *et al.,* 2019). Chickens of all ages are the primary hosts, while spontaneous infection has been observed in peafowl, pheasants (Crawshaw and Boycott, 1982), turkeys (Portz *et al.,* 2008), and ducks (Yamada *et al.,* 1980). The key predisposing variables for the fast spread of the virus include a confined raising environment and overlapping litter rotation cycles. The virus is disseminated directly from infected/vaccinated/ latent virus bearing birds by respiratory exudates, faeces (Roy *et al.,* 2015), and feather follicles (Davidson *et al.,* 2016), as well as indirectly through contaminated cages, litter, equipment, labours, dust, and infected carcasses. Biofilm in stagnant water (Ou *et al.,* 2011), mealworms, and darkling beetles are other unnatural sources of viruses (Ou *et al.,* 2012). Gowthaman *et al.,* (2014) found that layer birds > 6 weeks old and broilers > 2 weeks old were more sensitive. The authors recently conducted an airborne sampling of ILTV testing utilising an SKC Biosampler® and an alkaline PEG solution-filled collecting tank and discovered that the samples were variably positive but the virus' viability was not proven (Brown *et al.,* 2020). The epizootics are characterized by 80-90%morbidity and 10-80 %mortality (Seddon and Hart, 1935). According to the findings, non-vaccinated flocks have a significant seroprevalence of ILTV (72 %), suggesting that backyard fowl play a role in the disease's epidemiology (Hernandez-Divers *et al.,* 2008). Chicken embryo origin (CEO) strains are said to produce more severe respiratory illness than Tissue culture origin (TCO) strains, hence the death rate in outbreaks caused by CEO revertant strains is greater than in outbreaks occurring by TCO revertant strains (Garcia, 2017). CEO vaccine-like virus and Recombinant ILT virus have recently been linked to outbreaks in Egypt (Bayoumi *et al.,* 2020).

2.5. Virus pathogenesis & replication

When chickens are naturally infected with ILTV, the virus infects the mucosa of the nasal, conjunctival, and harderian glands initially, rather than the lower respiratory tract, and plays a key role in the clinical development of the disease (Beltran *et al.,* 2017). The virus has been found in the trachea, lung, cecum, kidney, pancreas, thymus, and oesophagus in addition to the upper respiratory tract (Wang *et al.,* 2013), however, no viraemia has been recorded (Chang *et al.,* 1977). The virus may be found in the ganglion of the trigeminal nerve as early as 2 days after infection (Oldoni *et al.,* 2009), and it can be reactivated when stressed (Bagust, 1986). William *et al.* (1992) investigated several latency locations and discovered that ILTV may be identified in the ganglion of the trigeminal nerve on 31, 45, and 63 days after infection with occasional viral shedding. Following that, latency-associated transcripts inside infected-cell polypeptide 4 (ICP4) were discovered, along with two microRNAs (miRNAs) that directly cleave ICP4 to maintain the balance of lytic and latent infection (Waidner *et al.,* 2011). Infected immune cells, notable macrophages, have been blamed for the systemic dissemination of ILTV to multiple organs (Calnek *et al.,* 1986).

Like other alphaviruses, ILTV replicates in a lytic cycle. The gene gC facilitates viral entry without interacting with heparan sulphate, allowing virus fusion inside cells (Kingsley and Keeler, 1999). DNA duplication and packaging of virus particles occur in the nucleus, resulting in basophilic intranuclear inclusion bodies 12 hours in early after infection (Reynolds *et al.,* 1968). Mahmoudain *et al.* (2012) were the first to classify genes into Immediate Early (IE), Early (E) and Late (L) genes. Immediate Early (IE) genes are transcribed within 1hour of infection, whereas Early (E) genes (β1 and β2) are transcribed in 4-16 hours (Prideaux *et al.,* 1992), and late(L) genes (γ1 and γ2) are transcribed in 16-32 hours, and in the cytoplasm, the corresponding proteins are translated (Gowthaman *et al.,* 2020). They also show that the ICP4 gene is the only IE gene. It was also shown that glucose and glutamine are necessary for the transcription of viral immediate early and early genes, respectively, even though it stimulates their metabolism, indicating that it keeps a balance between infection and host cell death (Qiao *et al.,* 2020). In this rolling process of DNA, replication concatemers are produced, cut, and packed into separate nucleocapsids. The envelope is derived from the nuclear membrane's

inner lamellae. The endoplasmic reticulum provides the second envelope, following which the virions aggregate in the cytoplasm. When it reaches the cytoplasm, tegument proteins are carried to the trans-Golgi, where they are re-enveloped during the second phase of budding. Exocytosis or cell burst are used to develop and release them (Granzow *et al.,* 2001). The Src gene has recently been shown to regulate ILTV invasion in a cellular fattyacids metabolism-dependent way, as well as ILTV CPE. Activating host Src not only inhibits viral multiplication but also has a pathogenic consequence (Wang *et al.,* 2019). Animal studies might be used to evaluate ILTV replication features in respiratory and conjunctival lining cells (Kirkpatrick *et al.,* 2006). Conversely, in vitro research is more popular due to ethical concerns over inter-animal variance in vivo animal investigations. Chicken embryo kidney cells (CEK) have been identified as one of the most susceptible cell lines for replicating ILTV and studying its cytopathic effects (CPE). Watrach and Hanson (1963) found CPE as early as 18 hours after infection, seeing alterations such as cell fusion, development of multinucleate, cytoplasmic vacuolations containing inclusion bodies, cell degeneration, and cell detachment. In vitro replication properties and pathogenesis of ILTV have also been studied using tracheal organ cultures from chicken embryos (Reddy *et al.,* 2017).

2.6. Antigenicity

Although many assays like immunofluorescence tests (Jordan and Chubb 1962), viral neutralisation (Devlin *et al*., 2011), and cross-protection studies show that ILTV strains are antigenically identical. Variation in virulence has been seen in chicken embryos and cell culture (Hidalgo *et al.,* 2003). The ILTV envelop glycoproteins appear to be the most powerful immunogenic protein in chickens, inducing both humoral and cell-mediated immune responses (York and Fahey 1990). Glycoprotein G (gG), one of the envelope glycoproteins, has been found to aid viral entrance (Tran *et al.,* 2000), and cell-to-cell dissemination (Nakamichi *et al.,* 2002) as well as being a broad-spectrum viral chemokine binding protein (vCKBP). The gG binds to the C, CC, and CXC subfamilies chemokines, preventing chemokine-receptor interactions. It also prevents chemokines from attaching to glycosaminoglycans, which is necessary for chemokine function in the host. (Bryant *et al.,* 2003). The vCKBP of ILTV (gG) activates innate immune responses by attracting certain populations of immune cells during the early stages of infection. (Devlin *et al.,* 2010).

2.7. Prophylaxis and control

Chicken vaccination is the most used way of controlling ILT in chickens. Live attenuated vaccines of a chicken embryo (CEO) and tissue culture origin (TCO) are available, and they are made by serially passing strains via chicken embryo or primary chicken cell culture (Menendez *et al.,* 2014) and zone vaccination, particularly with the CEO vaccine, has been a successful approach in curtailing large outbreaks of the disease (Dufour-Zavala, 2008). They produce potent antiviral immunity that can persist for up to a year after 15–20 weeks (Neff *et al.,* 2008). Birds can be vaccinated with the first dosage when they are 6-8 weeks old, and a booster dose when they are 12-15 weeks old (Gingerich and Carver, 2006). Live attenuated viruses have a negative reputation for returning to their original virulence and failing to provide lifetime sterile immunity, resulting in huge outbreaks in flocks (Samberg *et al.,* 1971; Rodriguez-Avila *et al.,* 2007). To circumvent the limitations of live attenuated viruses, biotechnological technologies are being employed to genetically remove replication-dependent genes (Pavlova *et al.,* 2013). However, the antigen of these non-replicable viruses is only present at the site of inoculation, they do not stimulate the immune system as much as the CEO and TCO vaccines do. Gergen *et al.* (2019) employed the F gene, gene gD, and gene gI of the ILTV double recombinant HVT vector vaccine to exhibit more than 90% protection against velogenic NDV, ILTV, and Marek's disease. The vectored vaccination confers significant protection, but it is subject to residual replication, latency and transfer to unvaccinated.ILTV gB, gC, gD, gI, gJ, TK, UL0, UL35, and UL47 have been vectored using vectors like HVT, NDV, and FP (Davison *et al.,* 2006; Vagnozzi *et al.,* 2012; Yu *et al.,* 2017).A successful vaccination must have a titre of $>10^2$ plaque-forming units/ml and be administered by routes other than the oral route (Raggi and Lee, 1965).

The goal of the present study is to perform a preliminary study that will serve as a basis for scientific investigations on chicken innate immune responses to ILTV. Most significantly, it will determine whether ILTV triggers the pyroptosis markers (NLRP3, Caspase-1, and GSDMD). Once the involvement of pyroptosis has been established, pyroptotic inhibitors may be used to block the cell death pathway, and the expression of pyroptotic markers can be examined to see if the infected cell's proinflammatory machinery has been turned off. We can

determine how ILTV-infected respiratory epithelial cells die and the molecular mechanism that causes inflammatory lesions while doing so. Additionally, the ability of pyroptotic inhibitors to prevent or diminish inflammation may be assessed.

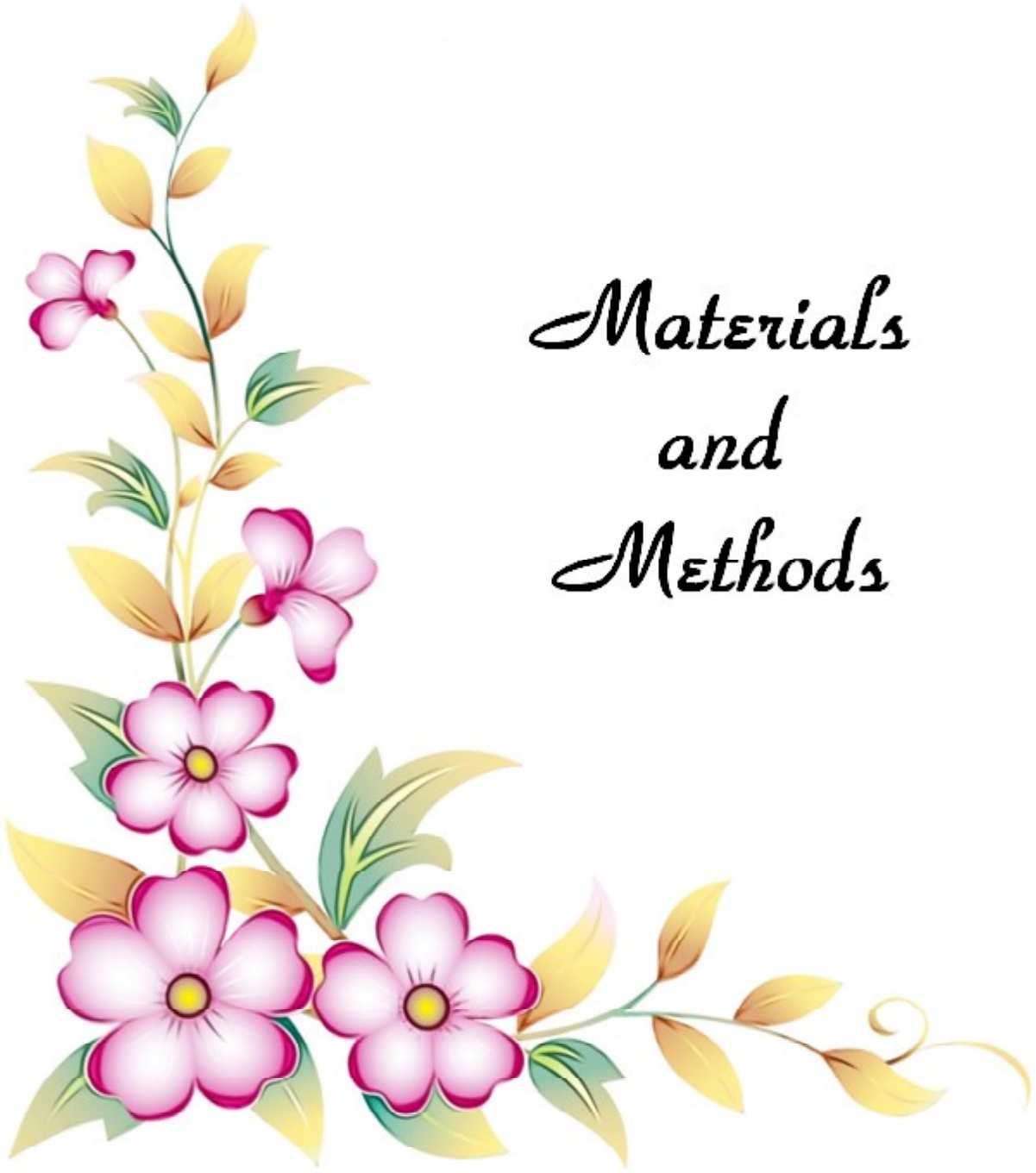

Materials and Methods

3 MATERIALS AND METHODS

3.1 Experimental Materials

3.1.1 Chemicals and Molecular biology reagents

a) Antibiotic Antimycotic Solution 100X liquid (Cat. No. A002, Himedia, India)

b) Bay 11-7082 (Cat. No. 183483, MP Biologicals, U.S.A)

c) Cell culture Grade Phosphate Buffered Saline (PBS) (Cat. No. TL1101-500ml, Himedia, India)

d) Disulfiram (Cat. No. 0218314925, MP Biomedicals, U.S.A)

e) DMEM (Cat. No. AL0064, Himedia, India)

f) DMSO (Cat. No. 276855, Sigma, U.S.A)

g) Foetal bovine serum (Cat. No. 1270-106, Gibco, Dublin, Ireland)

h) LHC-9 medium (Cat. No. 12680013, Gibco, Dublin, Ireland)

i) Lipopolysaccharide (LPS) (Cat. No. L-8274, Sigma-Aldrich, U.S.A)

j) M199 Medium (Cat. No. AL014A, Himedia, India)

k) MTT (Cat. No. 88417, Sigma-Aldrich, U.S.A)

l) Nigericin (Cat. No. 183319, MP Biologicals, U.S.A)

m) TRIZIN (Cat. No. G31C, GCC Biotech, India)

n) Trypan Blue (0.4%) (Cat. No. K940-100ml, Amresco, USA)

o) Trypsin-EDTA (TCL014, Himedia, India)

3.2 Commercial Kits

a) CytoTox96 Non-radioactive cytotoxicity assay kit (Cat. No. G1780, Promega, Madison, WI)

b) R2D 1st strand cDNA synthesis kit (Cat. No. G4641, GCC Biotech, India)

c) LysoTracker® Deep Red -1 mM solution in DMSO (Cat. No. L1242, Invitrogen™, USA)

d) SYBR Green/ ROX qPCR Master Mix (2X) (Cat. No. K0222, Thermo Scientific, Lithuania)

e) SYTOX® Green nucleic acid stain- 5 mM Solution in DMSO (Cat. No. S7020, Invitrogen™, USA)

3.3 Glassware and Plastic Ware

The glasswares used in the present study was from Borosil (India) and Schott Duran (Germany). They were washed thoroughly and sterilized as per the prescribed protocols. The plastic wares used in the present study were procured from Tarsons (India). Disposable syringes used in this study were from Dispovan (India). The plastic wares were either certified to be free from DNase and RNase activity or were DEPC treated and autoclaved to render them nuclease free. T25 flasks, 96 well plates, 6 well plates, (NEST Biotechnology, Wuxi, China), 100µm pore sized cell filter (Cat. No. 352360, Corning, Galendale, Arizona), Nalgene™ Sterile Syringe filters (Thermo Fischer Scientific, China) were used for current study cell culture system.

3.4 Scientific equipments

Standard equipment and instruments available in the Avian Disease Section, Division of Pathology and Central Instrumentation Facility, ICAR-IVRI were utilised for the requisite purpose. Specifications of the instrument/equipment were given at appropriate places in the text wherever necessary. The major equipments used in the study are of national and international brands. They are listed below:

- BioRAD CFX96 Touch real-time PCR machine
- CO_2 Incubator (Eppendorf, Germany)
- ELISA plate reader (Thermo Scientific, Germany)
- Gel electrophoresis systems (GeNei, India)
- Inverted microscope (Olympus, Japan)

- Laminar airflow (Alpha linear, India)
- Microcentrifuge (Thermo, Germany)
- Microwave oven (Samsung, Korea)
- PCR Systems: Master Cycler (Applied Biosystems, USA)
- Refrigerated Centrifuge (Thermo Scientific, Germany)
- Spectrophotometer (Multiscan Sky, Thermo Fisher Scientific, USA) at A260/280
- Ultra-low temperature freezer (-80°C) (New Brunswick Scientific, USA)
- UV transilluminator in a MultiImage™ Light Cabinet (Alpha Innotech Corporation, USA)
- Variable volumes of Finnpipette (ThermoScientific, USA)
- Vortex mixer (spinix, USA)

3.5 Buffers, media and reagents

Double distilled water was used for the preparation of all aqueous solutions and autoclaved at 121°C for 15 minutes. Common reagents like PBS (pH 7.2) were prepared as per standard procedures.

3.6 Oligonucleotide Primers

The details of the primers used and other relevant details in the current study are mentioned at required places. All the primers with desired sequences were procured from Eurofins Genomics India Pvt. Ltd (Bangalore). Aliquots of the working solution were prepared in nuclease free water (Fermentas, EU) to achieve a concentration of 10 pmol/µl.

3.7 Virus

For the current study, a freeze-dried ILT virus procured from the Avian Disease Section, Division of Pathology repository, IVRI was passaged via CAM route of embryonated chicken eggs was used for the further experiments

3.8 *In-vitro* culture of chicken epithelial cells

3.8.1 Preparation of tracheal epithelial cell (TEC) culture

Avian tracheal epithelium cell culture was prepared according to Zaffuto *et al.* (2008).

1) 18-days old chicken embryos were used for the isolation of avian tracheal epithelial cells. The surface of the eggs was cleaned with 70% ethanol before dissecting them.
2) A circular hole at the broad end of the egg was created with a sterile scissor, after removing the shell of the eggs, the underlying membrane was removed using another sterile forceps.
3) With the help of sterile toothed forceps, the chicken embryo was removed by holding the neck. The yolk sac was cut with a sterile scissor, and then the embryo was placed in a sterile petridish.
4) The chicken embryo was decapitated from the neck, by making an incision with sterile scissors and making sure that the anterior portion of the neck is still intact.
5) The anterior portion of the neck was exposed by making an incision on the commissure of the beak and skin, and all the way towards the carina.
6) The trachea was teased out with small sterile forceps by removing the fascia and fat surrounding it. An incision at the caudal and cranial part of the trachea was taken to remove it.
7) The trachea was placed and rinsed in a clean petri dish with 0.1% DL-dithiothreitol (DTT), and subsequently in plain DMEM in another Petri dish. Ten more tracheas were isolated in a similar manner.
8) These tracheas were transferred to a beaker containing 10ml of dissociation solution (DS) for 2 hrs in a 5% CO_2 incubator.
9) After incubation, 3ml of FBS was added to it to stop the dissociation reaction, rigorously pipetted, and finally the solution was filtered using a 100 μm pore sized cell filter.
10) The solution mixture was transferred to a sterile 50ml conical tube to which 10 ml of DMEM was added and centrifuged at 200xg for 10 mins.
11) The supernatant was discarded and the cell pellet was resuspended in 2.5 ml of each LHC-9 medium and DMEM.
12) The cells were then transferred to a sterile T25 flask and incubated in a 5% CO_2 incubator. The attachment of epithelial cells was monitored after 24 hrs.
13) The cells were maintained by changing the media after 5 days. Subsequently, a haemocytometer was used for cell counting.

14) The epithelial cells were distributed on respective flasks/plates and used for further experiments and were monitored for attachment every following day.

3.8.2 Preparation of chicken embryo kidney cell (CEKC) culture:

Chicken embryo kidney cell culture was prepared using a modified protocol by Chomiak *et al.* (1960) and was used as an alternative primary cell culture.

1) Two 20-days old embryonated chicken eggs were taken and cleaned with methylated spirit.
2) With sterile scissors, a circular hole was cut at the broad end of the egg. The eggshell was removed and the underlying membrane was pulled out with sterile small forceps.
3) The chicken embryo was located and with the help of sterile forceps, it was placed on a sterile petridish. The yolk sac and the amnion were cut with sterile scissors and discarded along with the egg.
4) The chicken embryo was decapitated by taking a cut at the neck and removing the head. Then the embryo was placed on the rostral recumbency and an incision was taken at the midline of the synsacral region.
5) The body cavity was exposed to locate the kidney lobules at the wall of the synsacrum and gently the kidney lobules were transferred to a clean Petri dish having DMEM.
6) The kidneys were teased out and transferred to a clean beaker containing 5 ml of 0.25% trypsin-EDTA The tissue was incubated in trypsin for 10 mins with a magnetic stirrer.
7) The solution was then filtered through a 100 µm pore-sized cell filter into an ice jacketed 50 ml conical tube, to which 2.5 ml of FBS was added to stop the trypsinization reaction.
8) Growth medium with 10% FBS was added to the 20 ml mark in the conical tube and centrifuged at 200 x g to get a cell pellet.
9) The cell pellet was resuspended in 5 ml of growth medium and then transferred to a T25 flask and incubated in a 5% CO_2 incubator. The attachment of epithelial cells was monitored after 24hrs.

10) The cells were maintained by changing the media to 1% maintenance media after 3 days. Subsequently, a haemocytometer was used for cell counting.

11) The epithelial cells were seeded on respective cell culture plates/flasks and used for further experiments.

3.9. Determination of appropriate doses for pyroptotic induction and inhibition

3.9.1a Pyroptotic induction : Induction of pyroptosis in CEKC culture was carried out in two steps, as per the protocol described by den Hartigh and Fink (2018) with slight modifications. Priming by lipopolysaccharide (LPS) and activation via both LPS as well as nigericin were done. The determined standard dose was used for the entire study.

3.9.1b Standardization of pyroptotic induction dose for LPS 96 well plates with 2×10^4 cells per well were subjected to five different doses of LPS at three different time intervals (6hpi, 12hpi, and 24hpi) as depicted in **Table 2**. The cytotoxicity assessment was done using a commercial Cytox 96 assay kit.

Table 2. Treatment with LPS and nigericin in 96 well plates

LPS doses (µg/ml)	For Priming (3hrs) volumes taken		For Activation (1hr) volumes taken	
	Maintenance media (µl)	LPS (µl)	Maintenance media (µl) + LPS (µl)	Nigericin (µl)
0.5	99.959	0.041	99.9	0.1
1	99.92	0.08	99.9	0.1
2.5	99.79	0.208	99.9	0.1
5	99.584	0.416	99.9	0.1
10	99.17	0.83	99.9	0.1

3.9.2a Pyroptosis inhibition: LPS/Nigericin induced cells were treated with Bay 11- 7082 and Disulfiram separately and in combination to ascertain a safe dose that inhibits LPS/Nigericin mediated pyroptosis in CEKC.

3.9.2b Standardisation of inhibitors dose: The dose of Bay 11-7082 and Disulfiram separately and in combination was determined by adding these inhibitors to pyroptotic induced cells. Priorly, these cells were induced by LPS/nigericin by the dose standardised in section 3.9.1b. Following pyroptotic induction, different doses of Bay 11-7082 and disulfiram were added according to the **Table 3** and then the cells were incubated at 37°C, 5% CO_2 incubator for different time intervals (6, 12, 24 hrs). The cytotoxicity assessment was done using a commercial Cytox 96 assay kit.

Table 3. Treatment with different doses of Bay 11-7082 and disulfiram in each well of 96 well plates

Concentration of inhibition (µM)	Volumes used for Bay 11-7082 (µl)	Volumes used for Disulfiram (µl)
1	0.01	0.04
2	0.02	0.08
5	0.05	0.2
10	0.1	0.4

3.9.3 Methodology followed before subjecting CEK cells to Cytox 96 assay kit

The methodology used in this study was done as per the method described by den Hartigh and Fink (2018) with slight modifications. The pyroptotic cell lysis was assessed by measuring the release of cytoplasmic enzyme LDH using a Cytotox 96 non-radioactive cytotoxicity assay kit. The assay was performed in triplicate as per the manufacturer's instructions.

Briefly, 2×10^4 cells per well, in 200 µL of maintenance media (without antibiotics), in triplicates were plated in a 96-well flat bottom tissue culture plate. A total of 9 wells were seeded for each treatment (3 spontaneous lysis, 3 total lysis, and 3 for the experimental setup) for the desired time intervals (6, 12, 24 hrs). The following day, the respected wells were replaced with 100 µl of M-199 maintenance media without antibiotics containing 2.5µg/ml LPS and incubated for 3 to 4 hr at 37°C and 5% CO_2. After priming, 100 µl of M-199 maintenance media was added without antibiotics + LPS containing 10 µM nigericin to the

experimental wells, 100 µl of M-199 maintenance media without antibiotics + LPS to the spontaneous wells, and 80 µl of M-199 maintenance media without antibiotics + LPS to the total lysis wells. The final concentration of nigericin was 5 µM. The cells were incubated at 37°C and 5% CO2 incubate for 1 hr in order to activate pyroptosis. Further, 20 µL of lysis buffer (provided with the cytotoxicity kit) was added to lyse the cells in the lysis wells 30 minutes before the conduction of the cytotoxicity assay. The cells were lysed by vigorous pipetting to ensure complete lysis of cells. Cell supernatant was collected at respective time intervals (6, 12, 24 hrs) for cytotoxicity assay.

3.9.4 Detection of LDH release using Cytotox 96 assay

1. 50 µl of supernatants of respective time interval samples from each well was transferred to a new, flat bottomed assay plate (kept the wells in the same order as the experimental plate). Additionally, three wells of medium only and three wells of medium + lysis buffer to be used as blanks for the OD readings was included.
2. 50 µl of the reconstituted substrate was added to each well and incubated at room temperature protected from light for 10 min.
3. 50 µl of stop solution provided with the kit was added to each well and the absorbance was measured at 490 nm within 1 hr of adding the stop solution.
4. The average values of the culture medium background was subtracted from all values from wells containing cells.

The results were calculated as % Cytotoxicity (% LDH release) using the following

$$\text{Percent cytotoxicity} = \left\{ \frac{\text{OD experimental} - \text{OD spontaneous}}{\text{OD total lysis} - \text{OD spontaneous)}} \right\} \times 100$$

3.10 Blocking pyroptotic cell death

After assessing cytotoxicity, the cells were treated with the standardized dose obtained from Section 3.9.2b of pyroptotic inhibitors disulfiram and Bay 11-7082 separately and in combination at six different intervals, including 24 hours, 12 hours, and 6 hours pre-ILTV infection and 6 hours, 12 hours, and 24 hours post-ILTV infection. Suitable controls were included in the experiment. Groups are depicted below in **table 4** and **Fig. 2**.

Table 4. Experimental groups for various treatments

Experimental group	PRE- ILTV infection				POST-ILTV infection		
	24hr	12 hr	6hr	Infection	6hr	12hr	24 hr
Group 1 (BAY 11-7082)	Epithelial cells + Bay	Epithelial cells + Bay	Epithelial cells + Bay	ILTV	Infected epithelial cells + Bay	Infected epithelial cells + Bay	Infected epithelial cells + Bay
Group 2 (Disulfiram)	Epithelial cells + disulfiram	Epithelial cells + disulfiram	Epithelial cells + disulfiram	ILTV	Infected epithelial cells+disulfiram	Infected epithelial cells+disulfiram	Infected epithelial cells+ disulfiram
Group 3 (BAY11-D7082+Disulfiram)	Epithelial cells with bay and disulfiram	Epithelial cells with bay and disulfiram	Epithelial cells with bay and disulfiram	ILTV	Infected epithelial cells with bay and disulfiram	Infected epithelial cells with bay and disulfiram	Infected epithelial cells with bay and disulfiram
Group 4 Mock control (Experimental control)	Epithelial cells	Epithelial cells	Epithelial cells	(No virus)	Epithelial cells + PBS	Epithelial cells + PBS	Epithelial cells + PBS
Group -5 Virus control	Epithelial cells	Epithelial cells	Epithelial cells	(ILTV)	Epithelial cells +virus	Epithelial cells +virus	Epithelial cells +virus

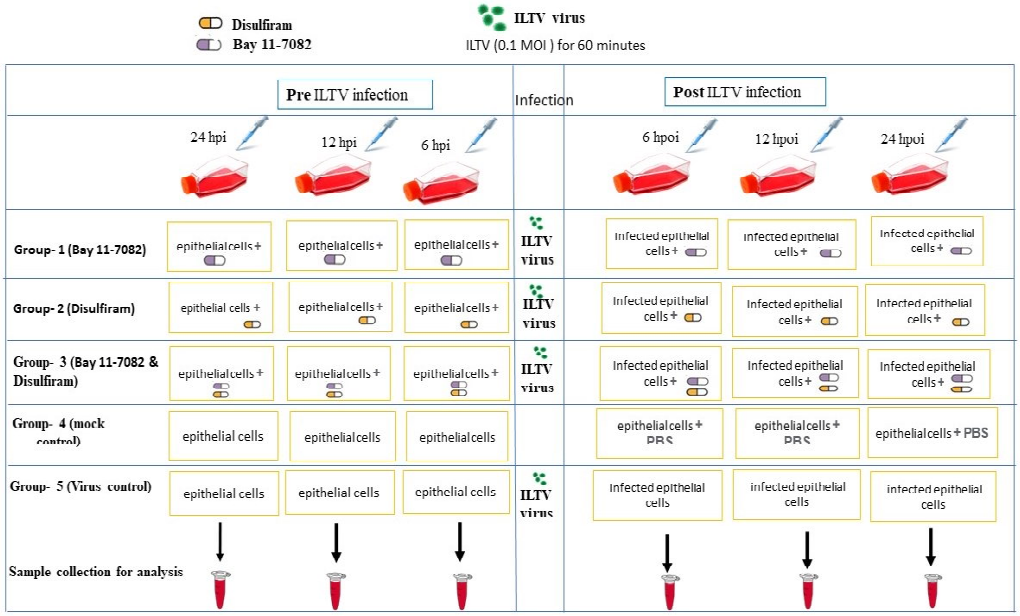

Fig. 2. Schematic representation of experimental design groups for various treatments

3.10 a) Pyroptotic Inhibition treatment for the adhered cells of experimental groups (1,2,3): The standardised doses of BAY 11-7082 and disulfiram were added for the designed experimental groups at pre infection and post infection.

3.10 b) Mock infection of CEK cells (Group-4): 10µl and 1µl of PBS was added to the T25 flask and 96 well plate which acted as a control for the molecular studies.

3.10 c) Source of virus for the virus control group (Group-5): ACAM passaged freeze-dried virus from the Avian Disease Section, Division of Pathology, IVRI with a standardized infection of a multiplicity of infection (MOI) 0.1 was used for the experiment. Its persistence was determined by calculating viral titres using the Reed and Muench method to achieve $\log_{10}TCID_{50}$.

3.10 d) Infection of the CEK cells: Infection of a multiplicity of infection (MO1) 0.1 was given for 60 mins to T25flask, 35mm and 96 well plate and then the media was overlaid with maintenance media containing pyroptotic inhibitors treatment Bay11-7082, disulfiram separately and in combination. The cells were pelleted and collected in Trizol reagent at regular intervals (24, 12, 6 pre-ILTV infections and 6, 12, 24 post-ILTV infections) in Eppendorf tubes and stored at -20°C and used for further molecular study. The 96 well plates were also

used to measure parameters for the periodic detection of pyroptosis (24, 12, 6 pre-ILTV infections and 6, 12, 24 post-ILTV infections).

3.11 Detection of pyroptosis inhibition

3.11.1 Determination of cell viability by MTT assay

The MTT (3-[4,5-dimethylthiazol-2-yl]-2,5 diphenyl tetrazolium bromide) assay was done following the procedures by Meerlo et al. (2011) with slight modifications. Briefly, 2×10^4 cells per well in 150µl of culture media was seeded in flat bottomed 96 well culture plates. The control and blank wells were also kept. Followed by cell seeding, the plate was incubated for 48hr and the media was replaced with fresh culture media containing different treatments of Bay 11- 7082 (10µM), Disulfiram (10µM), and a combination of both Bay 11- 7082 & Disulfiram (5+5 µM). Followed by incubation at 37 °C, 20 µl of the medium was substituted by the addition of 20µl of MTT solution at specified time points of the proposed experimental groups (24, 12, 6 pre-ILTV infections and 6, 12, 24 post-ILTV infections). After the addition of the MTT reagent, the plate was incubated for 4 h at 37°C with 5% CO_2. Soon after incubation the solution in all wells was aspirated and discarded, followed by the addition of 150 µl of DMSO into each well using a multichannel pipette to dissolve the formed formazan crystals. Repeated pipetting was done to dissolve the insoluble formazan crystals. Optical density was measured at 595nm in a microplate reader and cell viability was calculated based on the formula given below.

$$\text{Cell viability} = \left\{ \frac{(\text{OD of treated well} - \text{Mean OD of blank wells}}{\text{Mean OD of control wells} - \text{Mean OD of blank wells}} \right\} \times 100$$

- Treatment: wells containing respective pyroptotic inhibitors (Bay11-7082, Disulfiram separately and in combination) treatments.
- Control wells containing cells but no treatment.
- Blank wells: without cells only the media containing treatment wells.

3.11.2 Detection of plasma membrane integrity

The SYTOX green nucleic acid staining was done according to the kit manufacturer protocol provided with slight modifications. The integrity of the cell membrane was assessed by SYTOX green nucleic acid staining. This dye easily penetrates cells with compromised plasma membranes and yet will not cross the membranes of a live cell.

Preparation of chicken embryo epithelial cells for SYTOX green staining:

1. Briefly, the isolated chicken embryo epithelial cells were cultured in flat bottomed 96 well culture plates by seeding 2×10^4 cells per well in 150 µl of M199 culture media supplemented with 10% Fetal bovine serum and 1% antibiotic–antimycotic mix. Then they were subjected to subsequent analysis as well as microscopic observation of the cells.

2. Once cells had reached 70% confluence, the culture medium was replaced with the target pyroptotic inhibitors Bay11-7082 (10 µM), disulfiram (10 µM), separately and in combination at a final concentration of 5µM + 5µM contained media to the designed experiment wells and after that plates were incubated at 5% CO_2 incubator.

3. On the day of the experiment at selected time points (24, 12, 6 pre-ILTV infections and 6, 12, 24 post-ILTV infection) plates were chosen for the addition of prepared SYTOX Green solution to cover all the wells at the final concentration of 0.5 µM. Then cells were incubated at 37°C for 30 min, protected from light and the staining solution was removed. The cells were washed twice in 1X PBS. The cells were visualised under fluorescence microscope (green channel, ex. 488 nm, em. 523 nm) and the fluorescence was measured using a plate reader (1-s integration time).

3.11.3 Detection of lysosomal damage

The LysoTracker deep red assay was done according to the kit manufacturer protocol provided with slight modifications. The LysoTracker deep red fluorescence acidotropic probe assesses the integrity of lysosomes by labelling and tracking the acidic organelles in live cells. 1mM probe stock solution was diluted in the 1X PBS to make the final working concentration (65 nM).

Preparation of chicken embryo epithelial cells for LysoTracker deep red assay:

1. Isolated chicken embryo epithelial cells were grown on coverslips inside a 35 mm petri dish filled with 1.5 ml of culture medium.

2. Once cells had reached 70% confluence, the culture medium was replaced with the media containing pyroptotic inhibitors Bay11-7082 (10 μM), disulfiram (10 μM) separately and in combination at a final concentration of (5 μM + 5 μM) and after that plates were incubated at 5 % CO_2 incubator.

3. On the day of the experiment at selected time points (24, 12, 6 pre-ILTV infections and 6, 12, 24 post-ILTV infection) plates were chosen for the addition of prepared prewarmed (37 °C) probe-containing medium. Then cells were incubated at 37 °C for 1 hour, protected from light and the staining solution was removed. The cells were washed twice in 1X PBS and then 1.5 ml of plain M199 was added to the dishes. The fluorescence image from LysoTracker Deep Red was recorded using excitation at 647 nm and the emission range 660–680 nm.

3.12 Quantification of viral load by quantitative real time PCR

Post-infection with ILTV, the epithelial cells were harvested at different time intervals (6,12, 24, hpi). DNA was extracted, and absolute viral quantification was done using real-time PCR to amplify gC gene. The viral load was quantified using the following reaction: 10μl SYBR Green PCR Master mix, 0.3μl (10 pmol/μl), each forward primer and reverse primer **(Table 5)** along with 2 μl of DNA template and 7.4 μl of NFW to make up 25μl reaction. The cycling conditions were 5 min @ 95°C followed by 40 cycles of 95°C for 10 sec, 60°C for the 40sec and 25°C and hold of 2 min. Amplification and data acquisition was carried out using BioRAD CFX96 Touch real-time PCR machine.

The percentage of inhibition was calculated as follows: % inhibition = (1 - (average of compound-treated cells) / (average of control cells)) × 100 (Cao *et al.*, 2015)

Table 5. Details of primers used for Viral quantification

Sl. No	Target Gene	Oligonucleotide sequence (5'®3')	Amplicon size	Reference
1	ILTV gC	CCTTGCGTTTGAATTTTTCTGTTTC GTGGGTTAGAGGTCTGT	103 bp	Roy *et al.* (2015)

3.13 Evaluation of pyroptosis markers by relative real time PCR using SYBR green for the designed experimental groups

The relative gene expression for the evaluation of pyroptosis markers (Caspase-1, IL1β, IL -18) in the CEK cells for the designed experiment group was carried out in qualitative real time PCR. The control media group served as a calibrator, and GAPDH was used as an endogenous control (housekeeping gene).

3.13.1 RNA extraction:

Extraction of RNA from the CEK cells was carried out using TRIZIN (GCC Biotech, India) as per the manufacturer's protocol. The samples were centrifuged at 10,000 rpm for 4 mins and the cell pellet was dissolved in 1 ml of trizin and stored at -20°C. During the experiment, the stored samples were briefly taken out of the freezer and allowed to thaw at room temperature for 5 minutes. Then chloroform (100 µl) was added and vortexed for 30 secs after shaking vigorously. It was further incubated at room temperature for 2-3 minutes. The sample was centrifuged at 12000g for 15 mins at 4°C for the separation of phases. The aqueous phase at the top was collected and transferred to a new RNAse free microcentrifuge tube. To the collected aqueous phase isopropanol (250 µl) was added and kept at room temperature for 10 mins. Then it was centrifuged at 12,000g for 10 mins at 4°C. The supernatant was discarded without any disturbance to the RNA pellet. Washing of the pellet was done with 75% ethanol (500 µl). The mixture was centrifuged at 7,500g for 10 mins. After discarding the supernatant, the pellet was air dried. 20µl of RNAse-free water was added to dissolve the pellet and stored at -20°C till further use. Using a micro drop plate and a multimode spectrophotometer, the extracted RNA samples were analysed for purity and concentration. At 260 and 280 nm in wavelength, optical densities (OD) were determined.

3.13.2 Reverse Transcription for cDNA synthesis

Quanti Tect Reverse Transcriptase Kit™ was used to eliminate genomic DNA with 2 µl of gDNA wipe-out buffer and 7 µl RNAse free water from 5 µl of template RNA, followed by incubation in 42°C for 5 mins and snap chilled on ice. The reverse transcription of 14 µl of the previous reaction mixture was carried out with 1µl Quantiscript reverse transcriptase enzyme, 4ul 5X reverse transcriptase buffer and 1 µl of reverse transcriptase primer mix. The extension reaction was carried out in a thermal cycler at 42°C for 30 mins and denatured at 95°C for 3 mins. The synthesized cDNA was stored at -20°C until further use.

3.13.3 SYBR green based relative real-time PCR for pyroptosis marker gene expression

A qPCR machine (Biorad, CFX96, USA) was used to execute the qPCR reaction using SYBR Green/ ROX qPCR Master Mix (2X) (Thermo Scientific, Lithuania) to amplify all the target and house-keeping genes in CEKC culture samples collected from designed experiments. Details of the primers are listed in the **table 8**. The reaction mixture (**table 6**) was made for 10 µl in qPCR strips (Bio-rad) with optically clear flat caps (give products details) comprising of SYBR Green master mix 5µl, 0.2 µl each of forward and reverse primers, followed by template cDNA (20 ng), and nuclease free water up to 10µl. To verify the non-specific amplification, a no template control (NTC) reaction was carried out simultaneously. The table below lists the components in the reaction mixture.

Table 6. Components of reaction mixture used in real time PCR

Components	Volume (µl)
SYBR Green qPCR Master mix	5
Forward primer	0.2
Reverse primer	0.2
Template DNA	2
Nuclease free water Make up to	10

Following the preparation of the reaction mixture, the strips were either centrifuged or given a quick spin. The reaction conditions (**table 7**) were as follows: 95 °C for 15 min, then subjected to 40 cycles of 95 °C for 15 sec and 54-60 °C for 30 sec, and extension at 72°C for the 30s. The software-generated dissociation curve through 65-95 degrees Celsius validates the specificity of the target gene-specific product.

Table 7. Details of cyclic conditions followed in qPCR experiment

Step	Temperature	Time
Initial denaturation	95 °C	15min
Cyclic denaturation	95°C	15s
Annealing	54-60°C	30s
Extension	72 °C	30s
Number of cycles	40	
Melt curve	65-95°C	1 min each

Table 8. Details of primers used in relative Real time PCR for amplification of pyroptosis markers

Target Gene	Oligonucleotide sequence (5'→3')	Annealing temp(°C)	Reference
GAPDH	F-CACTATCTTCCAGGAGCGTGA	58	Coppo *et al.* (2018)
	R-CAGATGAGCCCCAGCCTTC		
Caspase-1	F-TAAGCACTTGAGACAGCGGGACG	58	Liu *et al.* (2016)
	R-GGATGTCCGTGGTCCCATTACTC		
IL-1β	F-CCAGAAAGTGAGGCTCAACA	58	Rasouli *et al.* (2015)
	R-GTAGCCCTTGATGCCCAGT		
IL-18	F-GAAGTGCTTCGTGCTGGAGT	60	Kolesarova *et al.* (2011)
	R-GAAGTGCTTCGTGCTGGAG		

3.13.4 Evaluation of fold expression of targeted genes

The calculation of $2^{-\Delta\Delta Ct}$ was performed as per Livak and Schmitten (2001).

Step 1 : Calculation of arithmetic mean of Ct values (mCt)

Step 2 : The values were normalized using the housekeeping gene (GAPDH) to target gene

ΔCt = mCt (Target gene) - mCt (Housekeeping gene)

Step 3 : The values were normalized using control values

$\Delta\Delta Ct = \Delta Ct$ (Experimental wells) - ΔCt (Control wells)

Step 4 : The relative quantity was calculated for the target gene

$2^{-\Delta\Delta Ct}$ = Relative quantity (Fold change in gene expression in experimental to that of control wells)

Standard error difference (SED) was calculated by the formula, SED = Square root of ((SD2 of endogenous control/n1) + (SD2 of target gene/n2).

3.14 Detecting expression of apoptotic and necroptosis markers by relative real time PCR using SYBR green:

Expression of apoptotic caspases-3, 8 and 9 as well as necroptotic markers RIP-1 and RIP-3 kinases (**Table 9**) were quantified by real time PCR and compared with control and pyroptosis induced groups to assess whether inhibition of pyroptosis could activate apoptotic/ necroptotic cell death pathways in ILTV infected cells. The control media group served as a calibrator, and GAPDH was used as an endogenous control (housekeeping g gene). Real time expression of these markers was done as per section 3.13.

Table 9. Details of primers used in relative Real time PCR for amplification of apoptosis & necroptosis markers

Target Gene	Oligonucleotide sequence (5'→3')	Annealing temp(°C)	Accession no. / Reference
Caspase-3	F-GAAGGAACACGCCAGGAAAC R-GCAAAGTGAAATGTAGCACCAA	57	NM_204725.1
Caspase-8	F-GTCTCCGTTCAGGTATCTGCT R-TCTCAATGAAAACGTCCGGC	58	NM_204592
Caspase-9	F-CCAACCTGAGAGTGAGCGATT R-GTACACCAGTCTGTGGGTCGG	58	AY057940
RIPK1	F-TGCCTTCTGTTCCTCACTGG R-CCTGCGTAGGTATTGCAGCTT	54	Zhirong *et al.* (2021)
RIPK3	F-ACATCCTTCGCTCACAGCAA R-ACCTGTGCTGCCTTCTCTCC	57	Wang *et al.* (2020)

3.15 Statistical analysis

Statistical analysis was carried out using JMP software using the analysis of variance (ANOVA) and t-test. Data were analysed using either two-way ANOVA or one-way ANOVA followed by Tukey's multiple comparison test to detect differences between the treated groups. Differences were considered significant where $p < 0.05$ or $p < 0.001$.

Results

4 RESULTS

4. *In vitro* culture of chicken epithelial cells

4.1 Preparation of tracheal epithelium cell (TEC) culture

The tracheal epithelial cells had polygonal morphology and got attached to cell culture plates 12hrs post seeding (Fig. 3A). The isolated avian tracheal cells showed circular morphology and no attachment was seen on the tissue treated plates after 24hrs (Fig. 3B). The unattached dead cells were seen floating in the maintenance medium. In order to counter the cell attachment problem, we modified our protocol in a few different ways.

1st Attempt: Serum free medium (BEGM, Gibco) with serum substitute (BIT 9500) for selective attachment of the epithelial cell was used, as we faced issues in the attachment of any cells in general. We added 5% foetal bovine serum 24hrs after harvesting the tracheal cells on the T25 flask. This was done to ensure the attachment of all the cells obtained in the final cell suspension. This resulted in overall limited attachment of epithelial cells as well as the fibroblasts which did not reach even 40% confluency. The cells eventually detached in two days without reaching 80% confluency which was a minimum requirement for the study.

2nd Attempt: Treatment of the harvested tracheas in dissociation solution for 2hrs which constitutes 0.2% protease that strips off epithelial cells from the mucosal lining was done. In order to mask the harsh treatment of protease, we treated the harvested tracheas for varying time periods like 30 mins, 60 mins and 90 mins. In flasks that were treated for 30 mins, 5% more attachment was seen, but unfortunately, the attached cells eventually died in 2 days without reaching the required confluency. Other treatments (60 mins & 90 mins) did not yield good growth of epithelial cells.

3rd Attempt: As previously mentioned we were using serum free medium BEGM and BIT 9500 serum substitute as a selective growth medium for tracheal epithelial cells, we switched to a different serum free growth medium named LHC-9 with B-27 supplement as a serum substitute. In this attempt, we observed an increase in the number of attached cells and were able to maintain the cells for 32hrs, when compared to the previous attempts. Unfortunately, the cultured avian tracheal cells could not survive for the required time duration for the experiment.

Due to the failure of Avian TEC cells to show standard growth for the propagation of ILTV, subsequent studies were performed in CEK cells.

4.2 Propagation of ILTV in chicken embryo kidney cells

Cells at 80% confluency were infected with CAM propagated ILTV of MOI=0.1. The virus was allowed to attach for 60 mins after which the media was changed to maintenance media, and cells were allowed to grow for 48hrs. Post 48hrs, cell aggregation, cell rounding and multinucleated syncytial cells as cytopathic effects were observed (Fig. 4B-D) while uninfected control cells did not show any changes other than mild cell rounding (Fig. 4A). Subsequently, these infected cells were freeze thawed and 200 µl of the inoculum was used to infect freshly prepared CEKC culture. This was repeated thrice. This passaged virus was further used for further experiments.

4.3 Determination of appropriate dose of LPS for pyroptotic induction based on cytotoxicity assessment by % LDH release:

Different doses of LPS (0.5 µg, 1 µg, 2.5 µg, 5 µg, and 10 µg) and 5 µM nigericin were used to standardise the dose for pyroptotic induction. Among 5 different doses of induction using LPS, we found that at 6,12 hr time intervals there was no significant difference between doses used but there was a significant difference at 24 hr (p value 0.048) (Fig. 5), but between induction doses, there was a significant difference (p value 0.025). Amongst various doses, the cells treated with 2.5 µg/ml of LPS displayed consistently low cytotoxic values throughout all time intervals, which was acceptable for further experiments to ascertain the safe concentration that induce pyroptosis and there was no significant difference in the percentage of LDH release over the all study time intervals at this dose. The inverted light microscope images of various

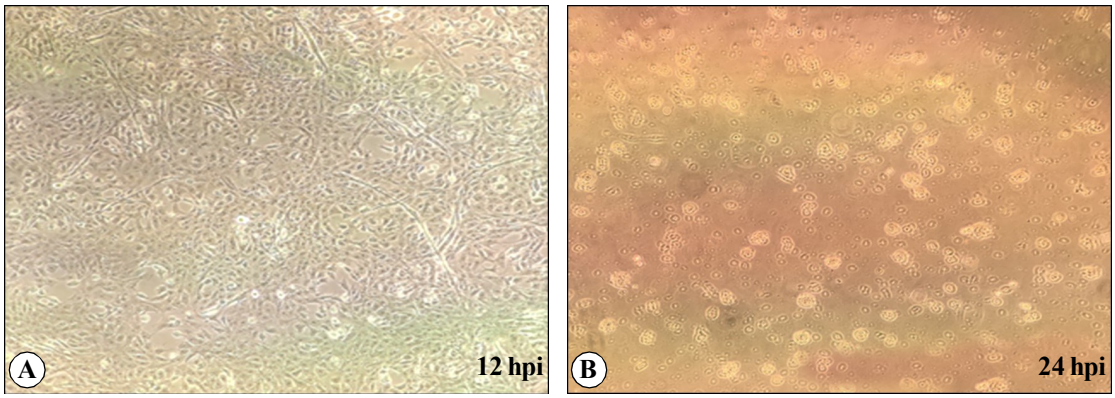

Fig. 3: A-B. Avian tracheal cell culture: A. Presence of proper attachment of avian tracheal cells characterized by typical polygonal morphology and minimum fibroblast attachment at 12hpi; B. Failure of tracheal epithelial cell attachment in the tissue culture plate showing rounded morphology after 24hrs post seeding

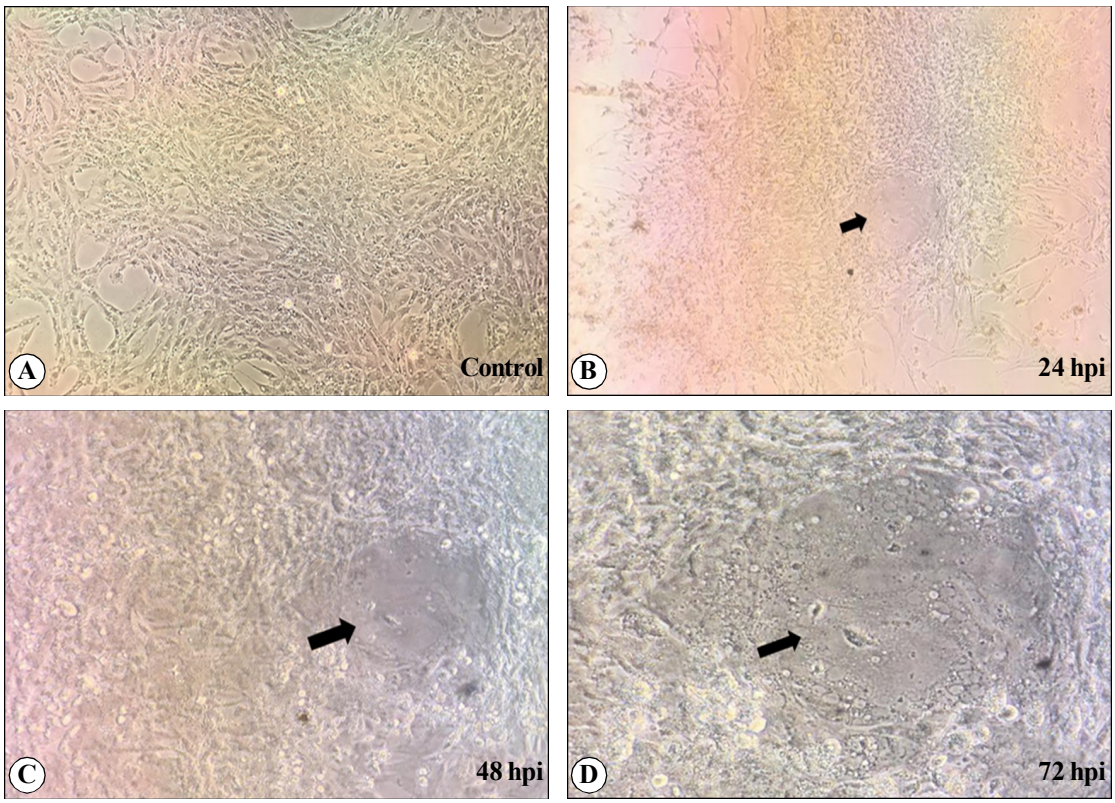

Fig. 4: A-D. Propagation of ILTV in CEK cell culture: A. uninfected CEK cells control with intact architecture. B-D. CEK cells showing cell death and cell rounding in clusters at 24hpi. CEK cells showing cell aggregation and cell death at 48hpi to 72hpi; (100x, 200x, 400x)

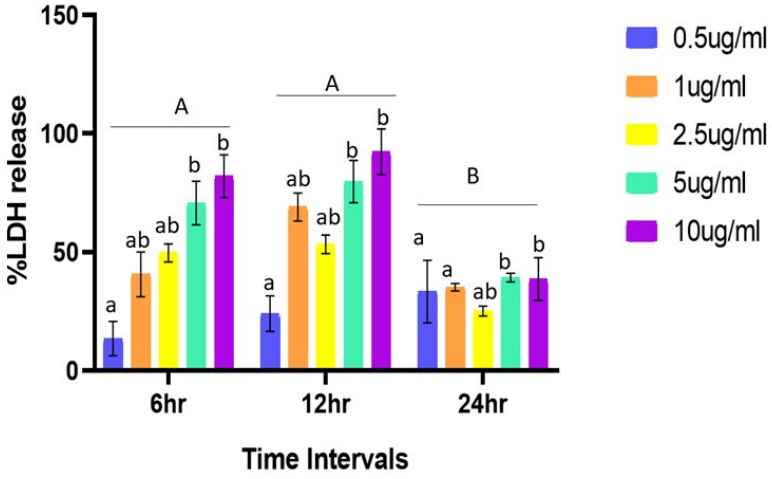

Fig. 5: Graph representing %LDH release in CEK cells at different time intervals treated with different doses of LPS.

(Bar with different superscript indicate significant difference at P<0.05. Capital letters denotes significant difference between time intervals whereas small letters denote significance difference between treatment doses.)

doses of LPS/ (5 µM) nigericin treated CEK cells exhibited morphological changes and characteristics of pyroptosis such as cell swelling and loss of cell extension process (Figure 6 B-D). A decrease in cell population was noted with the increase in the concentration of the LPS. While uninfected control cells did not show any changes other than mild cell rounding (Fig. 6 F)

Hence, 2.5 µg of LPS dose was chosen with 5µM of nigericin to induce pyroptosis for the standardisation of pyroptotic inhibitors.

Table 10. % LDH release assay values in CEK cells treated with different doses of LPS at different time intervals used for Pyroptosis Induction

LPS doses used for induction	6Hr	12Hr	24Hr
0.5 µg/ml	13.5[a]	24.02[a]	33.37[a]
1 µg/ml	40.65[ab]	69.02[ab]	35.12[a]
2.5 µg/ml	49.67[ab]	48.3[ab]	39.15[ab]
5 µg/ml	70.72[b]	79.75[b]	39.24[b]
10 µg/ml	82.05[b]	92.4[b]	38.61[b]

(Levels not connected by the same letter are significantly different between induction doses)

4.4 Standardisation of pyroptotic inhibition dose for Bay 11-7082

Bay 11-7082 was used to inhibit pyroptosis in cells induced with 2.5 µg of LPS and 5 µM nigericin. To standardise the dose of Bay 11-7082, varying concentrations (1 µM, 2 µM, 5 µM and 10 µM) were used and cell cytotoxicity was measured as % LDH release. We noticed that, across 4 different inhibition concentrations of Bay 11-7082, there was no significant difference between doses at 6 and 12 hr but there was a significant difference at 24 hr (p value 0.045) but between different inhibition concentrations there was significant difference (p value 0.032) (Fig. 7).

There was no significant difference in the % LDH release at 10 µM of Bay 11-7082 across all time points used. To determine the safe dose that prevents pyroptosis, a concentration of 10 µM was chosen since it caused less cytotoxicity in cells than other types of doses did across all time intervals.

4.5 Standardisation of pyroptotic inhibition dose for Disulfiram

Disulfiram was used to inhibit pyroptosis in cells induced with 2.5 µg of LPS and 5µM nigericin. To standardise the dose of disulfiram, varying concentrations (1 µM, 2 µM, 5 µM and 10 µM) were used and cell cytotoxicity was measured as % LDH release. We noticed that, across 4 different inhibition concentrations of disulfiram, there was no significant difference between doses at 6 and12 hr but there is a significant difference at 24 hr (p value 0.041) but between different inhibition concentrations there was significant difference (p value 0.047) (Fig. 8).

There was no significant difference in the % LDH release at 10 µM of Disulfiram across all time points used. Thus, a concentration of 10 µM was selected as a safe dose that inhibits pyroptosis since it had a lower cytotoxic effect on cells over all the time intervals than other concentrations.

4.6 Standardisation of pyroptotic inhibition dose for Bay 11-7082 &Disulfiram combination

Bay 11-7082 & disulfiram was used to inhibit pyroptosis in cells induced with 2.5 µg of LPS and 5µM nigericin. To standardise the dose of Bay 11-7082 & disulfiram combination, varying concentrations (5 µM +5 µM; 5 µM +10 µM; 10 µM +5 µM; 10 µM+ 10 µM) were used and cell cytotoxicity was measured as % LDH release. There is significance difference between (5 µM +5 µM;5 µM +10 µM; 10 µM +5 µM) combinations and (10 µM +10 µM) (p-value 0.046). But between (5 µM +5 µM;5 µM +10 µM; 10 µM +5 µM) combinations there was no significance difference and also the % LDH release was low when compared to (10 µM +10 µM) combination (Fig. 9). Hence 5 µM of Bay 11-7082 and 5 µM of Disulfiram was chosen as there was a very less % LDH release over all the time intervals to ascertain a safer concentration for pyroptotic inhibition.

4.7 Detection of pyroptosis inhibition

4.7.1 Determination of cell viability by MTT assay

In the current study, CEK were isolated and cultured in a 96 well plate for the proposed experimental design. Treatment of Bay11-7082 (10µM), disulfiram (10µM) and a combination

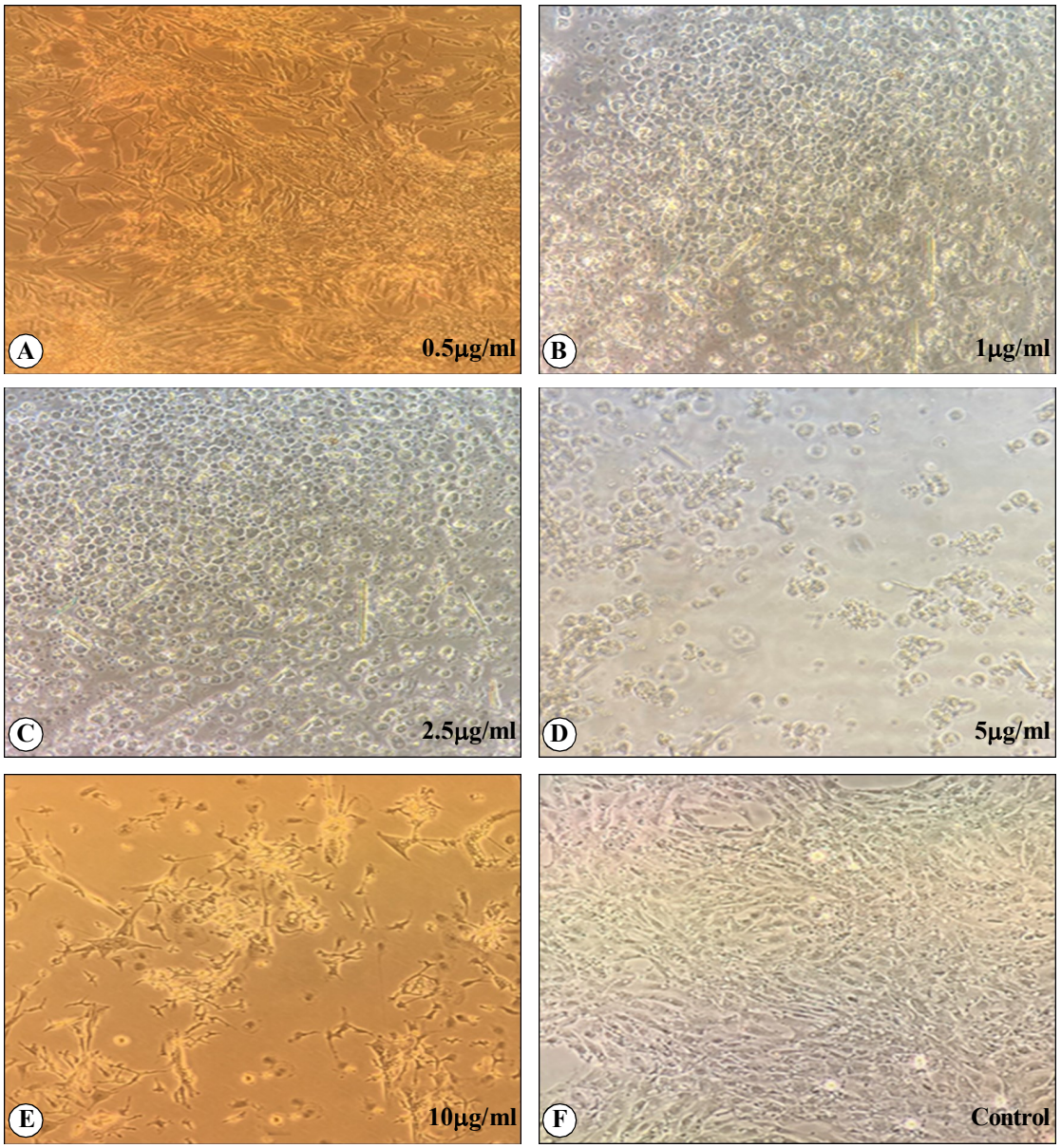

Fig. 6: **A-F: Representative images showing morphological changes at varying LPS doses used for pyroptosis induction(A-E). F. Normal CEK cells. Note at 1 µg/ml, 2.5 µg/ml, and 5 µg/ml characteristic of pyroptosis i.e., cell swelling with loss of extended processes; at 5&10 µg/ml dose there is cell shrinkage. A decrease in cell population was noted with the increase in the concentration**

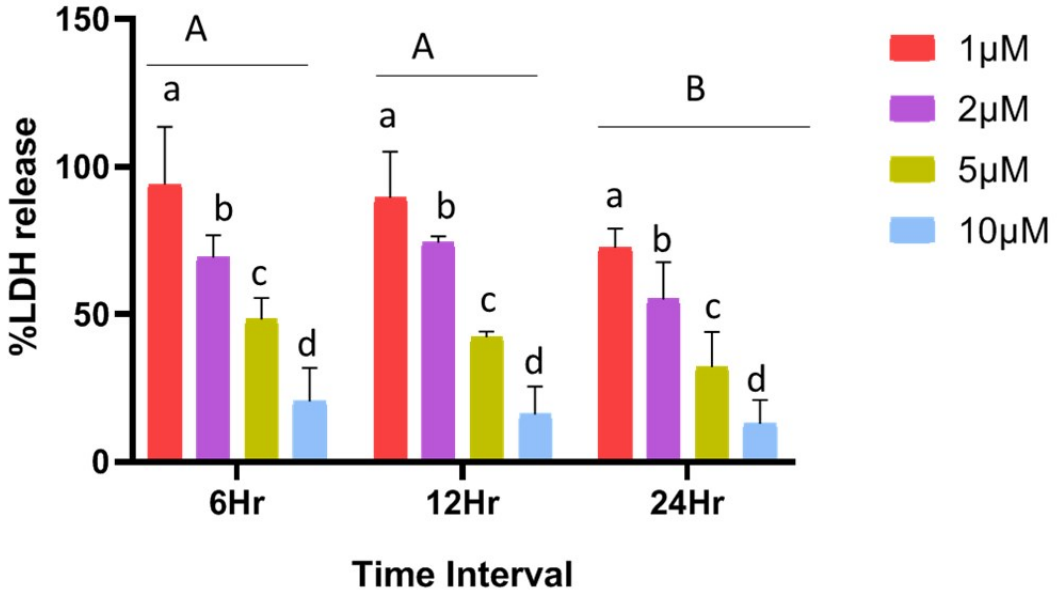

Fig. 7: Graph representing % LDH release in CEK cells at different time intervals treated with different doses of Bay 11-7082

Bar with different superscripts indicate significant difference at P<0.05. Capital letters denote significant difference between time intervals whereas small letters denote significant difference between treatment doses

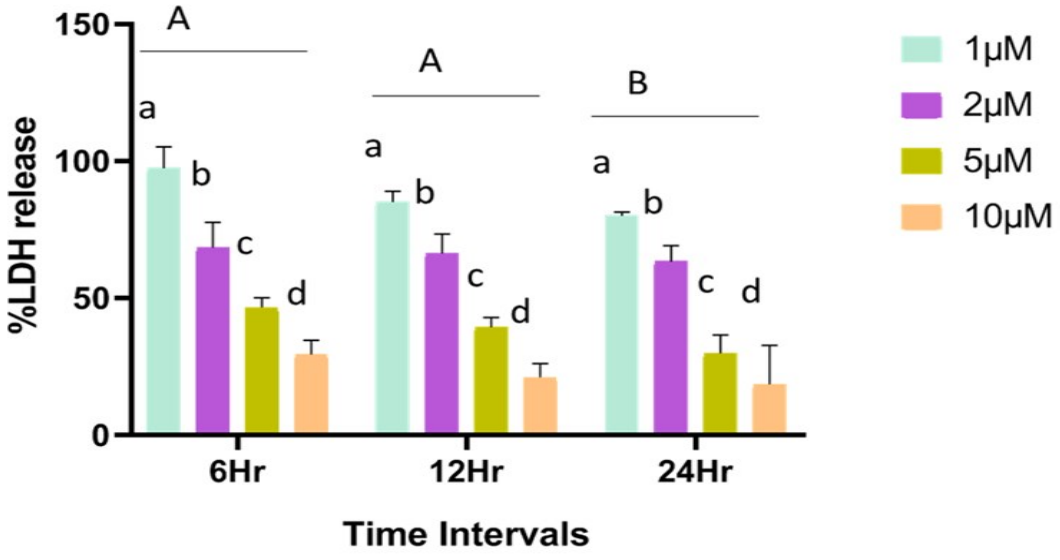

Fig. 8: Graph representing % LDH release in CEK cells at different time intervals treated with different doses of Disulfiram.

(Bar with different superscripts indicate significant difference at P<0.05. Capital letters denote significant difference between time intervals whereas small letters denote significant difference between treatment doses.)

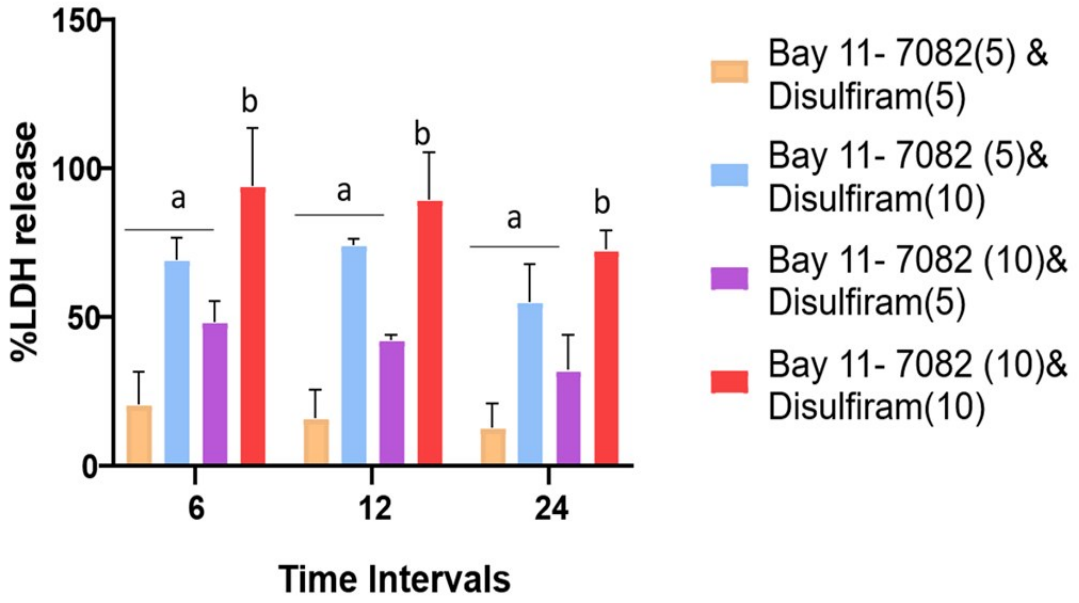

Fig. 9: Graph representing % LDH release in CEK cells at different time intervals treated with different doses of Bay 11-7082 & Disulfiram.

(Bar with different superscripts indicate significant difference between doses with in time $P<0.05$.)

of Bay 11 -7082 (5µM) & disulfiram (5µM) was given after the CEK cells attained 70% confluency in the culture plate. At 24 hr,12 hr, 6 hr pre-ILTV infections and 6 hr,12 hr, 24 hr post-ILTV infections of post-treatment CEK cell viability was determined by MTT assay.

In pre-ILTV infections, the combination group showed relatively constant cell survivability up to 24 hrs as compared to the control and other groups whereas bay treatment significantly reduced the cell viability as compared to disulfiram treated cells and control with p value <0.05 (Fig. 10a).

In post ILTV infection, the cell survivability of all treatment group cells was consistent till 24 hrs whereas the disulfiram treatment had relatively lower viability (Fig. 10b).

Table 11. Cell viability percentages of CEK cells determined by the MTT assay at various time points in the pre-infection treatment groups

Time Interval	(Pre ILTV infection) Treatment Groups		
	Group-1	Group-2	Group-3
24 Hr	81.12±5.49 [a]	85.11±6.646	95.16±2.788
12 Hr	78.22±2.13[b]	82.12±9.51	90.14±5.09
6 Hr	77.10±5.216 [c]	81.33±34.19	88.30±.111

(Levels not connected by the same letter are significantly different from control)

Table 12. Cell viability percentages of CEK cells determined by the MTT assay at various time points in the post -infection treatment groups

Time Interval	(Pre ILTV infection) Treatment Groups		
	Group-1	Group-2	Group-3
6 Hr	80.49±3.91	77.89±3.49	85.19±6.17
12 Hr	78.71±2.44	75.50±4.36	83.39±5.94
24 Hr	77.72±4.89	73.60±5.52	82.85±6.25

*In the control group cell viability was considered 100%.
Group-1 (Bay 11 -7082); Group-2 (Disulfiram); Group-3 (Bay 11 -7082 & disulfiram).

4.7.2 Detection of plasma membrane integrity by SYTOX green staining

To detect membrane integrity, CEK cells of different groups were stained with SYTOX green stain to visualise cell death under a fluorescent microscope. In the pre infection stage, as compared to control the number of sytox negative stained cells showed consistent fluorescence for up to 24 hours; whereas the bay treatment showed a disproportionately large number of sytox positive cells (Fig. 11A).

In the post-infection stage, all treatment groups showed sytox negative cells for up to 24 hours, however, the number of sytox positive cells was disproportionally increased with disulfiram treatment (Fig. 11B).

4.7.3 Detection of lysosomal damage by LysoTracker deep red assay

Lysotracker stain was used to stain the lysosomes of the cells of different treatment groups in pre and post infection groups at different time intervals. In pre-ILTV infections, the combination group showed relatively constant fluorescence for up to 24 hrs as compared to the mock control and other groups whereas with bay treatment the fluorescent stained cells decreased significantly as compared to disulfiram treated cells and mock control (Fig. 12A)

In post ILTV infection, all treatment group cells showed a constant number of lysosome-stain till 24 hours, however the fluorescence staining in the disulfiram treatment group was noticeably lower (Fig. 12B)

4.8 Quantification of viral load by quantitative real time PCR

Post-infection with ILTV & pyroptotic inhibitor treatment, for estimating virus copy number CEK cell samples were harvested at different time intervals (6,12, 24, hrs post infection). Cultures were detected with actively replicating virus at 6 hrs post infection in all the treatment groups. The log viral load detected at 6 hr poi for Group 1, Group 2 & Group 3 treatments were 3.62, 3.73 & 3.27 respectively (Fig. 13). There was a significant difference at 6hr (p value 0.039). As compared to Group 1 and Group 2 treatments over time intervals, the viral copy number for the Group 3 was significantly downscaled (p value 0.041). At 12 and 24 hr intervals, there was a steady decrease in virus load with no significant difference. With

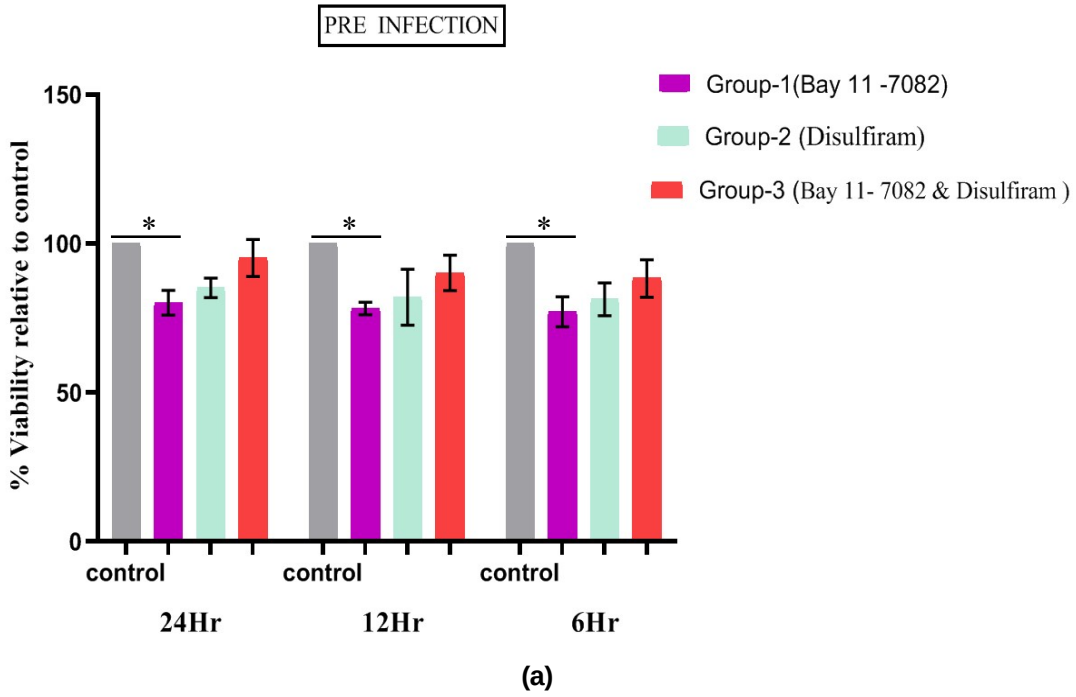

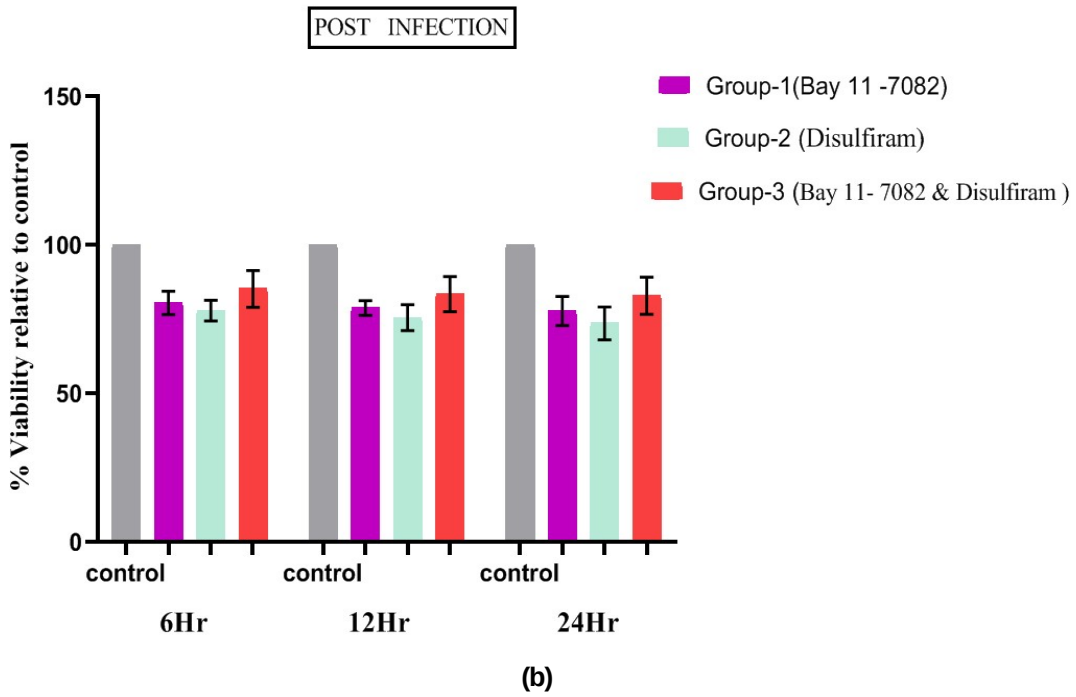

Fig. 10: a-b: Determination of cell viability by MTT assay. Graphs representing the percentage of viable cells ± SEM relative to cells treated for experimental groups at different time intervals of pre & post infection.
(*denotes the significant difference of $p<0.05$ from control between time intervals)

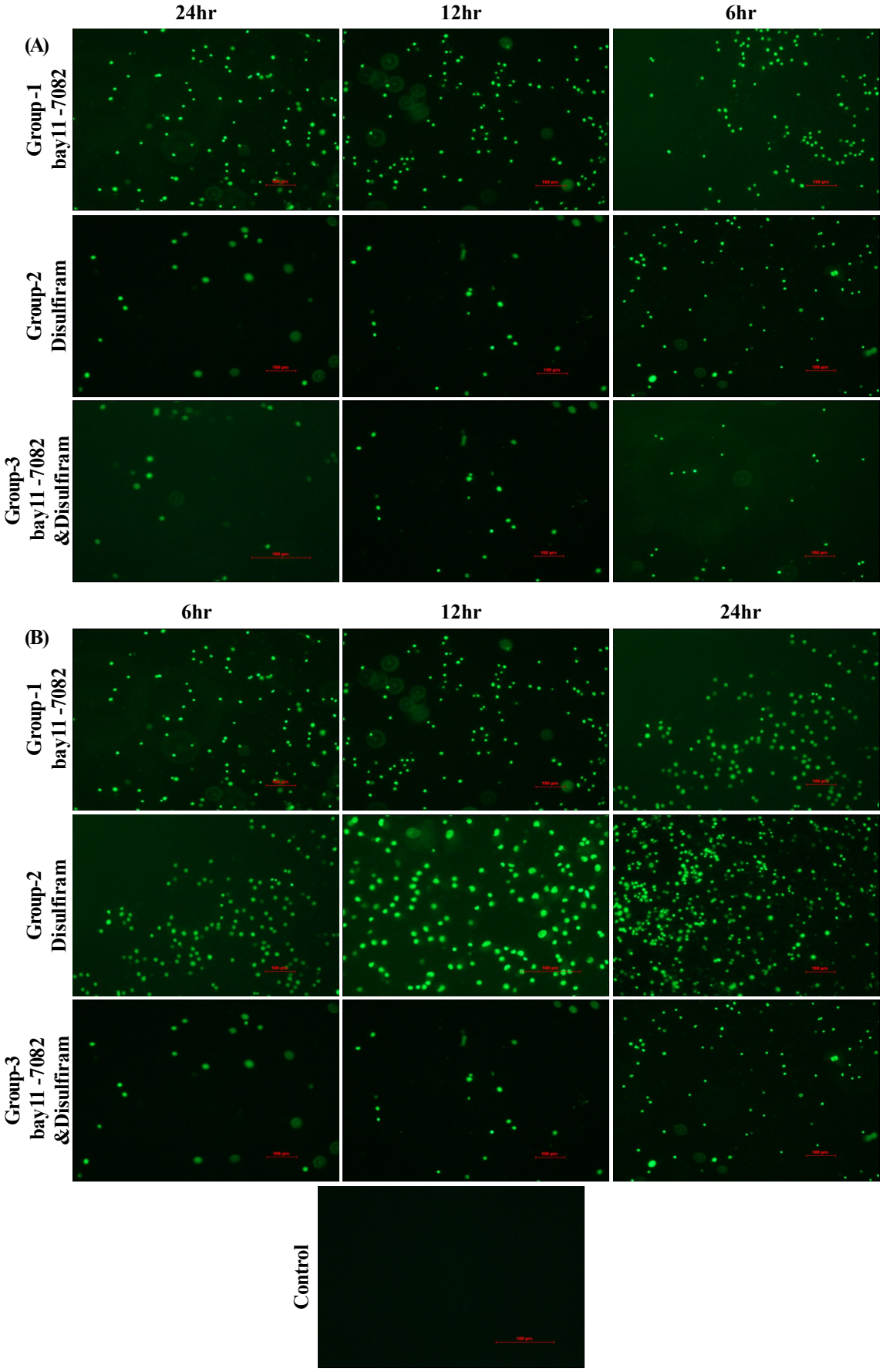

Fig. 11: A-B: Detection of plasma membrane integrity by SYTOX green staining.
Representative images showing lysotracker staining of Group 1, Group 2 and Group 3 at different time intervals of pre & post infection on CEK cells and mock control group

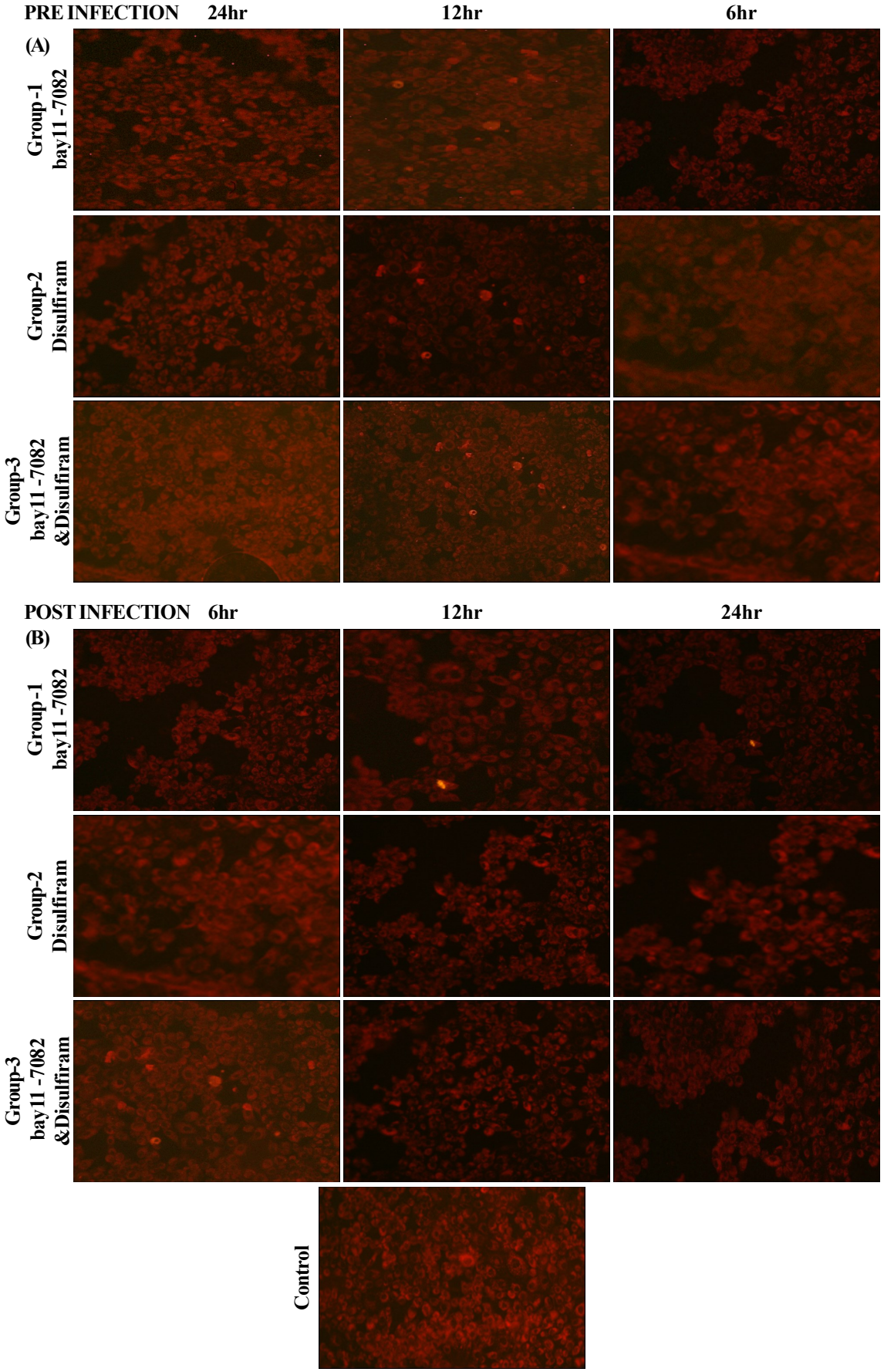

Fig. 12: A-B: Detection of lysosomal damage by LysoTracker deep red assay. Representative images showing Sytox green staining of Group 1, Group 2 and Group 3 at different time intervals of pre & post infection on CEK cells and mock control group

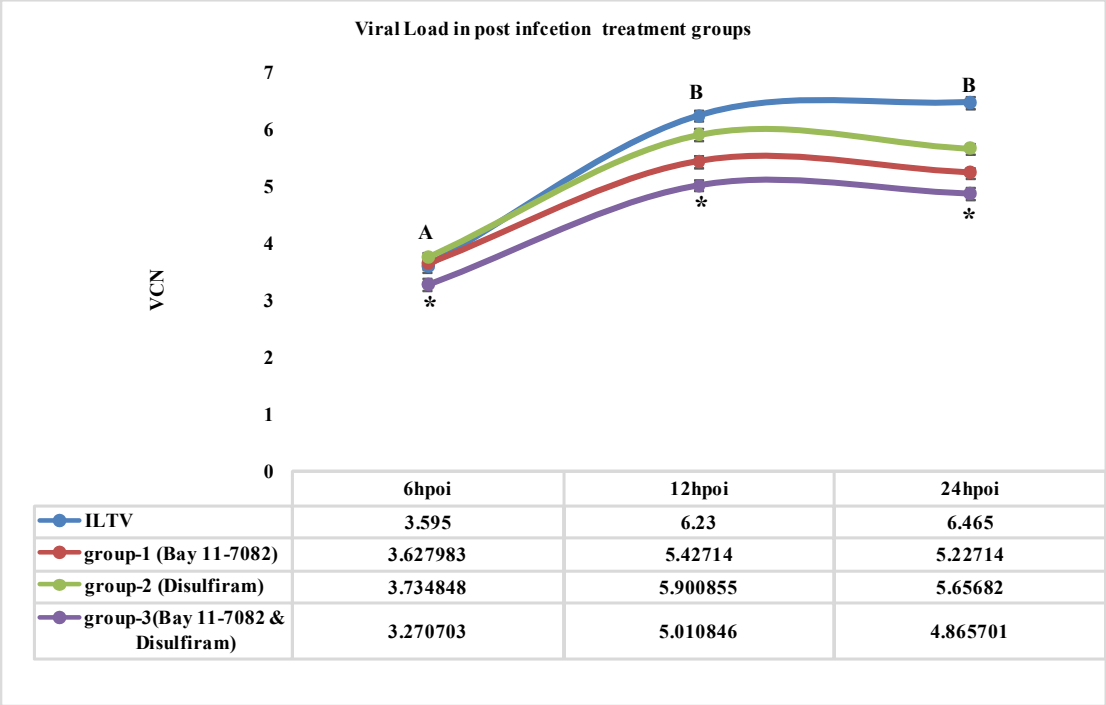

	6hpoi	12hpoi	24hpoi
ILTV	3.595	6.23	6.465
group-1 (Bay 11-7082)	3.627983	5.42714	5.22714
group-2 (Disulfiram)	3.734848	5.900855	5.65682
group-3(Bay 11-7082 & Disulfiram)	3.270703	5.010846	4.865701

Fig. 13: Graph showing viral copy number, estimated by SYBR green based absolute real time PCR in chicken embryo kidney cells post infection with ILTV (levels not connected by the same letter are significantly different between time points and * denotes significant difference within groups p<0.05)

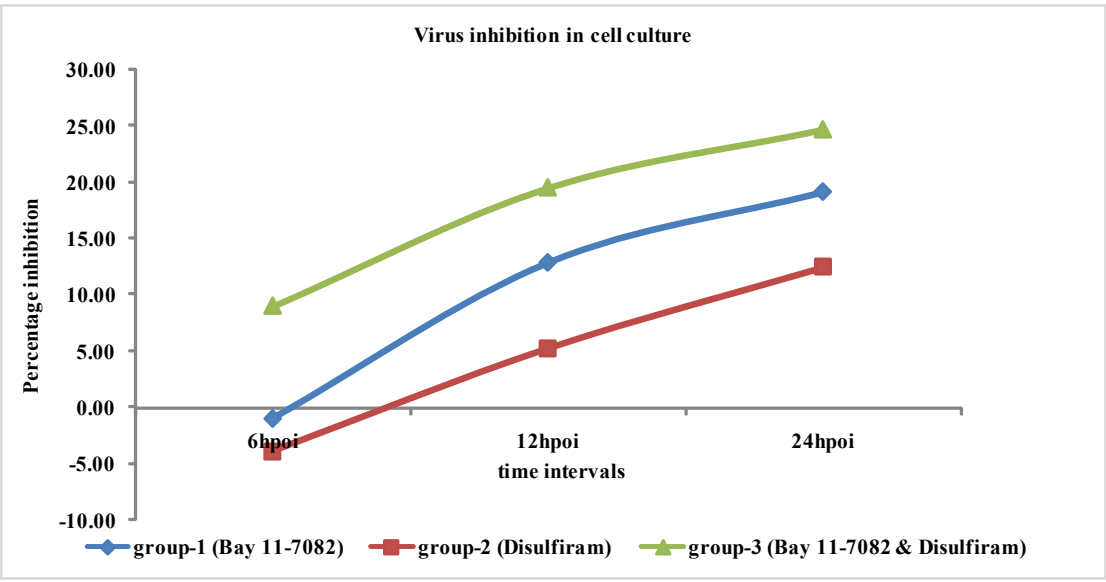

Fig. 14: Graph showing percentage inhibition at different time intervals in chicken embryo kidney cells post infection with ILTV

combination treatment, the percentage of viral inhibition was higher as compared to individual treatments (Figure 14). Between individual treatments of Bay 11-7082 and disulfiram, Bay 11-7082 treatment showed a higher percentage of viral inhibition.

4.9 Evaluation of pyroptosis markers by relative real time PCR using SYBR green for the designed experimental groups

4.8.1 The Expression pattern of caspase-1 during pre and post ILTV infection

There was no significant effect of treatment groups over time intervals in pre ILTV infection for the expression of caspase -1 but there was more significant difference between treatment groups with in time points with p value<0.001 (Fig. 15 A). Caspase-1 was significantly downregulated in all the treated groups as compared to the mock control over all the time intervals in the pre infection stage.

In post infection all treatment groups downregulated caspase-1 expression in the virus infected CEK cells, as compared to the mock control and virus control significantly (p value < 0.05) (Fig. 15 B). The combination of both drugs showed low caspase-1 expression across all the time intervals in post infection stage. This expression was lowest when compared to the mock group but at 12 hrs and 24 hrs, there was a steady decrease. When compared with virus control, all the treated groups showed low caspase-1 expression indicating its inhibition by the pyroptotic inhibitors.

4.9.2 The Expression pattern of during IL-1β pre and post ILTV infection

There was no significant effect of treatment groups over time intervals in pre ILTV infection for the expression of IL-1β but there was more significant difference between treatment groups with p value<0.001. The fold change for IL-1β expression was less in all the treated groups as compared to the mock control over all time intervals in the pre infection stage (Fig. 17 A).

In post infection in all treatment groups there was significant downregulation of IL-1β expression in the virus infected CEK cells, as compared to the mock control and virus control (pvalue < 0.05) (Fig. 17 B). The group treated with both drugs showed lowest IL-1β expression

across all the time intervals in the post infection stage. This expression was lowest when compared to the mock group but at 12 hrs and 24 hrs, there was a steady decrease in expression levels.

All the treated groups showed lower expression of IL-1β when compared to the virus control, indicating the blocking of IL-1β expression by pyroptotic inhibitors.

4.9.3 The Expression pattern of IL-18 during pre and post ILTV infection

There was no significant effect of treatment groups over time intervals in pre ILTV infection for the expression of IL-18 but there was high significant difference between treatment groups with p value<0.001 (Fig. 18 A). The Fold change for IL-18 expression is less in all the treated groups as compared to the mock control over all time intervals in the pre infection stage.

In post infection all treatment groups downregulated IL-18 expression in the infected CEK cells, as compared to the mock control and virus control significantly (pvalue < 0.05). The group treated with both drugs showed low IL-18 expression across all the time intervals in post infection stage. This expression was lowest when compared to the mock group but at 12 hrs and 24 hrs, there was a steady decrease in the expression levels. 1L-18 expression was low in the groups treated with Bay 11-7082, however high expression of IL-18 can be seen in the cells treated with disulfiram as compared to the mock group after 6hrs, indicating the varying effect of disulfiram on IL-18 expression (Fig. 18 B).

Decreased fold change of IL-18 can be seen in all the treated groups as the expression is low when compared with the virus control indicating the action of pyroptotic inhibitors on pyroptotic marker IL-18.

After blocking pyroptosis the following other types of cell deaths in ILTV infection had been double -checked using apoptosis and necroptosis markers:

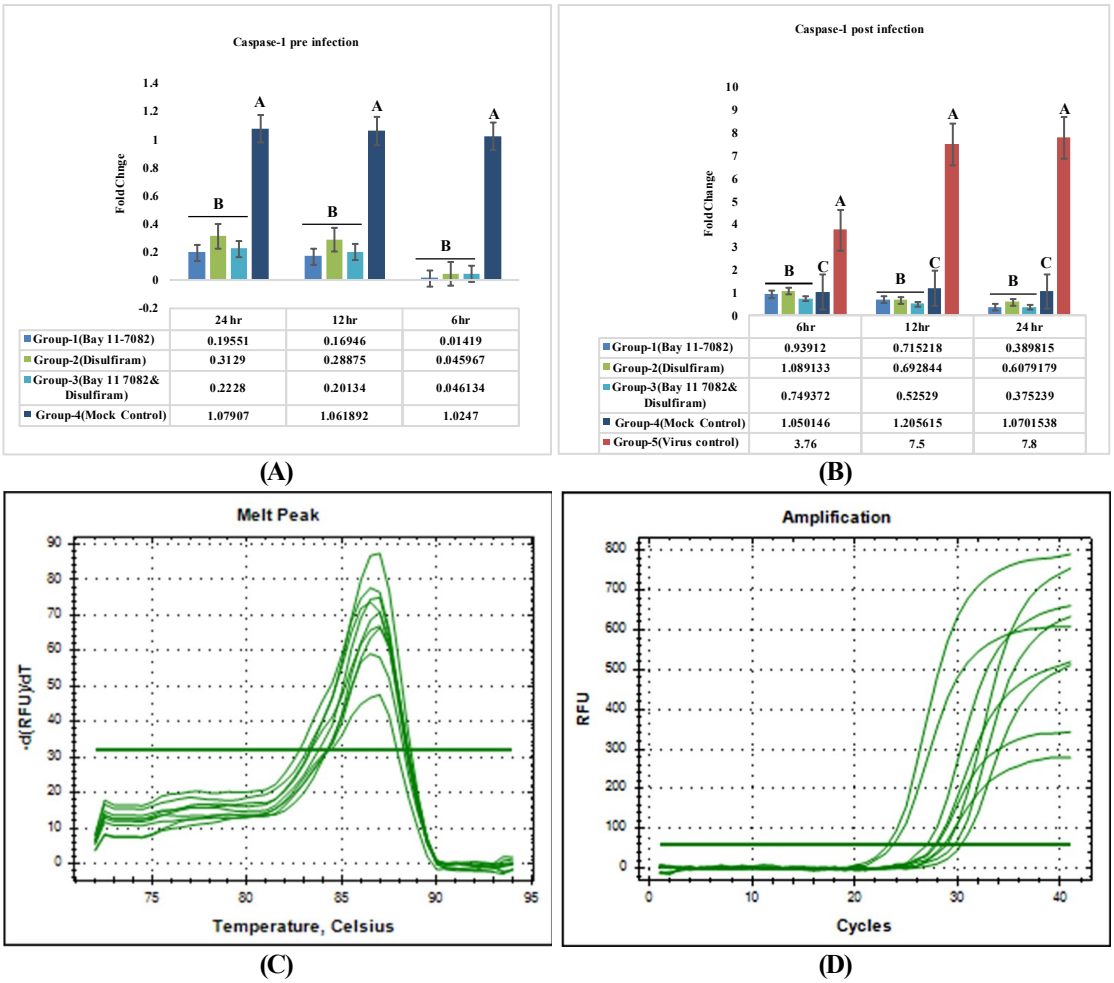

Fig. 15: A-D : Expression levels of Caspase-1 in all groups at different time intervals for pre and post ILTV infection : A,B. Graph ; C. Melt curve ; D. Amplification plot generated after SYBR green based relative real time PCR.

(Bar with different superscript indicate significant difference of P<0.05 from controls. values bearing different superscript between groups within time interval differ significantly)

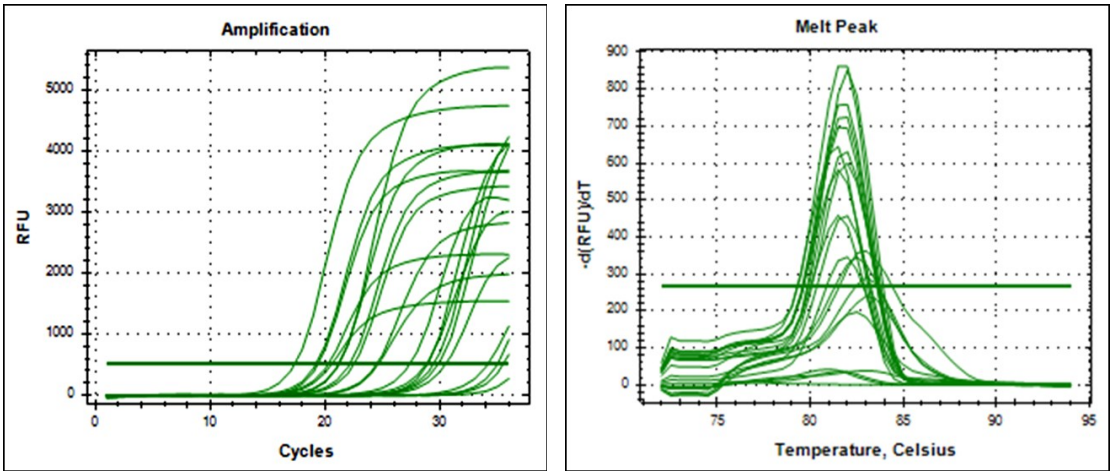

Fig. 16: Illustrated single peak amplification plot and dissociation curve generated during SYBR green based quantification of GAPDH

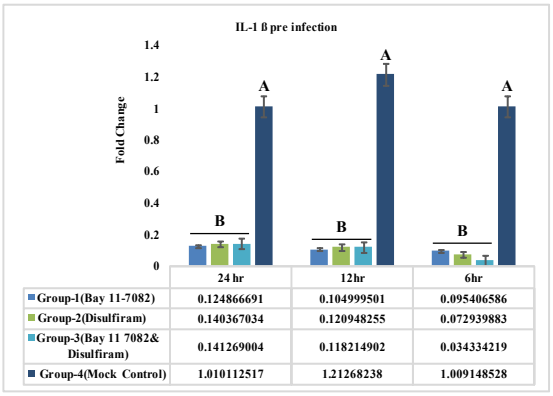

	24 hr	12hr	6hr
Group-1(Bay 11-7082)	0.124866691	0.104999501	0.095406586
Group-2(Disulfiram)	0.140367034	0.120948255	0.072939883
Group-3(Bay 11 7082& Disulfiram)	0.141269004	0.118214902	0.034334219
Group-4(Mock Control)	1.010112517	1.21268238	1.009148528

(A)

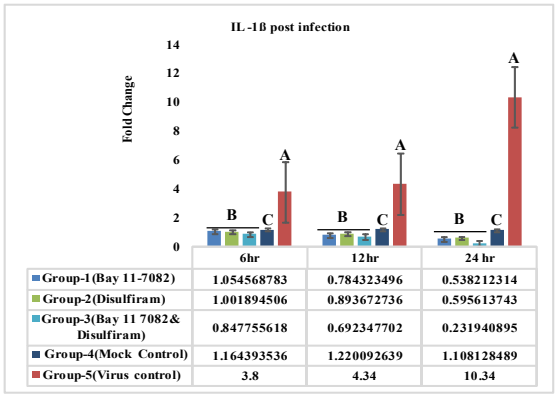

	6hr	12hr	24 hr
Group-1(Bay 11-7082)	1.054568783	0.784323496	0.538212314
Group-2(Disulfiram)	1.001894506	0.893672736	0.595613743
Group-3(Bay 11 7082& Disulfiram)	0.847755618	0.692347702	0.231940895
Group-4(Mock Control)	1.164393536	1.220092639	1.108128489
Group-5(Virus control)	3.8	4.34	10.34

(B)

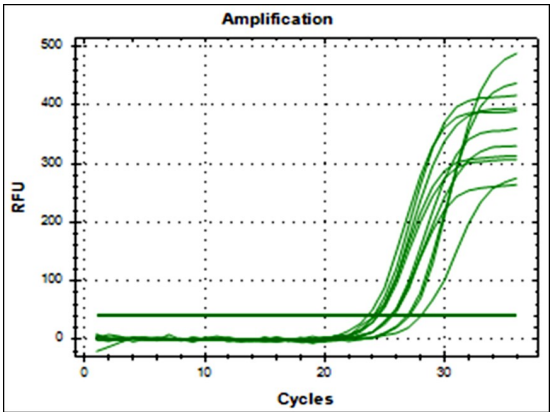

(C)

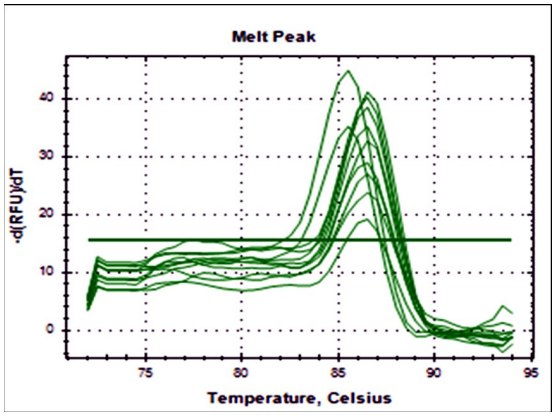

(D)

Fig. 17: A-D: Expression levels of IL-1â in all groups at different time intervals for pre and post ILTV infection: A, B. Graph; C. Amplification plot ; D. Melt curve generated after SYBR green based relative real time PCR.

(Bar with different superscript indicate significant difference of P<0.05 from controls. values bearing different superscript between groups within time interval differ significantly)

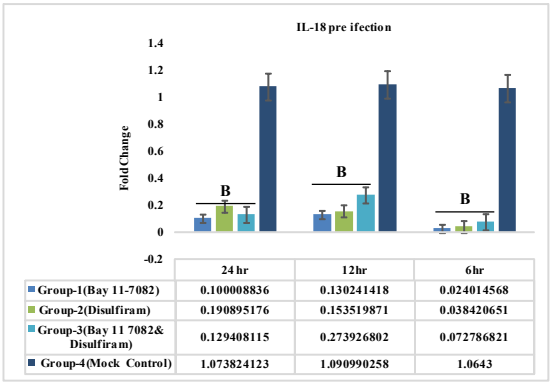

	24 hr	12hr	6hr
Group-1(Bay 11-7082)	0.100008836	0.130241418	0.024014568
Group-2(Disulfiram)	0.190895176	0.153519871	0.038420651
Group-3(Bay 11 7082& Disulfiram)	0.129408115	0.273926802	0.072786821
Group-4(Mock Control)	1.073824123	1.090990258	1.0643

(A)

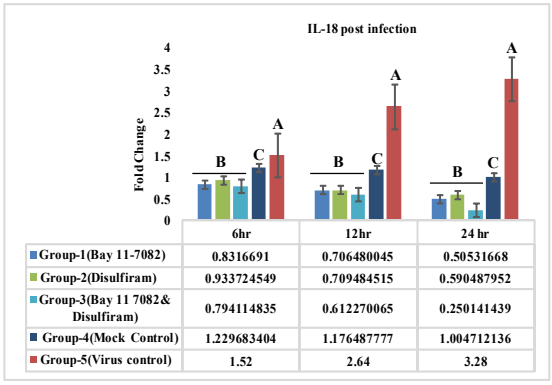

	6hr	12hr	24 hr
Group-1(Bay 11-7082)	0.8316691	0.706480045	0.50531668
Group-2(Disulfiram)	0.933724549	0.709484515	0.590487952
Group-3(Bay 11 7082& Disulfiram)	0.794114835	0.612270065	0.250141439
Group-4(Mock Control)	1.229683404	1.176487777	1.004712136
Group-5(Virus control)	1.52	2.64	3.28

(B)

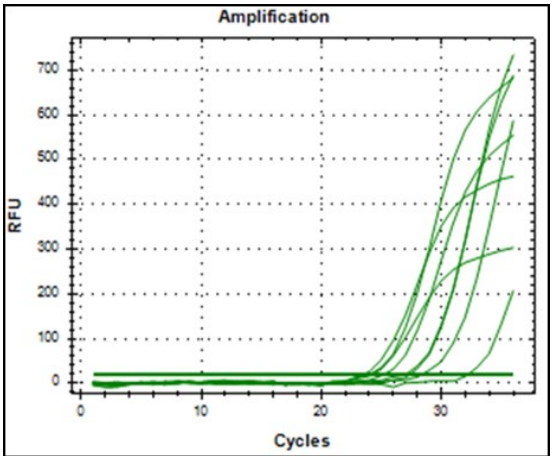

(C)

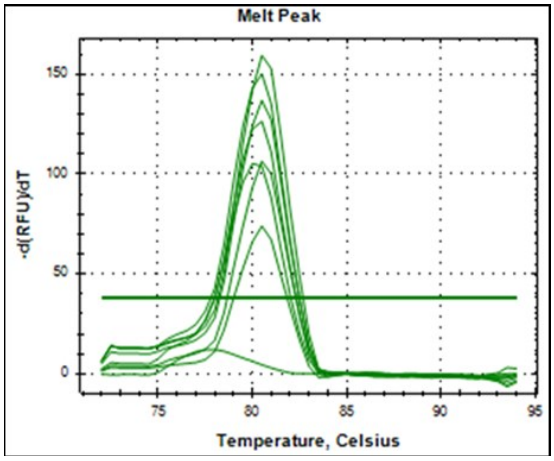

(D)

Fig. 18: A-D: Expression levels of IL-18 in all groups at different time intervals for pre and post ILTV infection : A,B. Graph; C. Amplification plot; D. Melt curve generated after SYBR green based relative real time PCR.

(Bar with different superscript indicate significant difference of $P<0.05$ from controls. values bearing different superscript between groups within time interval differ significantly)

4.10 Detection of apoptotic and necroptosis markers expression by qPCR

4.10.1 The Expression patterns of Apoptosis markers

4.10.1a The Expression pattern of caspase -3 post infection

There was a basal expression of caspase-3 in the treatment groups. There was significant difference between treatment groups within time as compared to mock control in post ILTV infection for the expression of caspase-3. The expression of Caspases-3 was upregulated compared to mock control and there was no significance difference between mock and virus control groups (Fig. 19)

4.10.1b The Expression pattern of caspase -8 post infection

There was a basal expression of caspase-8 in the treatment groups. There was significant difference between treatment groups within time as compared to mock control in post ILTV infection for the expression of caspase-8. The expression of Caspase-8 was down regulated compared to mock control and there was no significance difference between mock and virus control groups (Fig. 20).

4.10.1c The Expression pattern of caspase -9 post infection

There was a basal expression of caspase-9 in the treatment groups. There was significant difference between treatment groups with in time as compared to mock control in post ILTV infection for the expression of caspase-9. The expression of Caspase-9 was down regulated compared to mock control and there was no significance difference between mock and virus control groups (Fig. 21).

4.10.2 The Expression patterns of Necroptosis markers:

4.10.2a The Expression pattern of RIP K-1 post infection

The expression of RIP K-1 was upregulated in treatment groups and there was a significant difference between the treatment groups with in time when compared to the mock control and virus control. Expression of RIP K-1 was upregulated in Virus control as compared to mock control. (Fig. 22).

4.10.2b The Expression pattern of RIP K-3 post infection

The expression of RIPK-3 in treatment groups and virus control was downregulated when compared to mock control and there was no significant difference between the treatment groups, mock control and virus control (Fig. 23).

✍✍✍

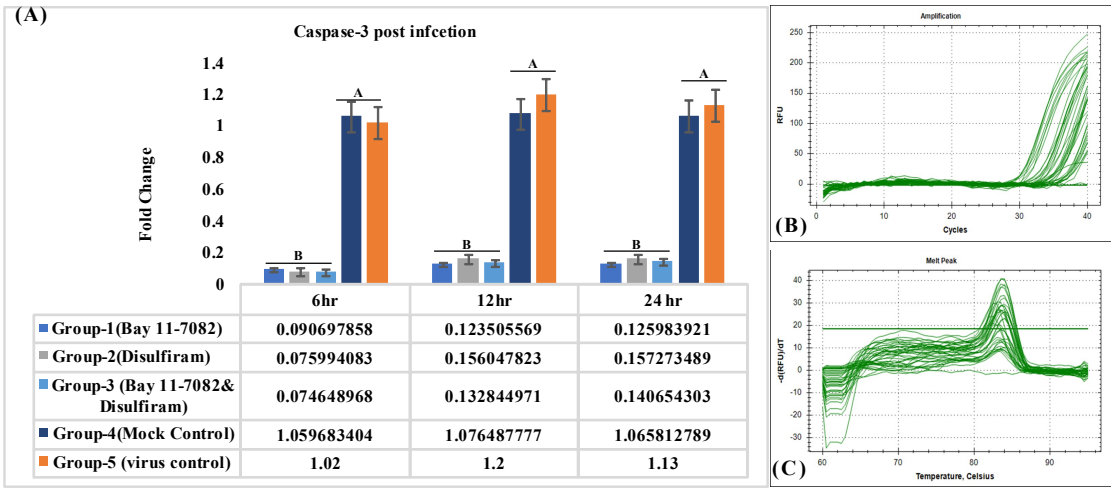

	6hr	12hr	24 hr
Group-1(Bay 11-7082)	0.090697858	0.123505569	0.125983921
Group-2(Disulfiram)	0.075994083	0.156047823	0.157273489
Group-3 (Bay 11-7082& Disulfiram)	0.074648968	0.132844971	0.140654303
Group-4(Mock Control)	1.059683404	1.076487777	1.065812789
Group-5 (virus control)	1.02	1.2	1.13

Fig. 19: A-C : Expression levels of Caspase-3 in all groups at different time intervals for post ILTV infection : A. Graph; B. Amplification plot; C. Melt curve generated after SYBR green based relative real time PCR.

(Bar with different superscript indicate significant difference of P<0.05 from controls. values bearing different superscript between groups within time interval differ significantly)

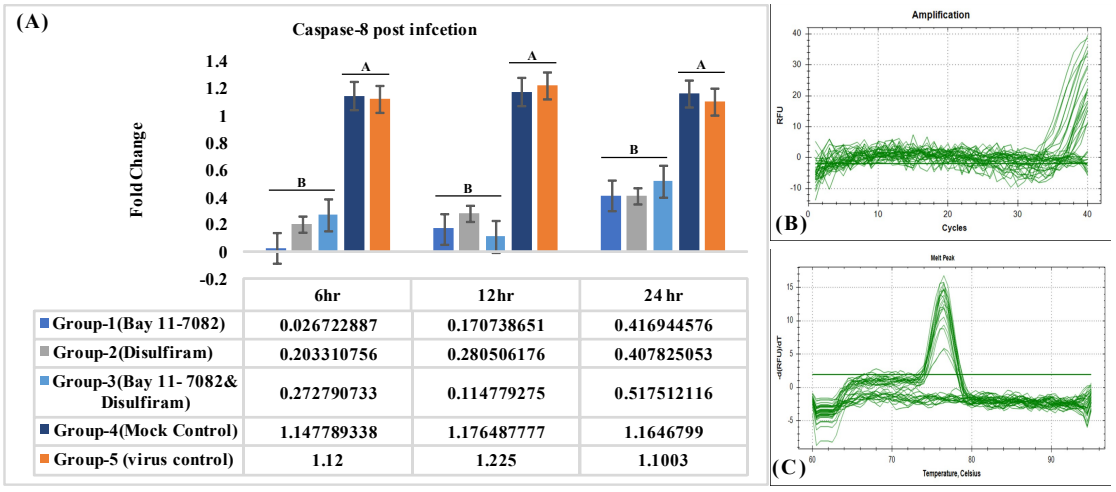

	6hr	12hr	24 hr
Group-1(Bay 11-7082)	0.026722887	0.170738651	0.416944576
Group-2(Disulfiram)	0.203310756	0.280506176	0.407825053
Group-3(Bay 11- 7082& Disulfiram)	0.272790733	0.114779275	0.517512116
Group-4(Mock Control)	1.147789338	1.176487777	1.1646799
Group-5 (virus control)	1.12	1.225	1.1003

Fig. 20: A-C :Expression levels of Caspase-8 in all groups at different time intervals for post ILTV infection : A. Graph ; B. Amplification plot ; C. Melt curve generated after SYBR green based relative real time PCR.

(Bar with different superscript indicate significant difference of P<0.05 from controls. values bearing different superscript between groups within time interval differ significantly)

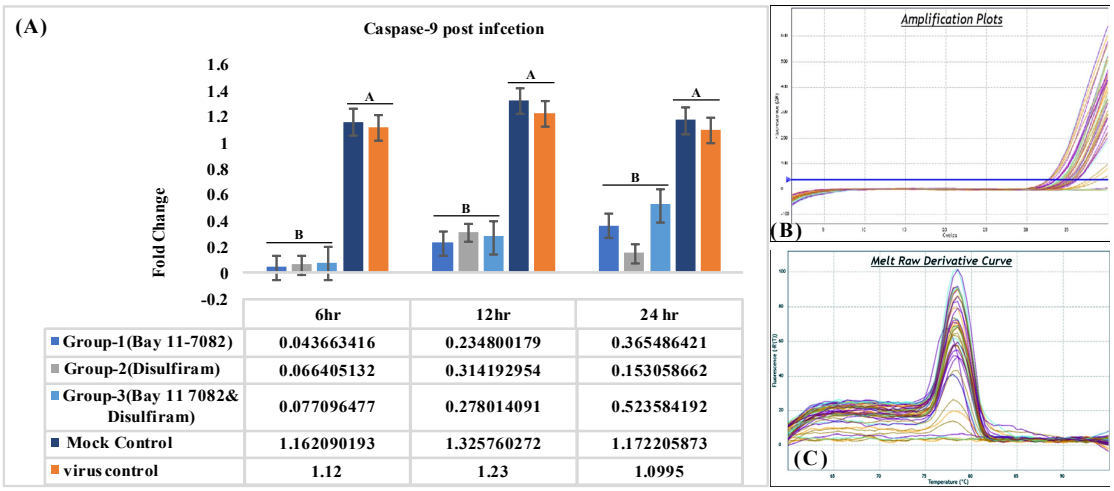

	6hr	12hr	24 hr
Group-1(Bay 11-7082)	0.043663416	0.234800179	0.365486421
Group-2(Disulfiram)	0.066405132	0.314192954	0.153058662
Group-3(Bay 11 7082& Disulfiram)	0.077096477	0.278014091	0.523584192
Mock Control	1.162090193	1.325760272	1.172205873
virus control	1.12	1.23	1.0995

Fig. 21: A-C: Expression levels of Caspase-9 in all groups at different time intervals for post ILTV infection : A. Graph ; B. Amplification plot ; C. Melt curve generated after SYBR green based relative real time PCR.

(Bar with different superscript indicate significant difference of P<0.05 from controls. values bearing different superscript between groups within time interval differ significantly)

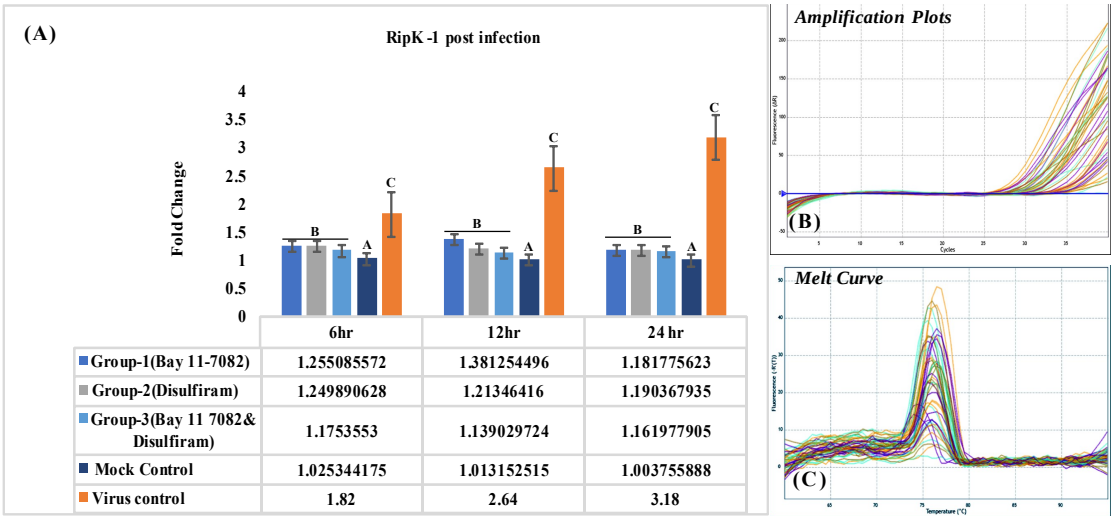

	6hr	12hr	24 hr
Group-1(Bay 11-7082)	1.255085572	1.381254496	1.181775623
Group-2(Disulfiram)	1.249890628	1.21346416	1.190367935
Group-3(Bay 11 7082& Disulfiram)	1.1753553	1.139029724	1.161977905
Mock Control	1.025344175	1.013152515	1.003755888
Virus control	1.82	2.64	3.18

Fig. 22: A-C: Expression levels of RIPK-1 in all groups at different time intervals for post ILTV infection : A. Graph ; B. Amplification plot ; C. Melt curve generated after SYBR green based relative real time PCR.

(Bar with different superscript indicate significant difference of P<0.05 from controls. values bearing different superscript between groups within time interval differ significantly)

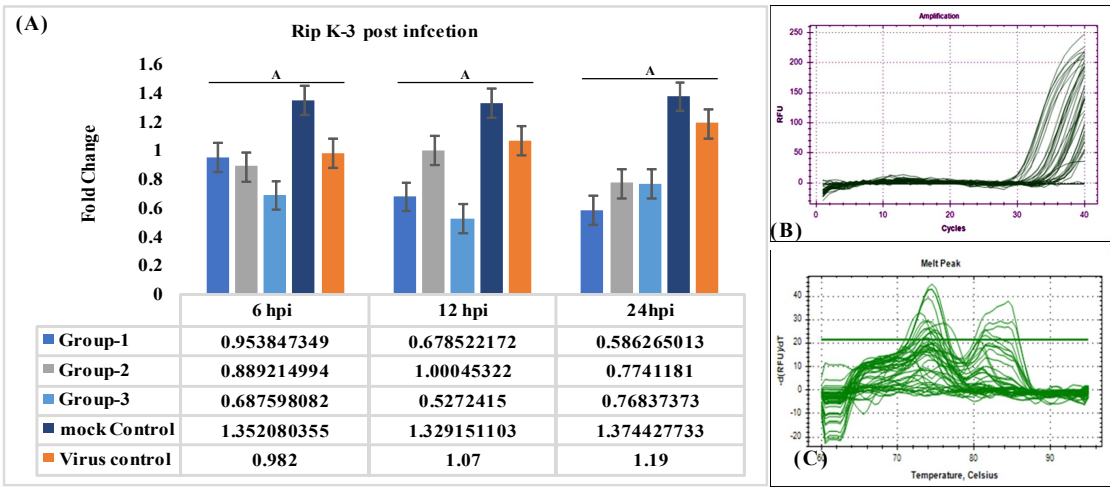

	6 hpi	12 hpi	24hpi
Group-1	0.953847349	0.678522172	0.586265013
Group-2	0.889214994	1.00045322	0.7741181
Group-3	0.687598082	0.5272415	0.76837373
mock Control	1.352080355	1.329151103	1.374427733
Virus control	0.982	1.07	1.19

Fig. 23: A-C: Expression levels of RIPK-3 in all groups at different time intervals for post ILTV infection : A. Graph ; B. Amplification plot ; C. Melt curve generated after SYBR green based relative real time PCR.

(Bar with different superscript indicate significant difference of P<0.05 from controls. values bearing different superscript between groups within time interval differ significantly)

Discussion

5 DISCUSSION

ILT is an acute and contagious disease majorly affecting the upper respiratory tract of chickens and characterised by respiratory distress, pump handle type breathing, gasping, rattling laryngeal sounds, 90-100% morbidity, 1-17% mortality and a considerable drop in egg production (Gowthaman *et al.,* 2014, Tamilmaran *et al.,* 2020). The first report was recorded by Singh *et al.,* in 1964 in India where they isolated the virus from field outbreaks by the CAM inoculation method. It has also been reported in some European countries of North America, Central America, South America, Caribbean, Europe and Asia (Hidalgo, 2003; Chacon and Ferreira, 2009; OIE, 2014; Magouz *et al.,* 2018). Other researchers had reported clinical cases of ILT in chickens with a history of high morbidity and considerable mortality and clinical signs of oculo-nasal discharges, conjunctivitis, respiratory distress, and gasping (Gowthaman *et al.,* 2020). Vaccination against ILTV is efficient in preventing infection. Aside from their efficacy, CEO and TCO vaccines have the unfavourable property of reverting to the virulent form upon bird-to-bird transmissions, resulting in vaccinal laryngotracheitis in the field (Dufour-Zavala, 2008; Chacon *et al.,* 2015). Vaccination can sometimes result in the development of latent carrier birds, which serve as a source of infection for unvaccinated populations (Bagust, 1986). Apart from vaccination, therapeutic approaches for ILTV must be explored further. Recent studies have found that pyroptosis plays an important role in many chicken infections. According to our hypothesis pyroptosis could be important in the pathogenesis of ILTV which causes intense inflammatory pathology in the conjunctiva and respiratory mucosa of chickens. Since elucidating the mode of cell death that aggravate inflammation in ILT will aid in identifying the root cause of inflammation, intervention strategies to block that specific cell death pathway

can be devised using inhibitors, which will help to reduce the negative effects of ILT virus-induced inflammation. Early work validated the presence of pyroptosis markers in naturally infected ILTV chickens as well as infected CEK cells (Kohale,2022). These observations are supported in the present work. Based on this, we assume that, by blocking this proinflammatory cell death pathway (pyroptosis), the pathology associated with exacerbated inflammation during ILT might reduce. Therefore, keeping this in view, the current study has been proposed with the objective to assess the effects of pyroptotic inhibitors on ILTV induced inflammation in epithelial cells of chicken origin.

Chicken tracheal cell culture has been used to study the infection of important respiratory viruses in birds, such as Newcastle disease and avian influenza (Zaffuto *et al.*, 2008). Although it is known that the trachea is the site of ILTV replication, studies on the isolation and behaviour of ILTV in chicken tracheal epithelial cell culture need to be explored. Indeed, many scientists have thoroughly analyzed various primary cultures and cell lines for the propagation of ILTV (Huges and Jones, 1988; Schnitzlein *et al.*, 1994; Portz *et al.*, 2008), in which they reported that Vero cell lines, Leghorn male hepatoma (LMH), and chicken embryo related (CER) primary cultures presented the optimal conditions for the growth of ILTV and showed cytopathic effect up to 96 hours. Even though LMH cell lines are mostly used for in-vitro studies in ILTV infections, primary cultures are the most effective at modelling in-vivo systems for exploring the immediate host response and infection pathways. Moreover, external proteases are needed for protein cleavage, hence this study was planned with an attempt to mimic the viral replication and host immune response in a system which acts as an exact replica of the site of viral replication in morbid birds. Apart from CER cultures, primary avian tracheal cell culture has never been attempted for the propagation of ILTV, while the trachea being one of the major sites for viral replication. We tried to standardise a protocol to establish an avian tracheal cell culture system to study viral replication and immediate host response according to the protocol given by Zaffuto *et al.* (2008). In this experiment, they were able to establish a growth curve for replication of NDV with low MOI confirming attachment, replication, the release of the virus and re-entry into the other cells. Unfortunately, in our experiment, we could not standardize the protocol for culturing tracheal epithelial cells even after several attempts that could facilitate the survival of tracheal cells throughout the experimental procedure. As an alternative method,

we opted for a chicken embryo kidney cell (CEK) culture system to study the effects of pyroptotic inhibitors on ILTV induced inflammation in epithelial cells of chicken origin.

For the present work, pre-propagated ILTV in CEK cells was used, and its persistence was determined by calculating viral titres using the Reed and Muench method to achieve $\log_{10}$TCID50 in the Avian Disease Section, Division of pathology, ICAR-IVRI. This was confirmed with a standard viral growth curve. Morphological changes like cell rounding, cell aggregation and cell death were noticed after 24 hpi and it persisted till 96 hpi when most of the monolayer was detached. Likewise, Portz *et al.,* (2008) observed a cytopathic effect 24 hours after inoculation of ILTV in CER cell lines.

Pyroptotic cell death is a very well-established feature of NLRP3 inflammasome activation either by canonical (caspase-1) or non-canonical (caspase-4, 5, 11) pathway that leads to GSDMD cleavage. Pyroptotic death elicits inflammation due to the release of cytosolic contents such as LDH, ATP, HMGB1 and IL-1α (Broz *et al.,* 2020). Activation of NLRP3 inflammasome is believed to be a two-step process (Latz *et al.,* 2013). In the two-signal model of inflammasome activation, "signal I/priming" (LPS or another pathogen-associated molecular pattern) induces the transcriptional upregulation of NLRP3 and pro inflammatory cytokines expression of pro-IL-1β and pro-IL-18, but fails to trigger maturation or release of these cytokine. For productive cytokine processing and secretion, a second signal ("signal II/ activation") induces processing of pro-cytokines to their active forms, which is then released into the extracellular space. This second signal is used for induction to carry out the processing of cytokines by a broad range of factors including PAMPs and DAMPs, e.g., nigericin toxin, extracellular ATP, as well as lysosomal destabilization agents such as silica and cholesterol crystals (Broz *et al.,* 2020). den Hartigh and Fink (2018) described the method where they activated caspase-1 via the NLRP3 inflammasome by treating murine bone marrow macrophages (BMM) with 100 ng/ml of LPS and 5μM of Nigericin and subsequent pyroptotic cell lysis is assessed by measuring the release of the cytoplasmic enzyme LDH. Likewise in the present study, we induced caspase-1 activated NLRP3 inflammasome mediated pyroptosis in CEK cells by different doses of LPS and (5μM) nigericin which increased the released LDH by compromising the cell membrane, suggesting the pyroptotic cell lysis. In our study, CEK

cells were treated with different doses of LPS like 0.5 µg/ml, 1 µg/ml, 2.5 µg/ml, 5 µg/ml, and 10 µg/ml to ascertain a safe dose that induces pyroptosis in CEK cells. According to our study, we found that 2.5 µg/ml of LPS and 5µM nigericin showed optimal cytotoxic levels by elevated LDH release inducing pyroptosis. This induction of pyroptosis is in line with the den Hartigh and Fink (2018).

The emerging studies suggest that the activation of the NLRP3 inflammasome promotes pyroptosis cell lysis and inhibiting this LPS-induced pyroptosis could be a promising therapeutic target for treating various inflammasome mediated diseases. Bay 11-7082 is a phenyl vinyl sulfone; it inhibits the NF-κB pathway through the blockade of the kinase activity of IKKβ. It inhibits its target proteins using the alkylation of essential nucleophilic residues, for example, cysteines (Zahid *et al.,* 2019). BAY 11-7082 has pharmacological activities that include anticancer, neuroprotective, and anti-inflammatory effects (Lee *et al.,* 2012). Bay 11-7082 is known to inhibit NF-κB (Hu *et al.,*2018) and NLRP3 Inflammasome activation in NG-5 Cell lines (Juliana *et al.,* 2010). . Disulfiram is an FDA-approved drug to treat chronic alcoholism, which inhibits pyroptosis by inhibiting N-GSDMD pore formation (Zhou *et al.,* 2022). Disulfiram has been repurposed to treat several diseases including cancer and bacterial infections and recently has been suggested as a potential therapy for COVID -19 infection (Blevins *et al.,* 2022). Recent findings have shown that disulfiram inhibits directly both canonical & non-canonical caspases and additionally IL-1β release by altering Cys191 of GSDMD, which in turn inhibits the formation of GSDMD pores and the subsequent pyroptosis in human and mouse cells (Hu *et al.,* 2020). According to Liu *et al.* (2016); Ruan *et al*. (2018) both these compounds were reported to covalently modify a conserved Cys in gasdermin D that is critical for pore formation. In support of existing knowledge, in the present study we used Bay11-7082 and Disulfiram in single and combination treatment to block the LPS /nigericin induced pyroptosis. Deng *et al.* (2020) studies stated that disulfiram inhibited NLRP3-dependent IL-1β secretion with an IC_{50} of 5 µM under LPS/ATP conditions in mouse macrophages. Jiang *et al.* (2017) studies stated that Bay 11- 7082 inhibited IL-1β production in BMDM's with an IC50 of 12 µM. In our study we inhibited LPS/Nigericin induced CEK cells with different doses of Bay11- 7082 and Disulfiram viz.,1 µM,2µM,5µM, and10 µM which is in agreement with the previous study reports. We found that Bay 11-7082 and disulfiram inhibited pyroptosis

induction at a concentration of 10μM when used separately and at a concentration of (5 μM +5 μM) Bay 11-7082 and disulfiram combination based on the % LDH release cytotoxic assessment. This is the first attempt where combination treatment of Bay 11-7082 and disulfiram were used to inhibit LPS/nigericin mediated NLRP3 inflammasome activation in CEK cells.

Our study on these inhibitor compounds on CEK cell viability assessment by MTT revealed that Bay 11-7082 significantly reduced the viability of cells whereas, Disulfiram did not affect the survivability of CEK cells. Similarly, in post infection, we observed that the combined treatment of compounds had an additive protective effect against ILTV infected epithelial cells rather than the individual drug treatment. As all of these findings were evident with the SYTOX green staining and Lyso tracker deep red assay.

To evaluate whether Bay 11-7082 and Disulfiram inhibit pyroptosis, we added these compounds to CEK cells and ILTV infected CEK cells and collected samples at time dependent manner to check the expression of pyroptosis markers via SYBR green based relative real time PCR. Hu *et al.* (2020) stated that disulfiram suppresses GSDMD as well as caspases. Bay 11-7082 and disulfiram are also capable of blocking GSDMD pore formation and pyroptosis by covalently modifying a conserved Cys (Cys192 in mouse and Cys191 in human GSDMD) that is essential for the formation of membrane pores (Hu *et al.*, 2018). In our study, we observed that there was downregulation of caspase-1, IL-1β, and IL-18 expression in all inhibitor treated post infection groups as compared to mock control and virus control further it was also observed that there was time dependent reduction in expression of caspase-1, IL-1β, and IL-18 in infected CEK cells by relative real time PCR. Bay 11-7082 was known to inhibit NF-κB activation, a key transcription factor in priming NLRP3 inflammasome and was more effective at inhibiting canonical inflammasome-dependent pyroptosis than disulfiram and the two drugs together had a synergistic protective effect in blocking pyroptosis although they were cytotoxic at the highest concentration tested. GSDMD plays a crucial role in the host response to microbial infection, including viruses. A key component of pyroptosis is the pore-forming protein gasdermin D; but according to previous reports, the GSDMD protein was not detectable in chickens. In this study, we observed that Disulfiram was less active than Bay 11-7082 in inhibiting pyroptosis in infected CEK cells. We interpret that this may be due

to the absence of target blocking of Disulfiram on GSDMD in chickens. Studies on the roles and functions of disulfiram on other members of chicken gasdermin are very scanty and need further investigation. All this evidence of detection of downregulated pyroptosis markers like caspase-1, IL-1β, and IL-18 in this study directs to the possibility of the role of Bay 11-7082 and Disulfiram in pyroptotic cell death pathway in ILTV infected CEK cells.

Calculation of viral copy number was done by absolute real time PCR to further confirm the amount of viral genome present after treatment with inhibitors in post infection groups. Results of quantitative PCR revealed a significant reduction in viral load with the combination treatment. Bay 11-7082, however, caused a greater reduction in viral load than the Disulfiram treatment. Zeng *et al.* (2021) reported that inhibition of NLRP3 inflammasome attenuated the release of COVID-19 related pro inflammatory cytokines in THP-1 cells and mice. Research findings strongly suggested that Bay 11-7082 suppressed NF-Kb signalling activity and limited the subsequent proinflammatory responses in virus-infected CEK cells, making it a potent inhibitor of pyroptosis. However, it was found that it is less viable for the cells than disulfiram in our study. Chen *et al.* (2022) reported that disulfiram inhibited viral replication by blocking Mpro protease and zinc ejection in the virus making the viral structure unstable and the subsequent virus lysis. It is not yet clear whether disulfiram has the capacity to block the efficiency of ILTV to enter host cells. The decreased viral load coincided with the observation of significant downregulation of pyroptosis markers in the real time PCR. The mechanistic details of the pyroptosis induced by ILTV and the functional consequences of pyroptosis have not been well elucidated.

Cell death pathways have long been considered to function in parallel with little or no overlap. However, to assess whether inhibition of pyroptosis could activate apoptotic/ necroptotic cell death pathways in ILTV infected cells. We evaluated the expression of apoptotic caspases-3, 8 and 9 as well as necroptotic markers RIP-1 and RIP-3 kinases by quantifying in real time PCR. Our results showed that there was no expression of apoptosis and necroptosis markers in ILTV infected cells as well as in post infection treatment groups. Reddy *et al.* (2014) studies suggested non-significant apoptotic cell death on ILTV affected cells of tracheal and conjunctival mucosae. The findings are in corroboration with our present study wherein

ILTV infected CEK cells, there was no expression of apoptosis markers was revealed in this study. Even though some studies reported that in addition to mediating endogenous apoptotic pathways, caspase-8 can also participate in the cleavage of gasdermin (GSDM) family proteins to induce pyroptosis (Xia *et al.,* 2020). Further research is needed to elucidate the role of gasdermin in chicken ILTV infected cells. Although the executive necroptosis marker RIPK-3 was not expressed in the post-infection treatment group cells, there was RIPK-1 expression in the infected CEK cells and treatment groups, suggesting the absence of the necroptosis pathway.

The present study served as the first step in using inhibitors targeting the pyroptosis pathway in ILTV infected Chicken epithelial cells to characterize the role of Bay 11-7082 and Disulfiram in the pathogenesis of ILTV, and we found the potential of targeting NLRP3 inflammasome induced pyroptosis as the immune intervention for the pathogenesis of ILTV in chickens. The results of the current research require further confirmation of these markers using various techniques. Other antipyroptosis inhibitors can also be studied further in order to block the dysregulation of an excessive pro inflammatory response caused by pyroptosis in ILTV infection, hence limiting morbidity and mortality and minimizing the economic losses to the poultry industry.

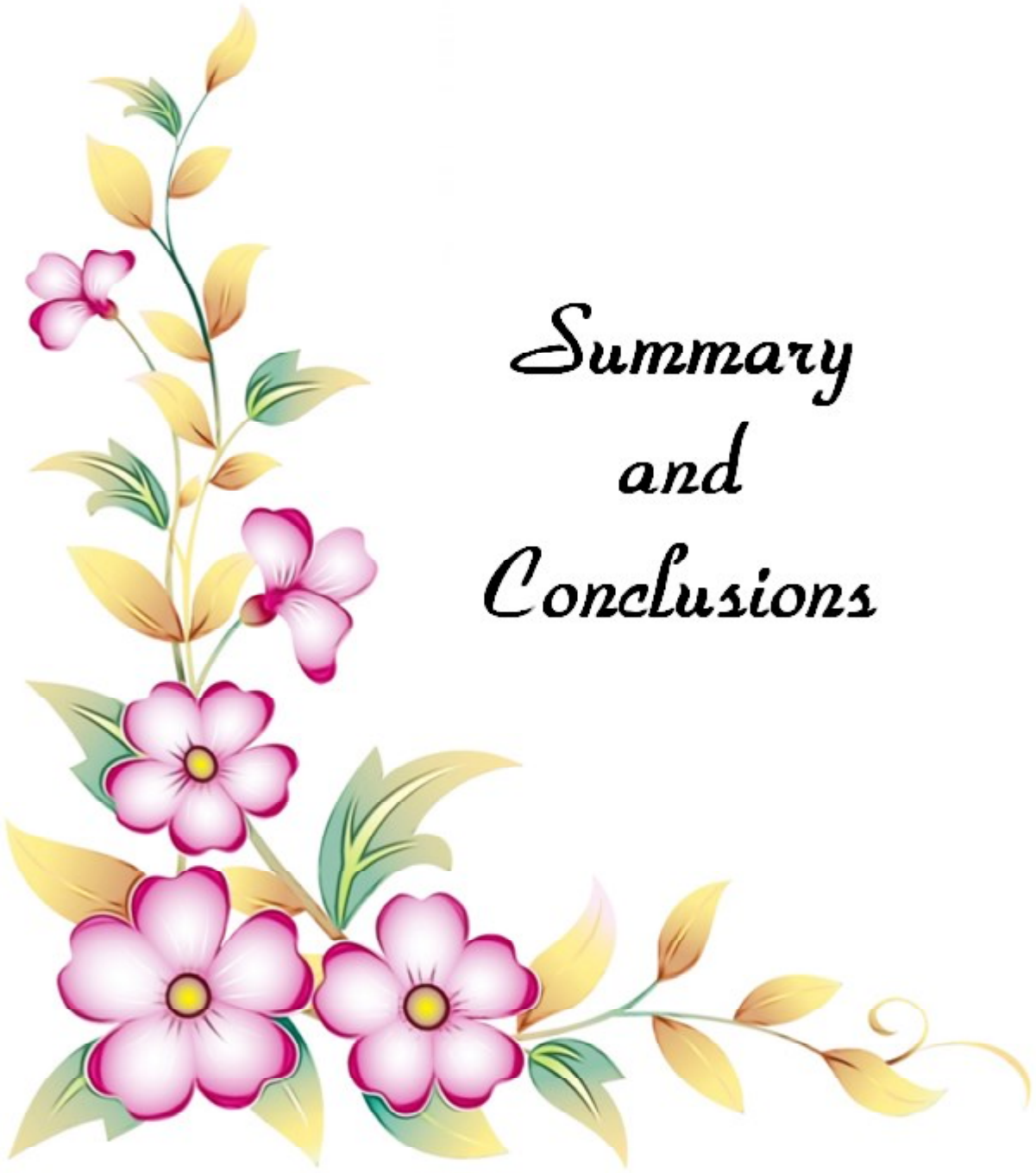

Summary and Conclusions

6 SUMMARY AND CONCLUSIONS

The present study was aimed to explore the effects of pyroptosis inhibitors on Infectious Laryngotracheitis Virus induced damage in chicken epithelial cells.

The entire research work was done on Chicken embryo kidney epithelial cells. Standardisation of doses for pyroptotic inhibitors like LPS & Nigericin was done based on the cytotoxicity assessment by % LDH release on CEK cells. The pyroptosis induction doses for LPS (2.5μg/ml) / Nigericin (5 μM) were standardised. Then, pyroptosis inhibition doses of Bay 11-7082 & disulfiram were standardized based on the % LDH release of the LPS/ Nigericin primed CEK cells. The doses for Bay 11-7082 (10 μM); Disufiram (10 μM); and for combination of Bay 11-7082 & Disulfiram (5 μM +5 μM) was standardized. These standardized doses were used for the entire experiment. In pre-ILTV infections, the combination group showed relatively constant cell survivability in MTT assay up to 24 hrs as compared to the mock control. Bay 11-7082 treatment significantly decreased the cell viability of CEK cells as compared to disulfiram alone treated cells and mock control. In post-ILTV infection, the cell survivability of all treatment groups was consistent till 24 hrs whereas the disulfiram treated group had relatively lower viability as evident by SYTOX green stain and Lyso tracker deep red assay. In SYBR green based real time PCR, the quantification of mRNA expression levels of pyroptosis markers in pre and post ILTV infection revealed that, pyroptotic markers (caspase-1, IL-1β and IL-18) expression was downregulated significantly in post-ILTV pyroptosis inhibitor-treated groups. All the inhibitors treated groups showed nearly equal efficacy in inhibiting pyroptosis but the combination had better results, notably at 12 & 24 hr. Even alone treatments of Bay 11- 7082 and Disulfiram downregulated the caspase 1, IL-1β, IL-18

mRNA expression in ILTV-infected CEK cells in a dose & time-dependent manner. This downregulation also matched with the viral load quantification calculations, where the virus copy number decreased in Bay 11- 7082 treatments when compared to disulfiram at periodic intervals. Compared to ILTV-infected CEK'S, the viral copy numbers were significantly decreased in combination treatments similar to the viral inhibition kinetics. Disulfiram is a potent GSDMD blocker but further studies are required to confirm its role as an executioner of pyroptosis in Avian cells. Through the results of our study we can assume that the downregulated expression of Caspase-1, IL-1β, IL-18 might be attributed due to some unexplored gasdermin blocking mechanism by Disulfiram.

To assess whether inhibition of pyroptosis could activate apoptotic/ necroptotic cell death pathways in ILTV infected cells. We evaluated the expression of apoptotic caspases-3, 8 and 9 as well as necroptotic markers RIP K-1 and RIP K-3 by quantifying in real time PCR. There was no expression of apoptosis and necroptosis markers in ILTV infected CEK cells as well as in pyroptosis blocked infected CEK cells. Hence Bay 11- 7082 and Disulfiram have proven antipyroptotic role in cultured CEK cells infected with ILTV characterised by a reduction in pyroptosis markers and the additional benefit of reduction in viral load. Therefore, pyroptotic inhibitors ameliorate the damage induced by ILTV in cultured CEK cells making it a potential therapeutic agent that can be used in flocks which are susceptible and suffering from ILTV infection.


Mini Abstract

7 MINI ABSTRACT

Avian infectious laryngotracheitis (ILT) is an upper respiratory disease that causes severe economic losses in the poultry industry, mainly due to high morbidity and mortality and reduced egg production. It is caused by *Gallidherpes virus-1* (GaHV-1) characterised by oculo-nasal discharges, conjunctivitis, respiratory distress, and gasping. One of the main reasons for desquamation is due to infiltration of proinflammatory cytokines in tracheal epithelial mucosa and cell death due to viral replication. Recently, there has been an increasing interest in pyroptosis due to its emerging role in pathogenesis of inflammatory diseases. The resurgence or re-emergence of ILT in vaccinated chicken flocks alters the hunt for therapeutic approaches. Since elucidating the mode of cell death that aggravate inflammation in ILT will aid in identifying the root cause of inflammation, intervention strategies to block that specific cell death pathway can be devised using inhibitors, which will help to reduce the negative effects of ILT virus-induced inflammation. To understand this, a study was carried out to analyse the effects of inhibitors on ITV induced inflammation in the chicken epithelial cell culture system. Here we standardized the dose of LPS for the induction of pyroptosis in CEK cells by % LDH release cytotoxic assessment. Then, doses of Bay 11-7082 and Disulfiram inhibitors were determined by % LDH release cytotoxic assessment for this standard dose of LPS/Nigericin primed CEK cells. Cell viability experiments done on assessing the effect of inhibitors on uninfected CEK cells (pre-infection) and ILTV infected CEK cells (post-infection) revealed that Bay 11-7082 treatment reduced the survivability of uninfected CEK cells whereas, in infected CEK cells, disulfiram treatment reduced the survivability. In-vitro gene expression studies of these Bay11-7082 and disulfiram inhibitors on ILTV infected CEK cells revealed remarkable downregulation of the expression of pyroptosis markers (caspase-1, IL-1β and IL-18). Similarly, these findings coincided with viral load quantification and viral inhibition calculation done at different time intervals. There was no evidence of expression of apoptosis or necroptosis markers after blocking the pyroptosis mediated pro inflammatory cytokine expression in ILTV infected CEK cells with inhibitors. Hence Bay 11- 7082 and Disulfiram have proven antipyroptotic role in cultured CEK cells infected with ILTV characterised by reduction in pyroptosis markers and the additional benefit of reduction in viral load. Therefore, pyroptotic inhibitors ameliorates the damage induced by ILTV in cultured CEK cells making a potent therapeutic agent that can be used in flocks which are susceptible and suffering with ILTV infection

लघु सारांश

8 लघु सारांश

एवियन संक्रामक लैरींगोट्रेकाइटिस (आईएलटी) एक ऊपरी श्वसन रोग है जो पोल्ट्री उद्योग में मुख्य रूप से उच्च रूग्णता और मृत्यु दर और अंडे के उत्पादन में कमी के कारण गंभीर आर्थिक नुकसान करता है। यह गैलिड हरपीज वायरस–1 के कारण होता है, जिसकी विशेषता नेत्र–नाकीय स्राव, नेत्रश्लेष्मलाशोथ, श्वसन संकट और हांफना हैं। इसके रोगजनन में ट्रेकिअल एपिथेलियल म्यूकोसा और कोशिका मृत्यु में प्रोइन्फ्लेमेटरी साइटोकिन्स की घुसपैठ मुख्य कारण है। हाल ही में, रोगों के रोगजनन में उभरती भूमिका के कारण पायरोप्टोसिस में रूचि बढ़ रही है। टीकाकरण किए गए चिकन झुंडों में आईएलटी का पुनरुत्थान या फिर से उभरना चिकित्सीय दृष्टिकोण के शिकार को बदल देता है। आईएलटी में सूजन को बढ़ाने वाले सेल डेथ के तरीके को स्पष्ट करने के बाद से सूजन के मूल कारण की पहचान करने में मदद मिलेली, उस विशिष्ट सेल डेथ पाथवे को ब्लॉक करने के लिए हस्तक्षेप रणनीतियों को अवरोधकों का उपयोग करके तैयार किया जा सकता है, जो आईएलटी वायरस–प्रेरित नकारात्मक प्रभावों को कम करने में मदद करेगा। इसे समझने के लिए, चिकन एपिथेलियल सेल कल्चर सिस्टम में आईएलटीवी प्रेरित सूजन पर अवरोधकों के प्रभावों का विश्लेषण करने के लिए एक अध्ययन किया गया था। यहां हमने सीईके कोशिकाओं में % एलडीएच रिलीज साइटोटोक्सिक मूल्यांकन द्वारा पायरोप्टोसिस को शामिल करने के लिए एलपीएस की खुराक को मानकीकृत किया। फिर, बे 11–7082 और डिसुलफिरम इनहिबिटर की खुराक एलपीएस/नाइजोरिसिन प्राइमड सीईके कोशिकाओं की इस मानक खुराक के लिए % एलडीएच रिलीज साइटोटोक्सिक मूल्यांकन द्वारा निर्धारित की गई थी। असंक्रमित सीईके कोशिकाओं (पूर्व–संक्रमण) और आईएलटीवी संक्रमित सीईके कोशिकाओं (संक्रमण के बाद) पर अवरोधकों के प्रभाव का आकलन करने पर किए गए सेल व्यवहार्यता प्रयोगों से पता चला कि बे 11–7082 उपचार ने असंक्रमित सीईके कोशिकाओं की उत्तरजीविता को कम कर दिया, जबकि संक्रमित सीईके कोशिकाओं में, डिसुल्फिरम उपचार ने उत्तरजीविता को कम कर दिया। आईएलटीवी संक्रमित सीईके कोशिकाओं पर इन बे 11–7082 और डिसुलफिरम अवरोधकों के इन–विट्रो जीन एक्सप्रेशन अध्ययनों से पाइरोप्टोसिस मार्करों (केस्पस–1, आईएल–1बीटा और आईएल–18) की अभिव्यक्ति में उल्लेखनीय गिरावट का पता चला है। इसी तरह, ये निष्कर्ष अलग–अलग समय अंतराल पर किए गए वायरल लोड क्वांटिफिकेशन और वायरल अवरोध गणना के साथ मेल खाते हैं। अवरोधकों के साथ आईएलटीवी संक्रमित सीईके कोशिकाओं में पायरोप्टोसिस मध्यस्थता समर्थक साइटोकिन अभिव्क्ति को अवरूद्ध करने के बाद एपोप्टोसिस या नेक्रोप्टोसिस मार्करों की अभिव्यक्ति का कोई सबूत नहीं था। इसलिए बे 11–7082 और डिसुलफिरम ने आईएलटीवी से संक्रमित सवंर्धित सीईके कोशिकाओं में पायरोप्टोसिस मार्करों में कमी और वायरल लोड में कमी के अतिरिक्त लाभ में एंटीपायरोपोटिक भूमिका साबित की है। इसलिए, पायरोप्टोटिक इनहिबिटर आईएलटीवी द्वारा प्रेरित सीईके कोशिकाओं में एक शक्तिशाली चिकित्सीय एजेंट बन सकता है जिसका उपयोग आईएलटीवी संक्रमण से पीड़ित मुर्गियों में किया जा सकता है।

References

9 REFERENCES

Aachoui, Y., Leaf, I.A., Hagar, J.A., Fontana, M.F., Campos, C.G., Zak, D.E., Tan, M.H., Cotter, P.A., Vance, R.E., Aderem, A. and Miao, E.A. 2013. Caspase-11 protects against bacteria that escape the vacuole. Science. **339**(6122): 975-978.

Aziz, T. 2010. Infectious Laryngotracheitis (ILT) targets broilers. World Poult. **25**: 17–18.

Bagust,T.J.and Johnson, M.A. 1995. Avian infectious laryngotracheitis: virus-host interactions in relation to prospects for eradication. Avian Pathol. **24**(3): 373–391.

Bagust, T. J. 1986. Laryngotracheitis (gallid 1) herpesvirus infection in the chicken 4. latency establishment by wild and vaccine strains of ILT virus. Avian Pathol. **15**(3): 581-595.

Bayoumi, M., El-Saied, M., Amer, H., Bastami, M., Sakr, EE. and El-Mahdy, M. 2020. Molecular characterization and genetic diversity of the infectious laryngotracheitis virus strains circulating in Egypt during the outbreaks of 2018 and 2019. Arch.Virol. **165**(3): 661–670.

Beach, J. R. 1926. The virus of infectious laryngotracheitis. Science**. 68**: 570-580.

Beltran, G., Williams, S.M., Zavala, G., Guy, J.S., Garcia, M. 2017. The route of inoculation dictates the replication patterns of the infectious laryngotracheitis virus (ILTV) pathogenic strain and chicken embryo origin (CEO) vaccine. Avian Pathol. **46**(6): 585–593.

Blevins, H.M., Xu, Y., Biby, S., and Zhang, S. 2022. The NLRP3 inflammasome pathway: a review of mechanisms and inhibitors for the treatment of inflammatory diseases. Front. Aging Neurosci. 14.

Blakey, J., Stoute, S., Crossley, B., Mete, A. 2019. Retrospective analysis of infectious laryngotracheitis in backyard chicken flocks in California, 2007-2017, and

determination of strain origin by partial ICP4 sequencing. J. Vet. Diagn. Invest. **31**(3): 350–358.

Brennan, M.A. and Cookson, B.T. 2000. Salmonella induces macrophage death by caspase 1 dependent necrosis. Mol. Microbiol. **38**(1): 31-40.

Brown, L., Premaratna, D., Segal, Y. and Beddoe, T. 2020. Air sampling for detection of infectious laryngotracheitis (ILT) in commercial poultry flocks. BMC Res.Notes. **13**(1): 1-5.

Broz, P., Newton, K., Lamkanfi, M., Mariathasan, S., Dixit, V.M., and Monack, D.M. 2010a. Redundant roles for inflammasome receptors NLRP3 and NLRC4 in host defense against Salmonella. J. Exp. Med. **207**: 1745–1755.

Broz, P., von Moltke, J., Jones, J.W., Vance, R.E., and Monack, D.M. 2010b. Differential requirement for Caspase-1 autoproteolysis in pathogen-induced cell death and cytokine processing. Cell Host Microbe. **8**: 471–483.

Bryant, NA., Davis-Poynter, N., Vanderplasschen, A. and Alcami A. 2003. Glycoprotein G isoforms from some alphaherpesviruses function as broad-spectrum chemokine binding proteins. Embo J. **22**(4): 833–846.

Calnek, B.W., Fahey, K.J. and Bagust, T.J. 1986. In vitro infection studies with infectious laryngotracheitis virus. Avian Dis. **30**(2): 327–336.

Chacon, J.L. and Ferreira, A.J.P. 2009. Differentiation of field isolates and vaccine strains of infectious laryngotracheitis virus by DNA sequencing. Vaccine. **27**(48): 6731-6738.

Chacon, J. L., Nunez, L. F. N., Vejarano, M. P., Parra, S. H. S., Astolfi-Ferreira, C. S. and Ferreira, A. J. P. 2015. Persistence and spreading of field and vaccine strains of infectious laryngotracheitis virus (ILTV) in vaccinated and unvaccinated geographic regions, in Brazil. Trop. Anim. Health Prod. **47**(6): 1101–1108.

Chang, P.W., Sculco, F. and Yates, V.J. 1977. An in vivo and in vitro study of infectious laryngotracheitis virus in chicken leukocytes. Avian Dis. **1**: 492-500.

Chauhan, D., Vande Walle, L. and Lamkanfi, M. 2020. Therapeutic modulation of inflammasome pathways. Immunol. Rev.**297**(1): 123-138.

Chen, H. F., Hsueh, P. R., Liu, Y. Y., Chen, Y., Chang, S. Y., Wang, W. J., and Hung, M. C. 2022. Disulfiram blocked cell entry of SARS-CoV-2 via inhibiting the interaction of spike protein and ACE2. Am. J. Cancer Res. **12**(7): 3333.

Chen, H., Deng, Y., Gan, X., Li, Y., Huang, W., Lu, L., Wei, L., Su, L., Luo, J., Zou, B. and Hong, Y. 2020. NLRP12 collaborates with NLRP3 and NLRC4 to promote pyroptosis inducing ganglion cell death of acute glaucoma. Mol. Neurodegener. **15**(1): 1-16.

Chen, H.Y., Cui, P., Cui, B.A., Li, H.P., Jiao, X.Q., Zheng, L.L., Cheng, G. and Chao, A.J. 2011a. Immune responses of chickens inoculated with a recombinant fowlpox vaccine coexpressing glycoprotein B of infectious laryngotracheitis virus and chicken IL-18. FEMS Microbiol. Immunol. **63**: 289–295.

Chen, K.W., Monteleone, M., Boucher, D., Sollberger, G., Ramnath, D., Condon, N.D., von Pein, J.B., Broz, P., Sweet, M.J. and Schroder, K. 2018. Noncanonical inflammasome signaling elicits gasdermin D–dependent neutrophil extracellular traps. Sci. Immunol. **3**(26): 6676.

Chomiak, T.W., Luginbuhl, R.E. and Helmboldt, C.F. 1960. Tissue culture and chicken embryo techniques for infectious laryngotracheitis virus studies. Avian Dis.**4**(3): 235-246.

Cone, R.A. 2009. Barrier properties of mucus. Adv. Drug. Deliv. Rev. **61**(2): 75-85.

Coll, R. C., Hill, J. R., Day, C. J., Zamoshnikova, A., Boucher, D., Massey, N. L. and Schroder, K. 2019. MCC950 directly targets the NLRP3 ATP-hydrolysis motif for inflammasome inhibition. Nat. Chem. Biol. **15**(6): 556-559.

Coppo, M.J., Devlin, J.M., Legione, A.R., Vaz, P.K., Lee, S.W., Quinteros, J.A., Gilkerson, J.R., Ficorilli, N., Reading, P.C., Noormohammadi, A.H. and Hartley, C.A. 2018. Infectious laryngotracheitis virus viral chemokine-binding protein glycoprotein G alters transcription of key inflammatory mediators in vitro and in vivo. Virol. J. **92**(1).

Cover, M.S., 1996. The early history of infectious laryngotracheitis. Avian Dis. **40**(3): 494-500.

Crawshaw, G. J. and Boycott, B. R. 1982. Infectious laryngotracheitis in peafowl and pheasants. Avian Dis. **1**: 397-401.

D'Arcy, M.S. 2019. Cell death: a review of the major forms of apoptosis, necrosis and autophagy. Cell Biol. Int. **43**(6): 582-592.

Danielle, P. A., Mascarenhas, D. M., Cerqueira, M., Pereira, S. F., Fernanda, V. S., Castanheira, Talita D., Fernandes, Graziele Z., Larissa D., Dario, S. and Zamboni. 2017. Inhibition of caspase-1 or gasdermin-D enable caspase-8 activation in the Naip5/NLRC4/ASC inflammasome. PLoS Pathog. **13**(8):1006502.

Davidson, I., Raibshtein, I., Altori, A. and Elkin, N. 2016. Infectious laryngotracheitis virus (ILTV) vaccine intake evaluation by detection of virus amplification in feather pulps of vaccinated chickens. Vaccine. **34**(13): 1630-1633.

Davison, A.J., Eberle, R., Ehlers, B., Hayward, G.S., McGeoch, D.J., Minson, A.C., Pellett, P.E., Roizman, B., Studdert, M.J. and Thiry, E. 2009. The order herpesvirales. Arch. Virol. **154**(1): 171-177.

Davison, S., Gingerich, E. N., Casavant, S. and Eckroade, R. J. 2006. Evaluation of the efficacy of a live fowlpox-vectored infectious laryngotracheitis/avian encephalomyelitis vaccine against ILT viral challenge. Avian Dis. **50**:50–54.

den Hartigh, A. B. and Fink, S. L. 2018. Pyroptosis induction and detection. Curr. Protoc. Immunol. **122**(1): 52.

De Vasconcelos, N.M., Van Opdenbosch, N., Van Gorp, H., Parthoens, E. and Lamkanfi, M. 2019. Single-cell analysis of pyroptosis dynamics reveals conserved GSDMD-mediated subcellular events that precede plasma membrane rupture. Cell Death Differ. **26**(1): 146-161.

Deng, W., Yang, Z., Yue, H., Ou, Y., Hu, W. and Sun, P. 2020. Disulfiram Suppresses NLRP3 Inflammasome Activation to Treat Peritoneal and Gouty Inflammation. Free Radic. Biol. Med. **152**: 8–17.

Devlin, JM., Hartley, CA., Gilkerson, JR., Coppo, MJC., Vaz, P., Noormohammadi, AH., Wells, B., Rubite, A., Dhand, NK. and Browning GF. 2011. Horizontal transmission dynamics of a glycoprotein G deficient candidate vaccine strain of infectious laryngotracheitis virus and the effect of vaccination on transmission of virulent virus. Vaccine. **29**(34):5699–5704.

Devlin, J.M., Browning, G.F., Hartley, C.A., Kirkpatrick, N.C., Mahmoudian, A., Noormohammadi, A.H. and Gilkerson, J.R. 2006. Glycoprotein G is a virulence factor in infectious laryngotracheitis virus. J. Gen. Virol. **87**: 2839–2847.

Devlin, J.M., Viejo-Borbolla, A., Browning, G.F., Noormohammadi, A.H., Gilkerson, J.R., Alcami, A. and Hartley, C.A. 2010. Evaluation of immunological responses to a glycoprotein G deficient candidate vaccine strain of infectious laryngotracheitis virus. Vaccine. **28**: 1325–1332.

Dhama, K., Chakraborty, S., Tiwari, R., Verma, A.K., Saminathan, M., Amarpal, M.Y., Nikousefat, Z., Javdani, M. and Khan, R.U. 2014. A concept paper on novel

technologies boosting production and safeguarding health of humans and animals. Res. Opin. Anim. Vet. Sci. **4**(7): 353-370.

Dhani, S., Zhao, Y. and Zhivotovsky, B. 2021. A long way to go: caspase inhibitors in clinical use. Cell Death Dis. **12**(10): 1-13.

Ding, J., Wang, K., Liu, W., She, Y., Sun, Q., Shi, J., Sun, H., Wang, D.C. and Shao, F. 2016. Pore-forming activity and structural autoinhibition of the gasdermin family. Nature. **535**(7610): 111-116.

Doitsh, G., Galloway, N.L., Geng, X., Yang, Z., Monroe, K.M., Zepeda, O., Hunt, P.W., Hatano, H., Sowinski, S., Munoz-Arias, I. and Greene, W.C. 2014. Cell death by pyroptosis drives CD4 T-cell depletion in HIV-1 infection. Nature. **505**(7484): 509-514.

Dufour-Zavala, L. 2008. Epizootiology of infectious laryngotracheitis and presentation of an industry control program. Avian Dis.**52**(1): 1-7.

Duran, N. and Favaro, W.J. 2020. Pyroptosis: Physiological roles in viral infection. ArXiv. org.2006.15777.

Fahey, K.J., Bagust, T.J. and York, J.J., 1983a. Laryngotracheitis herpesvirus infection in the chicken: the role of humoral antibody in immunity to a graded challenge infection. Avian Pathol. **12**: 505–514.

Fahey, K. J., York, J. J., and Bagust, T. J. 1984. Laryngotracheitis herpesvirus infection in the chicken. II. The adoptive transfer of resistance with immune spleen cells. Avian Pathol. **13**(2): 265-275.

Fernandes-Alnemri, T., Yu, J.W., Datta, P., Wu, J. and Alnemri, E.S. 2009. AIM2 activates the inflammasome and cell death in response to cytoplasmic DNA. Nature. **458**(7237): 509–513

Fink, S.L. and Cookson, B.T., 2006. Caspase 1 dependent pore formation during pyroptosis leads to osmotic lysis of infected host macrophages. Cell Microbiol. **8**(11): 1812-1825.

Fuchs, W. and Mettenleiter, T.C. 1996. DNA sequence and transcriptional analysis of the UL1 to UL5 gene cluster of infectious laryngotracheitis virus. J. Gen. Virol. **77**(9): 2221-2229.

Galluzzi, L., Vitale, I., Aaronson, S. A., Abrams, J. M., Adam, D., Agostinis, P., and Turk, B. 2018. Molecular mechanisms of cell death: recommendations of the Nomenclature Committee on Cell Death 2018. Cell Death Differ. **25(3):** 486-541.

Gao, P., Chen, L., Fan, L., Ren, J., Du, H., Sun, M., Li, Y., Xie, P., Lin, Q., Liao, M. and Xu, C. 2020. Newcastle disease virus RNA-induced IL-1β expression via the NLRP3/ caspase-1 inflammasome. Vet. Res. **51**: 1-14.

Garcia, M., Spatz, SJ. and Guy JS. 2013. Infectious laryngotracheitis. In: Swayne DE, Glisson JR, McDougald LR, Nolan LK, Suarez DL, Nair V. Editors. Diseases of Poultry. Ames, Iowa. Blackwell Publishing. 161–179.

Garcia, M. 2017. Current and future vaccines and vaccination strategies against infectious laryngotracheitis (ILT) respiratory disease of poultry. Vet. Microbiol. **206**: 157-162.

Garcia, M. and Spatz, S. 2020. Infectious laryngotracheitis. Diseases of poultry. Volume 1. 14th ed. John Wiley and Sons, Inc. pp 189-209.

Gergen, L., Cook, S., Ledesma, B., Cress, W., Higuchi, D., Counts, D., Cruz-Coy, J., Crouch, C., Davis, P., Tarpey, I. and Morsey, M. 2019. A double recombinant herpes virus of turkeys for the protection of chickens against Newcastle, infectious laryngotracheitis and Marek's diseases. Avian Pathol. **48**(1): 45–56.

Gibbs, C. 1134. Infectious laryngotracheitis vaccination. Mass Agric. Exp. Stn. Bull. **295**:1-20.

Gingerich, E. and Carver, D.K. 2006. http:// agriculture.state.pa.us. Infectious Laryngotracheitis Virus (ILT) Facts. Pennsylvania. Accessed December 20, 2020.

Gobel, T.W., Schneider, K., Schaerer, B., Mejri, I., Puehler, F., Weigend, S., Staeheli, P. and Kaspers, B. 2003. IL-18 stimulates the proliferation and IFN-γ release of CD4+ T cells in the chicken: conservation of a Th1-like system in a nonmammalian species. J. Immunol. **171**(4): 1809-1815.

Gong, W., Shi, Y., and Ren, J. 2020. Research progresses of molecular mechanism of pyroptosis and its related diseases. Immunobiology, **225**(2): 151884.

Gowthaman, V., Kumar, S., Koul, M., Dave, U., Murthy, T.G.K., Munuswamy, P., Tiwari, R., Karthik, K., Dhama, K., Michalak, I. and Joshi, S.K., 2020. Infectious laryngotracheitis: Etiology, epidemiology, pathobiology, and advances in diagnosis and control–a comprehensive review. Vet. Q. **40**(1):140-161.

Gowthaman, V., Singh, S.D., Dhama, K., Barathidasan, R., Mathapati, B.S., Srinivasan, P., Saravanan, S. and Ramakrishnan, M.A. 2014. Molecular detection and characterization of infectious laryngotracheitis virus (Gallid herpesvirus-1) from clinical samples of commercial poultry flocks in India. VirusDisease. **25**(3): 345-349.

Gowthaman, V., Singh, S.D., Dhama, K., Srinivasan, P., Saravanan, S., Murthy, T.R.G.K. and Ramakrishnan, M.A. 2016. Molecular survey of respiratory and immunosuppressive pathogens associated with low pathogenic avian influenza H9N2 subtype and virulent Newcastle disease viruses in commercial chicken flocks. Poult. Sci. **54**(2): 179-184.

Granzow, H., Klupp, B. G., Fuchs, W., Veits, J., Osterrieder, N., and Mettenleiter, T. C. 2001. Egress of alphaherpesviruses: comparative ultrastructural study. Virol. J. **75**(8): 3675-3684.

Guey, B., Bodnar, M., Manié, S.N., Tardivel, A. and Petrilli, V., 2014. Caspase-1 autoproteolysis is differentially required for NLRP1b and NLRP3 inflammasome function. Proceedings of the National Academy of Sciences. **111**(48): 17254-17259.

Hafez, H.M. and Attia, Y.A., 2020. Challenges to the poultry industry: current perspectives and strategic future after the COVID-19 outbreak. Front. Vet. Sci.**7**:516.

Hayles, L.B., Hamilton, D. and Newby, W.C. 1976a. Transfer of parental immunity to infectious laryngotracheitis in chicks. Can. J. Comp. Med. **40**: 218–219.

Hernandez-Divers, SM., Villegas, P., Jimenez, C., Hernandez-Divers, SJ., Garcia, M., Riblet, SM., Carroll, CR., O'Connor, BM., Webb, JL. and Yabsley MJ. 2008. Backyard chicken flocks pose a disease risk for neotropic birds in Costa Rica. Avian Dis. **52**(4): 558–566.

Hidalgo, H. 2003. Infectious laryngotracheitis: A review. Rev. Bras. Cienc. Avic. **5**(3): 157–168.

Hughes, C.S. and Jones, R.C. 1988. Comparison of cultural methods for primary isolation of infectious laryngotracheitis virus from field material. Avian Pathol. **17**(2): 295-303.

Hu, J.J., Liu, X., Xia, S., Zhang, Z., Zhang, Y., Zhao, J., Ruan, J., Luo, X., Lou, X., Bai, Y. and Wang, J., 2020. FDA-approved disulfiram inhibits pyroptosis by blocking gasdermin D pore formation. Nat. Immunol. **21**(7):736-745.

Hu, J.J., Liu, X., Zhao, J., Xia, S., Ruan, J., Luo, X., Kim, J. and Lieberman, J., and Wu, H.2018. Identification of pyroptosis inhibitors that target a reactive cysteine in gasdermin D. bioRxiv.

Jiang, H., He, H., Chen, Y., Huang, W., Cheng, J., Ye, J., and Zhou, R. 2017. Identification of a selective and direct NLRP3 inhibitor to treat inflammatory disorders. J. Exp. Med. **214**(11): 3219-3238.

Johnson, K.E., Chikoti, L. and Chandran, B. 2013. Herpes simplex virus 1 infection induces activation and subsequent inhibition of the IFI16 and NLRP3 inflammasomes. Virol. J. **87**(9): 5005-5018.

Jordan FT., and Chubb R. 1962. The agar gel diffusion technique in the diagnosis of infectious laryngotracheitis (ILT) and its differentiation from fowl pox. Res Vet Sci. **3**(3):245–255.

Jorgensen, I. and Miao, E.A. 2015. Pyroptotic cell death defends against intracellular pathogens. Immunol. Rev. **265**(1):130-142.

Juliana, C., Fernandes-Alnemri, T., Wu, J., Datta, P., Solorzano, L., Yu, J.W., Meng, R., Quong, A.A., Latz, E., Scott, C.P. and Alnemri, E.S., 2010. Anti-inflammatory compounds parthenolide and Bay 11-7082 are direct inhibitors of the inflammasome. J.Biol. Chem. **285**(13): 9792-9802.

Kanneganti TD. 2010. Central roles of NLRs and inflammasomes in viral infection. Nat. Rev Immunol. **10**(10):688–698.

Kayagaki, N., Stowe, I. B., Lee, B. L., O'Rourke, K., Anderson, K., Warming, S. and Dixit, V. M. 2015. Caspase-11 cleaves gasdermin D for non-canonical inflammasome signalling. Nature. **526**(7575): 666-671.

Kingsley, D.H. and Keeler, C.L. 1999. Infectious laryngotracheitis virus, an alpha herpesvirus that does not interact with cell surface heparan sulfate. Virol. J. **256**(2): 213–219.

Kirkpatrick, N.C., Mahmoudian, A., Colson, C.A., Devlin, J.M. and Noormohammadi, A.H. 2006. Relationship between mortality, clinical signs and tracheal pathology in infectious laryngotracheitis. Avian Pathol. **35**(6): 449-453.

Kohale, S.K.2022. Pathology and Evaluation of Pyroptotic Markers in Chickens Naturally Affected with Infectious Laryngotracheitis Virus vis-a-vis in-vitro Evaluation of Pyroptotic Markers in Epithelial cells of Chicken origin. Thesis, M.V.Sc. Deemed University, IVRI, Izatnagar, India.

Kumar, R., Patel, S.K., Rami Reddy, B.V., Bhatt, M., Karthik, K., Gandham, R.K., Malik, Y.S. and Dhama, K., 2015. Apoptosis and other alternate mechanisms of cell death. Asian J. Anim. Vet. Adv. **10**(10):646-668.

Kuriakose, T. and Kanneganti, T.D. 2019. Pyroptosis in antiviral immunity. In: Current Topics in Microbiology and Immunology. Springer, Berlin, Heidelberg. 1-19 p.

Lamkanfi, M. and Dixit, V.M. 2014. Mechanisms and functions of inflammasomes. Cell. **157**(5):1013-1022.

Latz, E., Xiao, T.S., and Stutz, A. 2013. Activation and regulation of the inflammasomes. Nat. Rev. Immunol. **13**(6): 397-411.

Lee, Jaehwi. 2012. "BAY 11-7082 is a broad-spectrum inhibitor with anti-inflammatory activity against multiple targets."J.Inflamm.

Lee, S., Hirohama, M., Noguchi, M., Nagata, K. and Kawaguchi, A. 2018. Influenza A virus infection triggers pyroptosis and apoptosis of respiratory epithelial cells through the type I interferon signaling pathway in a mutually exclusive manner. Virol. J. **92**: 00396-18.

Lee, J.Y., Joon Jin, S., Ann, W., Xianyao, L., Huaijun, Z., Bottje, W.G., Byung-Whi, K. 2010. Transcriptional profiling of host gene expression in chicken embryo lung cells infected with laryngotracheitis virus. BMC Genom. **11**: 445–459.

Lee, J.Y., Song, J.J., Wooming, A., Li, X., Zhou, H., Bottje, W.G. and Kong, B.W. 2010. Transcriptional profiling of host gene expression in chicken embryo lung cells infected with laryngotracheitis virus. BMC Genom. **11**(1): 1-15.

Lee, S.W., Markham, P.F., Markham, J.F., Petermann, I., Noormohammadi, A.H., Browning, G.F., Ficorilli, N.P., Hartley, C.A. and Devlin, J.M. 2011. First complete genome sequence of infectious laryngotracheitis virus. BMC Genom. **12**(1): 1-6.

Lei, X., Zhang, Z., Xiao, X., Qi, J., He, B. and Wang, J., 2017. Enterovirus 71 inhibits pyroptosis through cleavage of gasdermin D. Virol.J. **91**(18): 01069-17.

Liao, J., Yang, F., Tang, Z., Yu, W., Han, Q., Hu, L., Li, Y., Guo, J., Pan, J., Ma, F. and Ma, X. 2019. Inhibition of Caspase-1-dependent pyroptosis attenuates copper-induced apoptosis in chicken hepatocytes. Ecotoxicol. Environ. Saf. **174**: 110-119.

Liu, X.L., Shan, W.J., Jia, L.J., Yang, X., Zhang, J.J., Wu, Y.R., Xu, F.Z. and Li, J.N., 2016. Avian leukosis virus subgroup J triggers caspase-1-mediated inflammatory response in chick livers. Virus Res. **215**:65-71.

Luo, J., Carrillo, J. A., Menendez, K. R., Tablante, N. L., and Song, J. 2014. Transcriptome analysis reveals an activation of major histocompatibility complex 1 and 2 pathways in chicken trachea immunized with infectious laryngotracheitis virus vaccine. Poult. Sci. **93**(4): 848-855.

Lupfer, C., Malik, A. and Kanneganti, T.D. 2015. Inflammasome control of viral infection. Curr. Opin. Virol. **12**: 38-46.

Magouz, A., Medhat, S., Abou Asa, S. and Desouky, A. 2018. Detection of infectious laryngotracheitis virus (Gallid herpesvirus-1) from clinically infected chickens in Egypt by different diagnostic methods. Iran. J. Vet. Res. **19**(3): 194.

Mahmoudian, A., Markhama, P.F., Noormohammadia, A.H. and Browninga, G.F. 2012. Kinetics of transcription of infectious laryngotracheitis virus genes. Comp. Immunol. Microbiol. Infect. Dis. **35**: 103-115.

Man, S.M. and Kanneganti, T.D. 2015. Gasdermin D: the long-awaited executioner of pyroptosis. Cell Res. **25**(11): 1183-1184.

Martinon, F. and Tschopp, J.J.C.D. 2007. Inflammatory caspases and inflammasomes: master switches of inflammation. Cell Death Differ. **14**(1): 10-22.

Martinon, F., Burns, K. and Tschopp, J. 2002. The inflammasome: a molecular platform triggering activation of inflammatory caspases and processing of proIL-β. Mol. Cell. **10**(2): 417-426.

May, H. G., and Tittsler, R. P. 1925. Tracheo laryngitis in poultry. J. Am. Vet. Med. Assoc. **67**: 229-231.

Menendez, K.R., García, M., Spatz, S. and Tablante, N.L. 2014. Molecular epidemiology of infectious laryngotracheitis: a review. Avian Pathol. **43**(2): 108-117.

Nadimpalli, M., Lee, SW., Devlin, JM., Gilkerson, JR. and Hartley CA. 2017. Impairment of infectious laryngotracheitis virus replication by deletion of the UL[-1] gene. Arch. Virol. **162**(6): 1541–1548.

Nakamichi, K., Matsumoto Y. and Otsuka H. 2002. Bovine herpesvirus 1 glycoprotein G is necessary for maintaining cell-to-cell junctional adherence among infected cells. Virol.J. **294**(1): 22–30.

Neff, C., Sudler, C. and Hoop, R. K. 2008. "Characterization of western European field isolates and vaccine strains of avian infectious laryngotracheitis virus by restriction fragment length polymorphism and sequence analysis." Avian Dis. **52**(2): 278-283.

OIE terrestrial manual. 2014. Ch. 2.3.3 Avian Infectious laryngotracheitis. 1–11.

Okondo, MC., Johnson, DC., Sridharan, R., Go, EB., Chui, AJ., Wang, MS., Poplawski, SE., Wu, W., Liu, Y. and Lai, JH. 2017. DPP8 and DPP9 inhibition induces pro-caspase-1- dependent monocyte and macrophage pyroptosis. Nat.Chem. Biol. **13**: 46–53.

Oldoni, I., Rodriguez-Avila, A., Riblet, S.M., Zavala, G. and Garcia, M. 2009. Pathogenicity and growth characteristics of selected infectious laryngotracheitis virus strains from the United States. Avian Pathol. **38**(1): 47-53.

Ou, S.C, Giambrone, J.J. and Macklin, K.S. 2012. Detection of infectious laryngotracheitis virus from darkling beetles and their immature stage (lesser mealworms) by quantitative polymerase chain reaction and virus isolation. J. Appl. Poult. Res. **21**(1): 33–38.

Ou, S.C., Giambrone, J.J. and Macklin, K.S. 2011. Infectious laryngotracheitis vaccine virus detection in water lines and effectiveness of sanitizers for inactivating the virus. J. Appl. Poult. Res. **20**(2): 223–230.

Pavlova, S., Veits, J., Mettenleiter, T.C. and Fuchs, W. 2013. Identification and functional analysis of membrane proteins gD, gE, gI, and pUS9 of Infectious laryngotracheitis virus. Avian Dis. **57**(2s1): 416-426.

Piccirillo, A., Lavezzo, E., Niero, G., Moreno, A., Massi, P., Franchin, E., Toppo, S., Salata, C. and Palù, G. 2016. Full genome sequence-based comparative study of wild-type and vaccine strains of infectious laryngotracheitis virus from Italy. PLoS One. **11**(2): 0149529.

Place, D.E. and Kanneganti, T.D., 2019. On the Road to Discovering the Elusive Executioner of Pyroptosis. J. Immunol. **202**(7):1911-1912.

Platnich, J.M. and Muruve, D.A. 2019. NOD-like receptors and inflammasomes: A review of their canonical and non-canonical signaling pathways. Arch. Biochem. Biophys. **670**: 4-14.

Portz, C., Beltrão, N., Furian, T.Q., Júnior, A.B., Macagnan, M., Griebeler, J., Rosa, C.A.V.L., Colodel, E.M., Driemeier, D., Back, A. and Schatzmayr, O.M.B. 2008. Natural infection of turkeys by infectious laryngotracheitis virus. Vet. Microbiol. **131**(1-2): 57-64.

Prideaux, C.T., Kongsuwan, K., Johnson, M.A., Sheppard, M. and Fahey, K.J. 1992. Infectious laryngotracheitis virus growth, DNA replication, and protein synthesis. Arch.Virol. **123**(1): 181-192.

Qiao, Y., Wang, Z., Han, Z., Shao, Y., Ma, Y., Liang, Y., Chen, Z., Wu, H., Cui, L., Zhang, Y. and Liu, S. 2020. Global exploration of the metabolic requirements of gallid alphaherpesvirus 1. PLoS Pathog. **16**(8): 1008815.

Raff, M., 1998. Cell suicide for beginners. Nature. **396**(6707):119-119.

Raggi, L.G. and Lee, G.G. 1965. Infections laryngotracheitis outbreaks following vaccination. Avian Dis. **9**(4): 559–565.

Rathinam, V.A., Jiang, Z., Waggoner, S.N., Sharma, S., Cole, L.E., Waggoner, L., Vanaja, S.K., Monks, B.G., Ganesan, S., Latz, E., Hornung, V., Vogel, S.N., Szomolanyi-Tsuda, E. and Fitzgerald, K.A. 2010. The AIM2 inflammasome is essential for host defense against cytosolic bacteria and DNA viruses. Nat. Immunol. **11**(5): 395–402

Rathkey, J.K., Zhao, J., Liu, Z., Chen, Y., Yang, J., Kondolf, H.C., Benson, B.L., Chirieleison, S.M., Huang, A.Y., Dubyak, G.R. and Xiao, T.S., 2018. Chemical disruption of the pyroptotic pore-forming protein gasdermin D inhibits inflammatory cell death and sepsis. Sci.Immunol. **3**(26): 2738.

Reddy, V.R., Trus, I. and Nauwynck, H.J. 2017. Presence of DNA extracellular traps but not MUC5AC and MUC5B mucin in mucoid plugs/casts of infectious laryngotracheitis virus (ILTV) infected tracheas of chickens. Virus Res. **227**: 135-142.

Reddy, V.R., Steukers, L., Li, Y., Fuchs, W., Vanderplasschen, A. and Nauwynck, H.J. 2014. Replication characteristics of infectious laryngotracheitis virus in the respiratory and conjunctival mucosa. Avian Pathol. **43**(5): 450-457.

Reynolds, H.A., Watrach, A.M. and Hanson, L.E. 1968. Development of the nuclear inclusion bodies of infectious laryngotracheitis. Avian Dis. **12**(2): 332–347.

Rodríguez-Avila, A., Oldoni, I., Riblet, S. and García, M. 2007. Replication and transmission of live attenuated infectious laryngotracheitis virus (ILTV) vaccines. Avian Dis. **51**: 905–911.

Roizman, B.A.P.E.P., 2001. The family Herpesviridae: a brief introduction. Fields virology.

Rossol, M., Pierer, M., Raulien, N., Quandt, D., Meusch, U., Rothe, K., Schubert, K., Schöneberg, T., Schaefer, M., Krügel, U. and Smajilovic, S. 2012. Extracellular

Ca2+ is a danger signal activating the NLRP3 inflammasome through G protein-coupled calcium sensing receptors. Nat. Commun. **3**(1): 1-9.

Roy, P., Islam, A.F., Burgess, S.K., Hunt, P.W., McNally, J. and Walkden-Brown, S.W. 2015. Real-time PCR quantification of infectious laryngotracheitis virus in chicken tissues, faeces, isolator-dust and bedding material over 28 days following infection reveals high levels in faeces and dust. J. Gen. Virol. **96**(11): 3338-3347.

Ruan, J., Xia, S., Liu, X., Lieberman, J. and Wu, H., 2018. Cryo-EM structure of the gasdermin A3 membrane pore. Nature. **557**(7703): 62-67.

Ruhl, S. and Broz, P. 2015. Caspase 11 activates a canonical NLRP3 inflammasome by promoting K+ efflux. Eur. J. Immunol. **45**(10): 2927-2936.

Samberg, Y., Cuperstein, E., Bendheim, U. and Aronvici, I. 1971. The development of a vaccine against avian infectious laryngotracheitis IV. Immunization of chickens with a modified laryngotracheitis vaccine in the drinking water. Avian Dis. **15**: 413–417.

Sarhan, J., Liu, B. C., Muendlein, H. I., Li, P., Nilson, R., Tang, A. Y. and Poltorak, A. 2018.Caspase-8 induces cleavage of gasdermin D to elicit pyroptosis during Yersinia infection. Proc. Natl. Acad. Sci. **115**(46): 10888-10897.

Sanders, CJ., Doherty, PC. and Thomas PG. 2011. Respiratory epithelial cells in innate immunity to influenza virus infection. Cell Tissue Res. **343**: 13–21

Shi, J., Zhao, Y., Wang, K., Shi, X., Wang, Y., Huang, H., Zhuang, Y., Cai, T., Wang, F. and Shao, F. 2015. Cleavage of GSDMD by inflammatory caspases determines pyroptotic cell death. Nature. **526**: 660–665

Schnitzlein, W.M., Radzevicius, J. and Tripathy, D.N. 1994. Propagation of infectious laryngotracheitis virus in an avian liver cell line. Avian Dis. **1**(1): 211-217

Schmid Burgk, J. L., Gaidt, M. M., Schmidt, T., Ebert, T. S., Bartok, E. and Hornung, V. 2015. Caspase 4 mediates non canonical activation of the NLRP3 inflammasome in human myeloid cells. Eur. J. Immunol. **45**(10): 2911-2917.

Seddon, H. and Hart, L. 1935. The occurrence of infectious laryngotracheitis in fowls in New South Wales. Aust. Vet. J. **11**: 11–221.

Shrivastava, G., Leon-Juárez, M., García-Cordero, J., Meza-Sánchez, D.E. and Cedillo-Barron, L., 2016. Inflammasomes and its importance in viral infections. Immunol. Res. **64**(5): 1101-1117.

Singh, S.B., Singh, G.R. and Singh, C.M. 1964. A preliminary report on the occurrence of infectious laryngotracheitis of poultry in India. Poult. Sci., **43**: 492 - 4.

Solberg, S. 2019. Caspase-1 mediated pro-inflammatory cytokine pathway in highly pathogenic H5N1 avian influenza infection in the non-human primate model. Thesis, Master's degree, University of Pittsburgh, Pennsylvania. 28 p.

Sollberger, G., Choidas, A., Burn, G. L., Habenberger, P., Di Lucrezia, R., Kordes, S. And Zychlinsky, A. 2018. Gasdermin D plays a vital role in the generation of neutrophil extracellular traps. Sci. Immunol. 3(26): 6689.

Srinivasan, P., Balachandran, CG., Murthy, T., Saravanan, S., Pazhanivel, N. and Mohan, B. 2012. Pathology of infectious laryngotracheitis in commercial layer chicken. Indian J. Vet. Pathol. **89**:75–78.

Stewart, M. K. and Cookson, B. T. 2016. Evasion and interference: intracellular pathogens modulate caspase-dependent inflammatory responses. Nat. Rev. Microbiol. **14**(6): 346.

Stowe, I., Lee, B. and Kayagaki, N., 2015. Caspase 11: arming the guards against bacterial infection. Immunol. Rev. **265**(1): 75-84.

Sun, Z., Nyanzu, M., Yang, S., Zhu, X., Wang, K., Ru, J., Yu, E., Zhang, H., Wang, Z., Shen, J. and Zhuge, Q. 2020. VX765 Attenuates Pyroptosis and HMGB1/TLR4/NF-κB Pathways to Improve Functional Outcomes in TBI Mice. Oxid. Med. Cell. Longev. **1**: 1-21.

Sun, L., Wang, H., Wang, Z., He, S., Chen, S., Liao, D. & Wang, X. 2012. Mixed lineage kinase domain-like protein mediates necrosis signaling downstream of RIP3 kinase. Cell.J. **148**(1-2): 213-227.

Takeuchi, O. and Akira, S. 2010. Pattern recognition receptors and inflammation. Cell.J.**140(**6):805-820.

Thureen, D.R. and Keeler, C.L. 2006. Psittacid herpesvirus 1 and infectious laryngotracheitis virus: comparative genome sequence analysis of two avian alphaherpesviruses. Virol. J. **80**(16): 7863-7872.

Tran, LC., Kissner, JM., Westerman, LE. and Sears, AE. 2000. A herpes simplex virus 1 recombinant lacking the glycoprotein G coding sequences is defective in entry through apical surfaces of polarized epithelial cells in culture and in vivo. Proc. Natl. Acad. Sci. **97**(4): 1818–1822.

Vagnozzi, A.E., Zavala, G., Riblet, S.M., Mundt, A. and Garcýa, M. 2012. Protection induced by commercially available live-attenuated and recombinant viral vector vaccines against infectious laryngotracheitis virus in broiler chickens. Avian Pathol. **41**(1): 21–31.

Vagnozzi, A.E., Beltrán, G., Zavala, G., Read, L., Sharif, S. and García, M. 2018. Cytokine gene transcription in the trachea, Harderian gland, and trigeminal ganglia of chickens inoculated with virulent infectious laryngotracheitis virus (ILTV) strain. Avian Pathol. **47**(5): 497-508.

Van Opdenbosch, N., Gurung, P., Vande Walle, L., Fossoul, A., Kanneganti, T.D. and Lamkanfi, M. 2014. Activation of the NLRP1b inflammasome independently of ASC-mediated caspase-1 autoproteolysis and speck formation. Nat. Commun. **5**(1):1-14.

Vareille, M., Kieninger, E., Edwards, M.R. and Regamey, N. 2011. The airway epithelium: soldier in the fight against respiratory viruses. Clin. Microbiol. Rev. **24**(1): 210-229.

Waidner, L.A., Burnside, J., Anderson, A.S., Bernberg, E.L., German, M.A., Meyers, B.C., Green, P.J., Morgan, R.W., 2011. A microRNA of infectious laryngotracheitis virus can downregulate and direct cleavage of ICP4 mRNA. Virol. J. **411**: 25–31.

Wang, L.G., Ma, J., Xue, C.Y., Wang, W., Guo, C., Chen, F., Qin, J.P., Huang, N.H., Bi, Y.Z. and Cao, Y.C. 2013. Dynamic distribution and tissue tropism of infectious laryngotracheitis virus in experimentally infected chickens. Arch. Virol. **158**(3): 659–666.

Wang, Z., Sun, B., Gao, Q., Ma, Y., Liang, Y., Chen, Z., Wu, H., Cui, L., Shao, Y., Wei, P. and Li, H. 2019. Host Src controls gallid alpha herpesvirus 1 intercellular spread in a cellular fatty acid metabolism-dependent manner. Virol. J. **537**: 1-13.

Watrach, A.M. and Hanson, L.E., 1963. Cytopathic effect of infectious laryngotracheitis virus in cultures of chicken embryo kidney cells. Proceedings of the Society for Experimental Biology and Medicine, **112**(1), 230-232.

Williams, R.A., Bennett, M., Bradbury, J.M., Gaskell, R.M., Jones, R.C. and Jordan, F.T. 1992. Demonstration of sites of latency of infectious laryngotracheitis virus using the polymerase chain reaction. J. Gen. Virol. **73** (9): 2415–2420.

Winterfield, R. W. and So, I. G. 1968. Susceptibility of turkeys to infectious laryngotracheitis. Avian Dis. **12**(1): 191-202.

Wu, X., Mao, X., Huang, Y., Zhu, Q., Guan, J., and Wu, L. 2020. Detection of proteins associated with the pyroptosis signaling pathway in breast cancer tissues and their significance. Int. J. Clin. Exp. Pathol. **13**(6): 1408.

Xia, S., Hollingsworth, L. R., and Wu, H. 2020. Mechanism and regulation of gasdermin-mediated cell death. Cold Spring Harb. Perspect. Biol. **12**(3): 036400.

Yamada, S., Matsuo, K., Fukuda, T. and Uchinuno, Y. 1980. Susceptibility of ducks to the virus of infectious laryngotracheitis. Avian Dis. **24**(4): 930–938.

Yoo, L., Hong, S., Shin, K.S. and Kang, S.J. 2011. PARP-1 regulates the expression of caspase-11. Biochem. Biophys. Res. Commun. **408**(3): 489-493.

York, JJ., and Fahey, KJ. 1990. Humoral and cell-mediated immune responses to the glycoproteins of infectious laryngotracheitis herpesvirus. Arch. Virol. **115**(3–4):289–297.

Yu, Q., Spatz, S., Li, Y., Yang, J., Zhao, W., Zhang, Z., Wen, G., Garcia, M. and Zsak, L. 2017. Newcastle disease virus vectored infectious laryngotracheitis vaccines protect commercial broiler chickens in the presence of maternally derived antibodies. Vaccine. **35**(5): 789–795.

Zaffuto, K.M., Estevez, C.N. and Afonso, C.L. 2008. Primary chicken tracheal cell culture system for the study of infection with avian respiratory viruses. Avian Pathol. **37**(1): 25-31.

Zhang, Z., Zhang, Y., Xia, S., Kong, Q., Li, S., Liu, X. and Lieberman, J. 2020. Gasdermin E suppresses tumour growth by activating anti-tumour immunity. Nature. 579(7799): 415-420.

Zhang, L., Xing, R., Huang, Z., Zhang, N., Li, X. and Wang, P. 2019. Inhibition of synovial macrophage pyroptosis alleviates synovitis and fibrosis in knee osteoarthritis. J.Inflamm. **1**: 11.

Zhou, Z., He, H., Wang, K., Shi, X., Wang, Y., Su, Y. & Shao, F. 2020. Granzyme A from cytotoxic lymphocytes cleaves GSDMB to trigger pyroptosis in target cells. Science. **368**(6494): 7548.

Ziemann, K., Mettenleiter, T. C. and Fuchs, W. (1998). Gene arrangement within the unique long genome region of infectious laryngotracheitis virus is distinct from that of other alphaherpesviruses. Virol. J. **72**(1): 847–852.

✍ ✍ ✍

Appendix

APPENDIX

BUFFERS AND REAGENTS

1) Phosphate Buffered Saline (PBS-10x)

Sodium chloride	80.0 g
Potassium chloride	2.0 g
Disodium hydrogen phosphate (Na_2HPO_4)	14.4 g
Potassium dihydrogen phosphate (KH_2PO_4)	2.4 g
Distilled Water to make	1000 ml

*Working solution of PBS (1x) was prepared by 1:10 dilution of the 10x stock in DW; and pH was adjusted to 7.4 if required.

2) Trisodium citrate buffer (1x) pH 6.0

Trisodium citrate dihydrate	2.94 g
Distilled water	1000 ml

3) Tris-Borate-EDTA (TBE) Buffer (5X)

Tris-base*	54.0 g
Boric acid	27.5 g
0.5 M EDTA (pH 8.0)	20.0 ml
Distilled water to make	1000 ml

* Tris and EDTA were mixed in 800 ml of autoclaved distilled water, stirred until dissolved completely. Then boric acid was added and stirred; the final volume was adjusted to 1000 ml with autoclaved distilled water and stored at room temperature. Working solution of TBE buffer (0.5x) was prepared by 1:10 dilution of the stock in DW.

4) 1M Tris (pH 8)

Tris base	12.10g
Distilled water	80.00ml

pH was adjusted to 8.0 by concentrated HCl and volume was adjusted to 100 ml by distilled water and sterilized by autoclaving.

5) 0.5M EDTA

Disodium ethylene diamine tetra acetate.$2H_2O$	18.61g
Distilled water	80.00ml

Sodium hydroxide pellet was added until and unless the pH became 8.0 keeping the solution on a magnetic stirrer. The final volume was adjusted to 100 ml and sterilized by autoclaving.

6) TE buffer (pH 8)

1 M Tris HCl (pH 8)	1.0ml
O.5 M EDTA (pH 8)	0.2 ml
Distilled water	98.8 ml

Sterilized by autoclaving.

7) Ethidium bromide

10 mg of ethidium bromide was dissolved in 1 ml of distilled water and stored in dark at 4°C.

8) Type 6X loading dye

Bromophenol blue	0.25%
Xylene cyanol	0.25%
Sucrose	40%

Stored at 4 °C

9) Dissociation solution

DMEM	999.878µl
Protease	20 µl
DNAse	2 µl
PS	100 µl

*Filter by 0.2µm syringe filter

10) Growth medium for ATE cells (20ml)

DMEM	10ml
LHC-9 medium	9.4ml
B-27 supplement (50X)	0.5ml
PS (100X)	0.1ml

*Filter by 0.2µm syringe filter

11) Alternative Growth medium for ATE (20ml)

DMEM	10ml
BEGM	9.4ml
BIT-9500	0.5ml
PS (100X)	0.1ml

* Filter by 0.2µm syringe filter

12) 10% Growth medium for CEK cells

FBS	5ml
M199 medium	44.5ml
Penicillin Streptomycin (PS)	0.5ml

* Filter by 0.2µm syringe filter

13) 1% Maintenance medium for CEK cells

FBS	0.5ml
M199 medium	49ml
Penicillin Streptomycin (PS)	0.5ml

*Filter by 0.2µm syringe filter

14) LPS stock solution (2.4mg/ml)

LPS	2.4mg
PBS	1ml

The working solution of LPS was prepared by 1:10 dilution of the stock solution in PBS to make a final concentration of (240ng/µl).

15) Nigericin stock solution(10mM)

Nigericin sodium salt	5mg
DMSO	669µl

16) Disulfiram stock solution (5 mM)

10 mg of Disulfiram was reconstituted with 6.74 ml of DMSO to make a 5 mM stock solution

17) Bay 11-7082 stock solution (20 mM)

5 mg of Bay 11-7082 was reconstituted with 1.2 ml of DMSO to make a 20 mM stock solution

18) MTT stock solution

MTT powder was dissolved in 1X PBS (5mg/ml) followed by filtration of the solution using a 0.22µm syringe filter in dark & aliquots of these solutions were prepared and stored at -20 f C in dark. MTT solution was used within 20 days once prepared.

VITAE

Name	:	**Dr. Parvatha Rama Sai Revathi**
Father's Name	:	Mr. P Chinna Rami Reddy
Mother's Name	:	Mrs. M Vijaya
Date of birth	:	22-08-1996
Permanent Address	:	D/no: -5-12-118/36 a4,Kongalaveedu Road, Near Three Taps,Giddalur,Prakasam District, Andhra Pradesh- 523357.
Email ID	:	revathi9reddy@gmail.com

Academic Qualifications:

Degree	Board/university	Year of passing	OGPA
B.V.Sc. & A.H.	College of Veterinary Science, Proddatur Sri VenkateswaraVeterinaryUniversity	2014-2019	7.91
M.V.Sc.	Indian Veterinary Research Institute (IVRI), Izatnagar Deemed University	2020-2023	8.106

M.V.Sc.Research title : ***Effects Of Pyroptotic Inhibitors On Infectious Laryngotracheitis Virus (ILTV) Induced Inflammation In Chicken Epithelial Cells***

Life membership

1. Indian Association of Veterinary Microbiologists, Immunologists and Specialists in Infectious diseases (IAVMI).

Fellowship/Awards

1. Institutional fellowship for pursuing M.V. Sc in Veterinary Microbiology at ICAR-IVRI.